Models for interfacial waves and their numerical integration

Hai Yen Nguyen

HAL Id: tel-00363790

https://theses.hal.science/tel-00363790

Submitted on 24 Feb 2009

N° ENSC-2008/98

THÈSE DE DOCTORAT
DE L'ÉCOLE NORMALE SUPÉRIEURE DE CACHAN

Présentée par

Hai Yen NGUYEN

pour obtenir le grade de

DOCTEUR DE L'ÉCOLE NORMALE SUPÉRIEURE DE CACHAN

domaine :

Mathématiques Appliquées

Sujet de la thèse :

MODÈLES POUR LES ONDES INTERFACIALES ET LEUR INTÉGRATION NUMÉRIQUE

Thèse présentée et soutenue à Cachan le 1er février 2008 devant le jury composé de :

M. Thomas J BRIDGES	Rapporteur
M. Paul CHRISTODOULIDES	Examinateur
M. Frédéric DIAS	Directeur de thèse
M. Jean-Michel GHIDAGLIA	Président du jury
M. Henrik KALISCH	Examinateur
M. Jean-Marc VANDEN-BROECK	Rapporteur

Centre de Mathématiques et de Leurs Applications

ENS CACHAN/CNRS/UMR 8536

61, avenue du Président Wilson, 94235 CACHAN CEDEX (France)

Remerciements

Je n'aurais pas mené à bien ce travail sans la disponibilité, l'attention et l'exigence de Frédéric Dias. Sa direction a été une chance, humaine et intellectuelle. Je souhaite lui exprimer toute ma gratitude.

Je remercie tout particulièrement les Professeurs Thomas J Bridges et Jean-Marc Vanden-Broeck d'avoir accepté de juger ce travail et d'en être les rapporteurs.

Je tiens à remercier très chaleureusement Jean-Michel Ghidaglia d'avoir accepté de présider le jury de cette thèse.

J'exprime mes remerciements à Henrik Kalisch et Paul Christodoulis pour leur participation au jury.

Mes trois années de thèse se sont déroulées dans un excellent environnement au sein du Centre de Mathématiques et de Leurs Applications de l'ENS Cachan. Je tiens à en remercier tous les membres, particulièrement l'équipe du secrétariat, Véronique, Virginie et Micheline ainsi que Pascal pour l'informatique.

Merci à Frédéric Pascal pour ses précieux conseils au niveau scientifique. Je remercie également Frédéric Chardard et Denys Dutykh pour nos discussions très enrichissantes. Mes pensées vont aussi à Hadi Rabbani Haghighi pour son aide dans la rédaction de ce manuscript.

Un grand merci également à l'équipe des doctorants du CMLA, qui contribuent largement à la convivialité du labo. Notamment, dans le désordre, Gabriele, Stéphanie, Jérémie, Jean-Pascal, Rodrigo, Filippo, Guido, Gael, Adina, Julie, Diego, Fikri, Neus, Ayman, Eric, Bruno, Camilo, Gonzalo, Mauricio, Gwendoline.

Ma famille et mes amis vietnamiens ainsi que Simone Chapron ont été présents pour m'encourager pendant toutes ces années. Je leur en suis infiniment reconnaissante.

Je remercie enfin de tout coeur Rafael Grompone von Gioi pour son soutien sans faille.

Introduction

L'eau couvre plus de 70% de la surface de la terre. Plusieurs phénomènes qui ont lieu à la surface de l'eau sont familiers à tout le monde depuis très longtemps, par exemple les ondes circulaires provoquées par une pierre jetée dans une mare, ou des vagues qui se brisent à l'approche de la plage. La théorie des ondes à la surface de l'eau est une source de problèmes mathématiques et physiques intéressants depuis au moins 150 ans.

Mais l'existence des ondes à l'intérieur du domaine aquatique a été découverte beaucoup plus tard. Ces ondes sont connues depuis quelques siècles sous le nom d'ondes internes et les études scientifiques sur ce sujet sont récentes. Les ondes internes qui ont lieu à l'interface de deux fluides superposés tels qu'une couche d'eau chaude s'étendant jusqu'à l'interface avec une couche d'eau plus froide, plus salée, sont appelées ondes à l'interface.

Cette thèse est consacrée à la modélisation numérique des ondes à l'interface. Nous limitons notre attention au régime où les amplitudes des ondes sont petites et leurs longueurs sont grandes.

Une brève présentation des ondes à l'intérieur du domaine aquatique, ainsi que certains modèles existants pour les ondes à l'interface de fluides, est donnée dans le premier chapitre. Nous décrivons également les trajectoires des particules à l'intérieur d'un fluide à deux couches superposées dans le cas où l'onde à l'interface est périodique et de petite amplitude.

Une discussion des équations de Boussinesq classiques, ainsi que de leurs avantages et de leurs extensions est incluse dans le deuxième chapitre. Ces équations fournissent des outils utiles pour la modélisation de notre problème.

Dans le troisième chapitre, nous dérivons un système de trois équations pour modéliser des ondes à l'interface en utilisant une méthode de perturbation. Pour simplifier,

nous supposons que les paramètres caractérisant la non-linéarité et la dispersion sont égaux.

Dans le chapitre quatre, un modèle alternatif à ce problème est proposé. Il s'agit d'un système de type Boussinesq, qui est libre de l'hypothèse où les paramètres caractérisant la non-linéarité et la dispersion sont égaux. Le cas critique, où le carré du rapport entre les épaisseurs de deux couches est égal à leur rapport de densité, est également étudié. Ce cas de figure est modélisable par un système de type Boussinesq avec des termes non-linéaires élevés au cube. Nous appelons cela un système de Boussinesq étendu.

Les simulations numériques sont présentées dans le cinquième chapitre. Elles montrent que ces deux systèmes de type Boussinesq conviennent pour la modélisation de la propagation ainsi que la collision entre deux ondes solitaires. Nous étudions à la fois la collision "head-on" et la collision "overtaking" entre deux ondes solitaires d'élévation ou deux ondes solitaires de dépression. Les ondes solitaires plates résolvant le système Boussinesq étendu sont également simulées. Le filtrage itératif permet d'obtenir, à partir des solutions approximatives, des ondes solitaires affinées qui se propagent de manière parfaitement stable. Ces ondes solitaires affinées sont utilisées afin d'étudier quantitativement les run-ups et les déphasages résultant des collisions de type inélastique entre deux ondes solitaires.

Mots clés: ondes à l'interface, ondes solitaires, ondes solitaires plates, équations de type Boussinesq, fluide à deux couches, collision "head-on", collision "overtaking", run-up, déphasage.

Introduction

Water covers more than 70% of the Earth's surface. Many phenomena which take place on the water surface are familiar to everyone since a long time ago, for example the rings spreading out from a stone thrown in a pool or waves breaking whenever they approach the beach. The theory of water waves (waves at the surface of water) have been a source of intriguing physical and mathematical problems for at least 150 years.

However the existence of waves in the interior of water domain was discovered much later. These waves have been known for centuries with the name internal waves and their scientific studies are recent. The internal waves that take place at the interface of two superposed fluids such as a warmer water layer extending down to the interface with a colder, more saline water layer, are called interfacial waves.

This thesis is devoted to the numerical modelling of the interfacial waves. We restrict our attention to the small amplitude, long-wave regime.

A short presentation of the internal waves as well as some existing models for interfacial waves is given in the first chapter. We describe also the trajectories of the particles in the interior of a two-layer fluid in the case where the interfacial wave is periodic and of small amplitude.

A discussion of the classical Boussinesq equations, their advantages and extensions is included in the second chapter. These equations provide useful tools for modelling our problem.

In the third chapter, we derive a system of three equations for modelling the interfacial waves by using a perturbation method. For simplicity, we assume that the nonlinearity and dispersion parameters are equal.

In chapter four, an alternative model for this problem is proposed. It is a Boussinesq system, which is free of the assumption that the nonlinearity and dispersion

parameters are equal. A critical case, where the square of the thickness ratio of the two layers equals to their respective density ratio, is also studied. It can be modeled by a Boussinesq system with cubic nonlinearities terms. We call this the extended Boussinesq system.

The numerical simulations are presented in the fifth chapter. They show that these two Boussinesq systems are convenient for modelling the propagation as well as the collision between two solitary waves. We study both the head-on collision and the overtaking collision between two solitary waves of elevation or two solitary waves of depression. The flat solitary waves solution to the extended Boussinesq system are also simulated. The iterative filtering permits to obtain, from the approximate solution, the clean solitary waves which propagate in a perfectly stable manner. Using these clean solitary waves, we investigate qualitatively the run-ups and the phase shifts resulting from the inelastic collisions between two solitary waves.

Keywords: Interfacial waves, solitary waves, flat solitary waves, Boussinesq equations, two-layer fluid, head-on collision, overtaking collision, run-up, phase shift.

Contents

Chapter 1

Internal waves overview

Internal waves are waves that travel within the interior of a fluid. They have been studied much later than water waves (waves at the surface of water). One of the earliest scientific observations of internal waves is that of Fridtjov Nansen, a Norwegian explorer, scientist and diplomat. Returning from a three year journey of FRAM expedition to Arctic Ocean with his crew in 1896, he brought to civilization a wealth of descriptions of unexplained natural phenomena; one of them was the dead water problem. Dead water is the nautical term for a strange phenomenon which can occur when a layer of fresh water rests on top of more dense, heavier salt water, without mixing of two layers. A ship travelling in such conditions may be hard to manoeuvre or can even slow down almost to a standstill. He discussed his observations on this phenomenon with Vilhelm Bjerknes, a famous Norwegian physicist and meteorologist. Vilhelm Bjerknes attributed the wave resistance to internal wave generated by the ship. More than one hundred years later, the knowledge of the flows due to internal waves, their generation and propagation in addition to the dead water problem is still partial.

The study of internal waves is motivated by human activities that take place more and more in the water environment. They are affected by wave motion. For example, to exploit oil in the ocean, long cables are usually used to connect ships or oil platforms floating on the sea surface with sub-sea drilling or production. Knowledge of the internal waves in addition to the wave and current effects at the ocean surface is important for the design of such constructions. Scientists try to quantify induced loads on submerged engineering constructions such as oil platforms and rail and road tunnels lying on the seabed. Work has been done on flows in fjords and at sills, motion in coastal water and sub-surface waves in a layered ocean, breaking

of internal waves and mixing processes in the ocean.

1.1   Internal waves

Internal waves are gravity waves that oscillate within the fluid medium. Internal waves that appear at the interface between two fluids of different densities are called interfacial waves. Fluids can be air, water, petrol, etc, and the fluid domain can be multiple layers with interfacial waves appearing at different interfaces. The simplest model is when a coating of oil lies over water. The stability of this configuration can be explained by everyone who knows that the density of water is larger than that of petrol, hence it is not surprising that an interface between these two fluids is established.

Water environment can be stratified by a rapid change in density with depth. In freshwater such as in lakes, this density change is usually caused by water temperature, while in seawater such as in oceans the density change may be caused by changes in salinity and/or temperature. Although internal waves are also observed in the atmosphere, this manuscript deals mainly with internal waves in the water environment.

Internal waves typically have much lower frequencies and higher amplitudes than surface gravity waves because the density differences (and therefore the restoring forces) within a fluid are usually much smaller than the density of the fluid itself.

Internal waves exist in different forms: standing waves, travelling waves, mix of these two waves, internal solitary waves, etc. As emphasized by Helfrich & Melville (2006) [30] in their recent survey article on long nonlinear internal waves, observations over the past four decades have demonstrated that internal solitary-like waves are ubiquitous features of coastal oceans and marginal seas. The main interest of my work is in interfacial solitary waves. A short introduction of this kind of wave is given in the next section.

1.1.1   Internal solitary waves

Solitary waves are nowadays well defined as long nonlinear waves consisting of a localized central core and a decaying tail. They were reported both at the surface and in the interior of fluids.
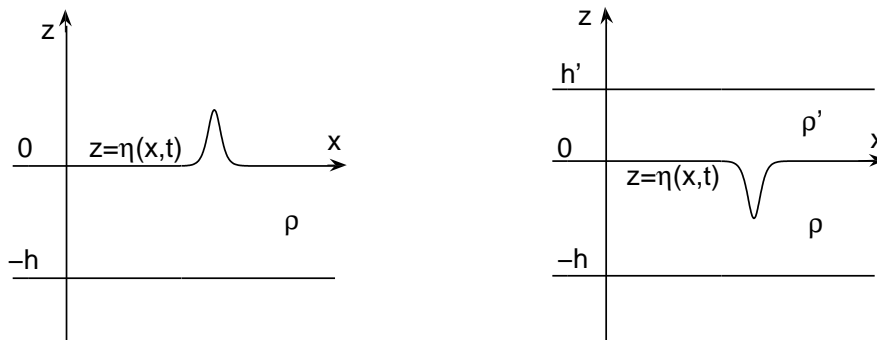
Figure 1.1: (a) Sketch of a solitary wave of elevation propagating at the surface of fluid with density ρ and depth h. (b) Sketch of a solitary wave of depression propagating at the interface between two fluid layers with different densities ρ' and ρ. The roof and the bottom of the fluid domain are flat and rigid boundaries, located respectively at $z = h'$ and $z = -h$.

Historically, a solitary wave was observed for the first time at the surface of water by John Scott Russell in 1834, while conducting experiments for other purposes. This discovery was described by his own words in the report on waves for the fourteenth meeting of the British Association for the Advancement of Science, in 1844:

"I was observing the motion of a boat which was rapidly drawn along a narrow channel by a pair of horses, when the boat suddenly stopped - not so the mass of water in the channel which it had put in motion; it accumulated round the prow of the vessel in a state of violent agitation, then suddenly leaving it behind, rolled forward with great velocity, assuming the form of a large solitary elevation, a rounded, smooth and well-defined heap of water, which continued its course along the channel apparently without change of form or diminution of speed. I followed it on horseback, and overtook it still rolling on at a rate of some eight or nine miles an hour, preserving its original figure some thirty feet long and a foot to a foot and a half in height. Its height gradually diminished, and after a chase of one or two miles I lost it in the windings of the channel. Such, in the month of August 1834, was my first chance interview with that singular and beautiful phenomenon which I have called the Wave of Translation".

In order to have an idea of the form of solitary waves, the readers who are not familiar with this terminology are invited to look at Figure 1.1.

The solitary waves take place whenever the nonlinear and dispersive effects are

balanced. For water waves, the nonlinearity is characterized by the ratio

$$\alpha = \frac{A}{h}$$

between the wave amplitude A and the water depth h while the dispersion is characterized by the ratio

$$\beta = \frac{h^2}{\ell^2}$$

between the square of the water depth and the square of the wavelength ℓ.

For two fluid layers, the thickness of the lower or upper layer can be used in the definition of β depending on the regime that one studies. For convenience, in this manuscript, h is defined as the thickness of the lower layer and h' is that of the upper layer. The primes are used to denote quantities in the upper layer.

The amplitude A of the solitary wave is defined as the maximum displacement from the undisturbed flow. The wavelength which appears in the above definition is given by

$$\ell = \frac{1}{A} \int_{-\infty}^{+\infty} \eta dx,$$

where η is the disturbance of the interface from its stationary position (it is usually a function of space and time variables).

Internal solitary waves are important for many practical reasons. They are ubiquitous in the coastal water and take place whenever strong tides and stratification occur in the neighbourhood of irregular topography. Figure 1.2 shows the locations of solitons (red point) observed around the world with a variety of remote and in-situ sensors. The present and future studies continue to complete this map especially in the open-ocean part. Internal solitary waves can propagate over several hundred kilometers and transport both mass and momentum. They also carry considerable velocity shear that can lead to turbulence and mixing. The mixing often introduces bottom nutrients into the water column, thereby fertilizing the local region, modifying the biological environment and re-suspending sediment. Internal solitary waves influence also acoustic propagation, radar observations and offshore engineering design. An early motivation to study them was the unexpected large stresses they imposed on offshore oil drilling rigs.
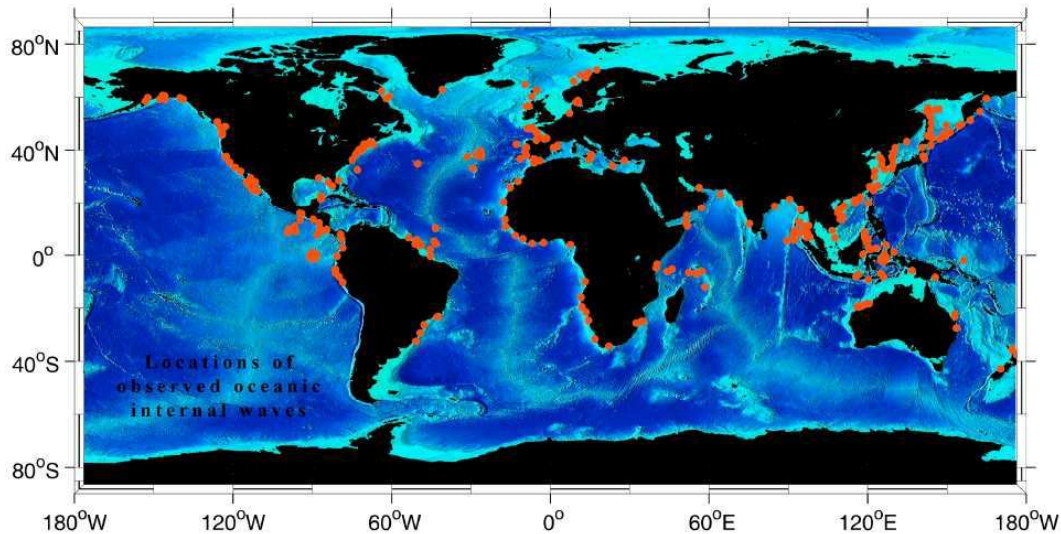
Figure 1.2: Locations of internal wave imagery and data presented in the Second Edition of the Atlas of Oceanic Internal Solitary Waves. The vast majority are satellite images. Lack of open-ocean sites reflects paucity of the data there. Picture taken from website http://www.internalwaveatlas.com/Atlas2_index.html

1.1.2   Observations

Interest in large internal waves began in the $1960s$ to $1970s$ thanks to the confluence of applied mathematics, remote sensing and development of ocean instrumentation, especially thermistor. One of the most dramatic early measurements took place in the Andaman Sea. A group of internal waves with height up to 80 m and length up to 2000 m was observed on the main thermocline at a depth of 500 m in water 1500 m deep.

As presented in Fig 1.2, internal solitary waves are widespread. Oceanographers found their existence in many regions around the world oceans, for example in strait, coastal zone and on continental margin, especially where the tidal flows take place over topography.

Fig 1.3a shows a solitary wave packet propagating toward the coast on the Oregon shelf. Wave amplitudes are 20 to 25 meters while the thickness of the upper layer is just of 7 m. As we know, the solar radiation is absorbed near the free surface of the upper layer. A region of warmer water, lower density was created and a pycnocline appeared at a depth of about 7 m. The colors indicate temperatures as indicated in the color bar.

a

b
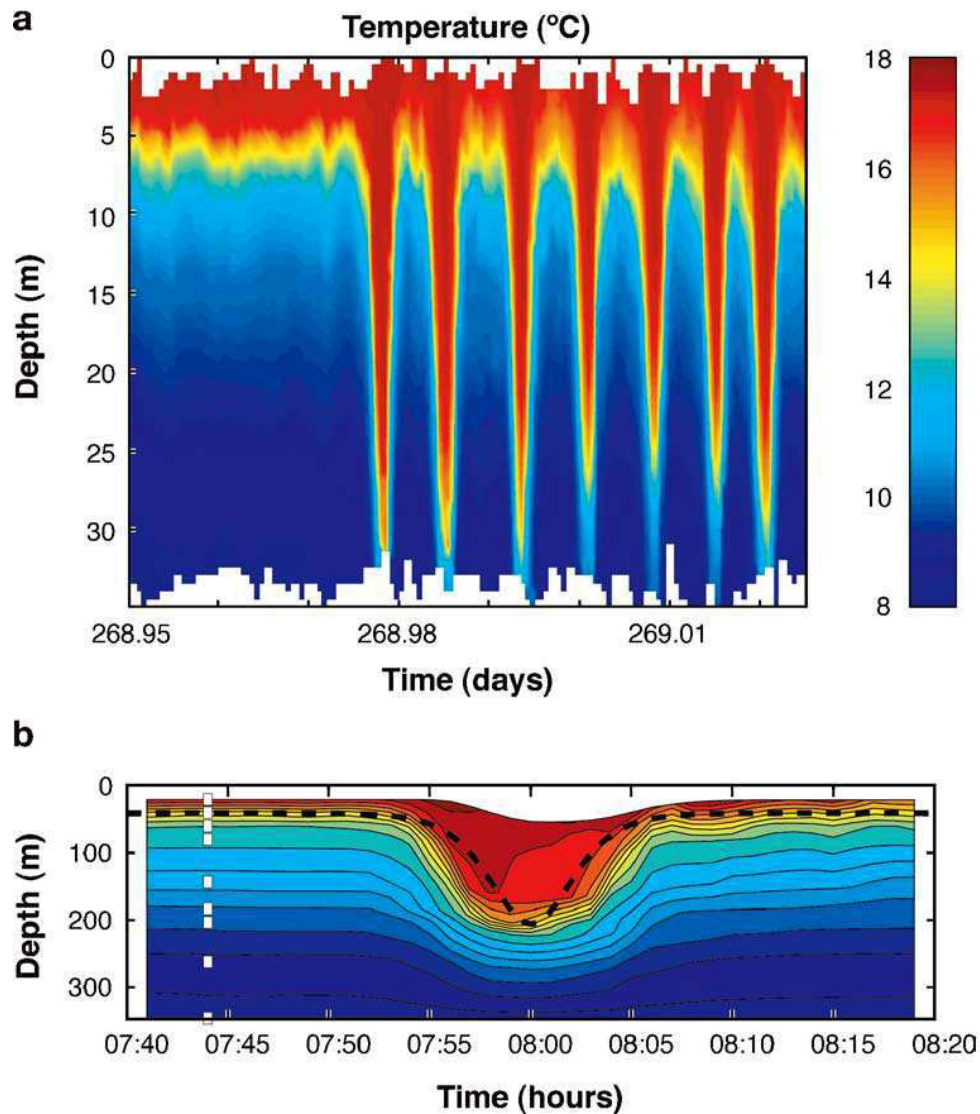
Figure 1.3: Large-amplitude internal waves observed with fixed thermistor arrays. (a) The leading portion of a wave packet observed in about 147 m of water, propagating toward the Oregon coast (Picture taken from Stanton & Ostrovsky (1998) [36]). The colors indicate temperatures as indicated in the color bar. (b) A single large wave in 340 m of water in the northeast South China Sea (Picture taken from Duda et al. (2004)). The temperature is contoured in intervals of 1°C, and the white squares indicate the thermistor locations. The dashed curve is the profile of a KdV solitary wave calculated using the background stratification.
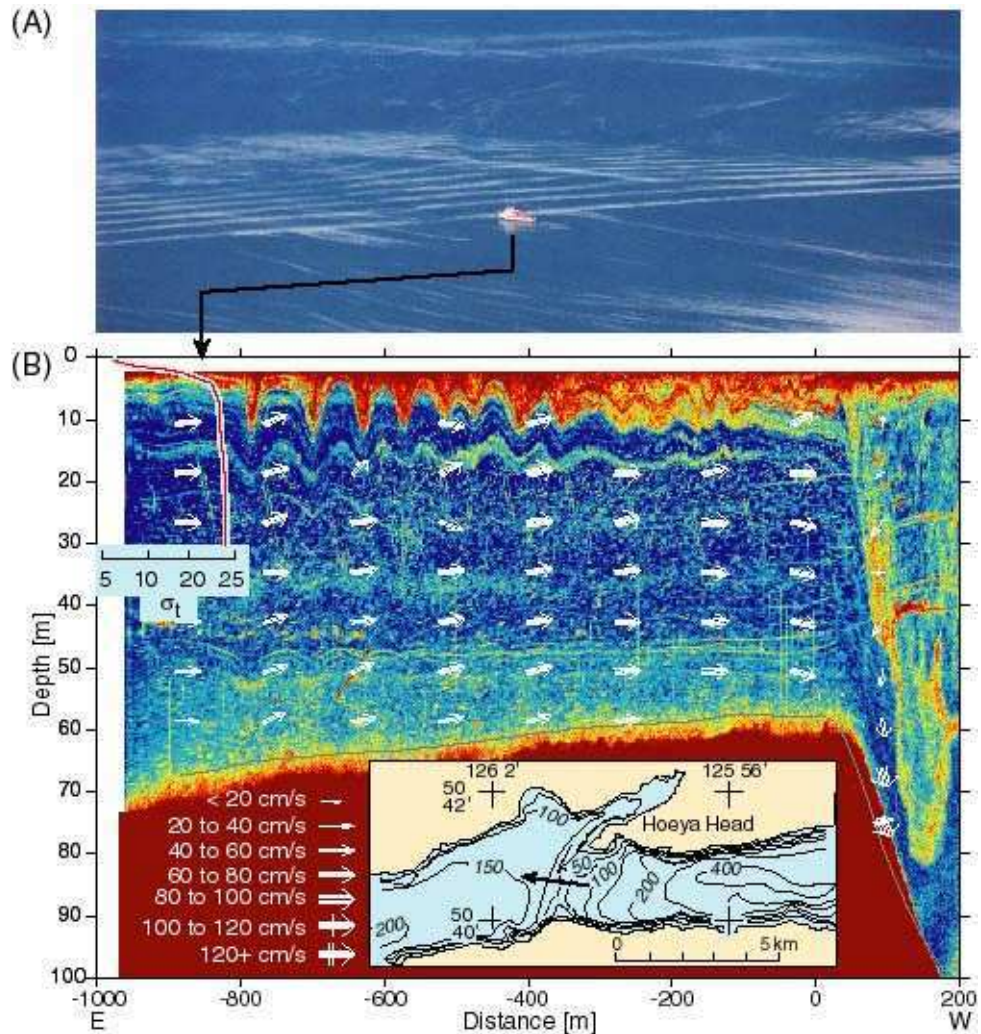
Figure 1.4: (A) Photograph of Canadian ship *Vector* crossing a packet of solitons in Knight Inlet, British Columbia. (B) Current vectors and acoustic profile during the time that current tidal attains a level near the maximum. Ship direction is with current. Solitons appear to have been generated before release of downstream pycnocline depression (Farmer & Armi (1999) [25]). Picture taken from website http://www.internalwaveatlas.com/Atlas2_index.html

Fig 1.3b illustrates the tendency of waves with amplitudes that are significantly large compared to the total depth to broaden and develop a flat crest. The amplitude is about 150 m in water of about 340 m total depth with upper layer depth of about 40 m. The dashed curve is the profile for a KdV solitary wave that Dula et al. (2004) calculated for the observation conditions, and illustrates that the observed wave is qualitatively different.

The measurements shown in Fig 1.4 were made in Knight Inlet, British Columbia, a 90 km long density stratified fjord with a 60 m sill separating two deep basins (Farmer & Armi (1999) [25]).

In the aerial photograph Fig 1.4A, the solitary waves can be seen as a surface modulation. Typically the waves form almost straight lines, consistent with the 2-dimensional behaviour of the flow near the channel center. Fig 1.4B is echo-sounder imaging which corresponds to the boat position in Fig 1.4A. It shows a series of solitary waves of amplitude 2 to 5 meters appearing in the pycnocline at a depth of 5 m. The density profile in red color on the upper left corner shows an abrupt jump in density with depth which creates two superposed fluid layers separated by an interface.

Although internal solitary waves are of interest in many contexts, their generation remains poorly understood. If the theoretical study of their generation and propagation is approximately correct, then they should occur whenever the combination of stratification, bathymetry, and current flow conspire to give the needed condition. It is apparent that these conditions happen frequently in coastal regions, especially during the summer.

1.2   Previous studies

Internal waves have been the subject of theoretical analysis for the last five decades because of their important role. Studies have been performed theoretically, numerically, as well as experimentally, especially for the simplest configuration: two layer fluid. If not specified, all discussions below will refer to two layer fluids.

In the following, we restrict ourselves to the case of internal waves at the interface of two superposed fluids. The lower fluid is of density ρ and depth h, and the lighter upper fluid is of density ρ' and depth h'. The stability of this configuration is ensured by $\rho' < \rho$. The density ratio $r = \rho'/\rho$ therefore takes values between 0 and 1. The case $r \approx 0$ corresponds to water waves while the case $r \approx 1$ corresponds

to two fluids with almost the same density such as an upper, warmer layer extending down to the interface with a colder, more saline layer. The thickness ratio $H = h'/h$ takes theoretical values between 0 and ∞. The displacement of the interface from the rest position is denoted by η.

Internal waves are called long waves if their wavelength is large compared to the thickness of at least one of the two layers. The long-wave regime contains the six following basic regimes:

- Korteweg-de Vries regime: two layers are of finite depth and one seeks the waves of small amplitude. This regime is characterized by $A/h \simeq A/h' \simeq (h/l)^2 \simeq (h'/l)^2 \simeq \beta \ll 1$.

- Finite-steepness for two finite layers: two layers are of finite depth and one seeks the waves of large interface deviations but small slope. This regime is characterized $(h/l)^2 \simeq (h'/l)^2 \simeq (A/l)^2 \simeq \beta \ll 1$.

- Benjamin-Ono regime: one of the two layers is infinite. Waves of small amplitude are considered. If one chooses the bottom layer to be infinite, this regime is characterized by $(h'/l)^2 \simeq (A/h')^2 \ll 1$.

- Small steepness for an infinite lower (or upper) layer: one of the two layers is infinite. The waves of large interface deviation and small slope are considered. If one chooses the bottom layer to be infinite, this regime is characterized by $(h'/l)^2 \simeq (A/l)^2 \simeq \beta \ll 1$.

- Intermediate Long Waves (ILW) regime: one of the two layers is very thin, the other layer is of finite depth. The waves of small amplitude are studied. If the lower layer is finite, the characterization of this regime is $(h'/l)^2 \simeq (A/h')^2 \simeq \beta \ll 1$; $\sqrt{\beta}h \simeq O(1)$

- Extension of ILW regime: one of the two layers is very thin, the other layer is of finite depth. This regime allows the study of large amplitude waves. If the lower layer is finite, the characterization of this regime is $(h'/l)^2 \simeq \beta \ll 1$; $\sqrt{\beta}h \simeq O(1)$

Craig et al. (2005) [16] used Hamiltonian perturbation theory for the long-wave limit to study these six regimes. They considered two cases, where the surface of the upper layer is bounded by a rigid lid or a free surface. They focused on quantifying the difference between these two configurations in the KdV regime. Their numerical and theoretical results show that: when the difference between the densities of

the two layers is large, there are a number of significant differences between both cases. But when $\rho - \rho'$ is small, the difference is small. This important remark was also mentioned in Evans & Ford (1996) [24]. The "rigid lid" configuration remains consequently popular for investigating internal waves even if it does not allow for generalized solitary waves. Generalized solitary waves are long nonlinear waves consisting of a localized central core and periodic non-decaying oscillations extending to infinity. Such waves arise whenever there is a resonance between a linear long wave speed of one wave mode in the system and a linear short wave speed of another mode (see Fochesato et al. (2005) [26]). Classical Korteweg-de Vries equation do not deal with the resonance, consequently can not exhibit generalized solitary waves. Dias & Il'ichev (2001) [21] have established a model which permits the generalized solitary wave solutions as the result of the resonance between a solitary wave and a periodic wave. The limit case, where the square of the thickness ratio is close to the density ratio, which possesses the broaden solitary wave and front solutions has been also discussed in this article.

For solitary waves, it is known that when the wave speed approaches a critical value the solution reaches a maximum amplitude while becoming indefinitely wider; these waves are often called 'table-top' waves. In the limit as the width of the central core becomes infinite, the wave becomes a front (see Dias & Vanden-Broeck (2003) [19]). Such behavior is conveniently modelled by an extended Korteweg-de Vries (eKdV) equation, i.e. a KdV equation with a cubic nonlinear term (see Funakoshi & Oikawa (1986) [27]). Sometimes the terminology 'modified KdV equation' or 'Gardner equation' is also used. KdV-type equations only describe one-way wave propagation. The natural extension toward two-way wave propagation is the class of Boussinesq systems.

Let's consider the Boussinesq system obtained by Craig et al. (2005) [16] for the KdV regime. This model can be applied to the case where the upper layer is bounded by a rigid lid. It is correct up to order β. In physical variables, this model can be written as

$$
\begin{aligned}
\partial_t \eta &= -\partial_x \Big(\frac{hh'}{\rho'h + \rho h'} u_I + \frac{1}{3} \frac{(hh')^2 (\rho'h' + \rho h)}{(\rho'h + \rho h')^2} \partial_x^2 u_I + \frac{\rho h'^2 - \rho' h^2}{(\rho'h + \rho h')^2} (\eta u_I) \Big) \\
\partial_t u_I &= -\partial_x \Big(g(\rho - \rho')\eta + \frac{1}{2} \frac{\rho h'^2 - \rho' h^2}{(\rho'h + \rho h')^2} u_I^2 \Big),
\end{aligned}
\tag{1.1}
$$

where $u_I = \rho u - \rho' u'$ is a combination of horizontal velocities at the interface.

It is evident that, in the case where the amplitude of the surface wave is relatively large compared to the thickness of the upper layer, the motion of the free surface influences the interface, so that the rigid lid assumption cannot be used.

Another model has been obtained by Choi & Camassa (1999) [13]

$$\eta_t - \left((h' - \eta)\bar{u}_1\right)_x = 0,$$
$$\bar{u}_{1t} + b_1\bar{u}_1\bar{u}_{1x} + (b_2 + b_3\eta)\eta_x = b_4\bar{u}_{1xxt} + O(\beta^3), \tag{1.2}$$

where $\bar{u}_1$ is the mean velocity of the upper layer

$$\bar{u}_1 = \frac{1}{1 - \eta}\int_\eta^1 u_1(x, z, t)dz,$$

and b_i are parameters given by

$$b_1 = \frac{\rho'h^2 - \rho h'h - 2\rho h'^2}{\rho'h^2 + \rho h'h}, \qquad b_2 = \frac{gh(\rho' - \rho)}{\rho'h + \rho h'},$$

$$b_3 = \frac{g\rho(\rho' - \rho)(h' + h)}{(\rho'h + \rho h')^2}, \qquad b_4 = \frac{1}{3}\frac{\rho'h'^2h + \rho h'h^2}{\rho'h + \rho h'}.$$

This model is a special case of the fully nonlinear model $(3.19) - (3.22)$ that Choi & Camassa (1999) [13] have established for finite amplitude, long-wave regime. In the fully nonlinear model, no assumption on the wave amplitude has been made. They used perturbation theory based only on the small parameter β. Therefore the model can be used to study waves of not only intermediate but also small and larger amplitude (compared to the depth of two layers). In the limit, when the wave amplitude becomes small, the fully nonlinear model restricts to the Boussinesq equations (1.2). Note that Choi & Camassa did not use the definition of β given in section 1.1.1. For them $\beta = h'^2/\ell^2$. This difference does not change anything, because in the configuration that we discuss $h'/h = O(1)$. The set of equations (3.19)–(3.22) in Choi & Camassa (1999) [13] is the two-layer version of the Green-Naghdi equations and it was recently extended to the free-surface configuration (see Barros et al. (2007) [2]).

It is worth pointing out that the models (1.1) and (1.2) are applicable for two-way propagation waves. For unidirectional waves, they reduce to the Korteweg-de Vries (KdV) equation.

Solitary waves for two-layer flows have also been computed numerically as solutions to the full incompressible Euler equations in the presence of an interface by various authors – see for example Laget & Dias (1997) [34]. Similarly fronts have been computed for example in Dias & Vanden-Broeck (2003) [19] and Dias & Vanden-Broeck (2004) [20].

1.3   Trajectories of the particles

The trajectories of particles moving under a surface wave are well-known. On the other hand, we haven't found any description of particle trajectories for interfacial waves. This is why we include it here.

Let us briefly study the trajectories of the particles in the interior of the configuration sketched in Figure 1.1b for small amplitude periodic interfacial waves.

Two incompressible and inviscid fluids with densities ρ and ρ' fill respectively the lower and upper layer of the fluid domain which is bounded below by a flat bottom at $z = -h$ and above by a rigid roof at $z = h'$.

We assume that the displacement $\eta(x, t)$ of waves at the interface $z = 0$ is very small and the flows are potential with ϕ and ϕ' respectively the velocity potentials of the lower and upper fluids.

At the leading order, where the small quantities are ignored, one has the following linear equations and linear boundary conditions:

The equations for the conservation of mass for the lower and upper layer respectively are

$$\Delta\phi = 0, \tag{1.3}$$

$$\Delta\phi' = 0. \tag{1.4}$$

The impermeability along the two rigid boundaries gives:

$$\phi_z = 0 \quad \text{at} \quad z = -h, \tag{1.5}$$

$$\phi'_z = 0 \quad \text{at} \quad z = h'. \tag{1.6}$$

The kinematic conditions along the interface give

$$\eta_t - \phi_z = 0 \quad \text{at} \quad z = 0, \tag{1.7}$$

$$\eta_t - \phi'_z = 0 \quad \text{at} \quad z = 0. \tag{1.8}$$

The dynamic boundary condition imposed on the interface leads to

$$\rho(\phi_t + g\eta) = \rho'(\phi'_t + g\eta) \quad \text{at} \quad z = 0. \tag{1.9}$$

One looks for ϕ of the form

$$\phi(x, z, t) = (C \cosh kz + D \sinh kz)e^{i(kx-\omega t)},$$

where C and D are arbitrary constants.

This expression verifies automatically (1.3). Substituting it into the boundary condition (1.5) yields

$$\left[k(C \sinh kz + D \cosh kz)e^{i(kx-\omega t)}\right]_{z=-h} = 0.$$

One deduces from the previous equation the relation between the constants C and D:

$$D = C \tanh kh.$$

Substituting the previous equation into the expression for ϕ, one has

$$\begin{aligned}
\phi(x, z, t) &= C\left(\cosh kz + \tanh kh \sinh kz\right)e^{i(kx-\omega t)} \\
&= C\left(\frac{e^{kz} + e^{-kz}}{2} + \frac{e^{kh} - e^{-kh}}{e^{kh} + e^{-kh}}\frac{e^{kz} - e^{-kz}}{2}\right)e^{i(kx-\omega t)} \\
&= C\frac{e^{k(h+z)} + e^{-k(h+z)}}{e^{kh} + e^{-kh}}e^{i(kx-\omega t)}.
\end{aligned}$$

Thus,

$$\phi(x, z, t) = C\frac{\cosh k(h+z)}{\cosh kh}e^{i(kx-\omega t)}. \tag{1.10}$$

Similarly, one looks for ϕ' of the form

$$\phi'(x, z, t) = (A \cosh kz + B \sinh kz)e^{i(kx-\omega t)},$$

where A and B are arbitrary constants. This expression of ϕ' verifies automatically the condition (1.4). Demanding that ϕ' formally satisfy the boundary condition (1.6) leads to

$$\left[k(A \sinh kz + B \cosh kz)e^{i(kx-\omega t)}\right]_{z=h'} = 0.$$

One deduces from the previous equation that

$$B = -A \tanh kh'.$$

Substituting this equation into the expression of ϕ' yields

$$\begin{aligned}
\phi'(x, z, t) &= A\left(\cosh kz - \tanh kh' \sinh kz\right)e^{i(kx-\omega t)} \\
&= A\left(\frac{e^{kz} + e^{-kz}}{2} - \frac{e^{kh'} - e^{-kh'}}{e^{kh'} + e^{-kh'}}\frac{e^{kz} - e^{-kz}}{2}\right)e^{i(kx-\omega t)} \\
&= A\frac{e^{k(h'-z)} + e^{-k(h'-z)}}{e^{kh'} + e^{-kh'}}e^{i(kx-\omega t)}.
\end{aligned}$$

Finally, one has

$$\phi'(x, z, t) = A\frac{\cosh k(h' - z)}{\cosh kh'}e^{i(kx-\omega t)}. \tag{1.11}$$

We will use the kinematic conditions at the interface (1.7) and (1.8) to find out the relation between the two constants A and C. From these two equations, one has

$$\phi_z = \phi'_z \quad \text{at} \quad z = 0.$$

Substituting (1.10) and (1.11) into the previous equation yields

$$Ck\frac{\sinh k(h + z)}{\cosh kh}e^{i(kx-\omega t)} = -Ak\frac{\sinh k(h' - z)}{\cosh kh'}e^{i(kx-\omega t)} \quad \text{at} \quad z = 0.$$

Therefore

$$C = -A\frac{\tanh kh'}{\tanh kh}.$$

Thus, one can express ϕ' in terms of C:

$$\phi'(x, z, t) = -C\frac{\cosh k(h' - z)\tanh kh}{\sinh kh'}e^{i(kx-\omega t)}. \tag{1.12}$$

Substituting this expression into (1.8) yields

$$\eta_t = Ck(\tanh kh)e^{i(kx-\omega t)}$$

Integrating the previous equation with respect to t, one obtains

$$\eta(x, t) = \frac{iCk}{\omega}(\tanh kh)e^{i(kx-\omega t)}, \tag{1.13}$$

assuming that the mean value of $\eta(x, t)$ is 0.

Now we look for the **dispersion relation**.

The condition (1.9) can be written as

$$\phi_t + g\eta = \frac{\rho'}{\rho}(\phi'_t + g\eta) \quad \text{at} \quad z = 0.$$

Let $r = \rho'/\rho$, the previous equation becomes

$$\phi_t - r\phi'_t + (1 - r)g\eta = 0 \quad \text{at} \quad z = 0. \tag{1.14}$$

Using (1.10) and (1.12), one has

$$
\begin{aligned}
\phi_t|_{z=0} &= (-i\omega)C\frac{\cosh k(h + z)}{\cosh kh}e^{i(kx-\omega t)}|_{z=0} \\
&= -i\omega Ce^{i(kx-\omega t)}.
\end{aligned}
$$
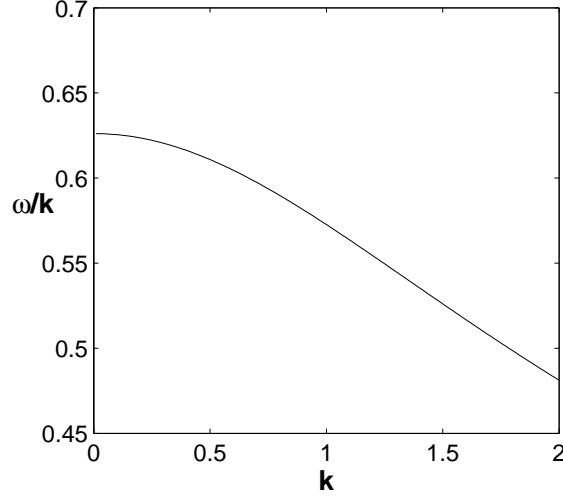
Figure 1.5: Dispersion relation (1.15) for the right-running wave of small amplitude, periodic interfacial waves with parameters $h = 1m$, $h' = 0.6m$, $r = 0.9$.

and

$$
\begin{aligned}
\phi'_t|_{z=0} &= i\omega C \frac{\cosh k(h' - z)\tanh kh}{\sinh kh'} e^{i(kx - \omega t)}|_{z=0} \\
&= i\omega C \frac{\tanh kh}{\tanh kh'} e^{i(kx - \omega t)}.
\end{aligned}
$$

Substituting the two previous expressions and (1.13) into (1.14) yields

$$
-i\omega C e^{i(kx - \omega t)} - r i\omega C \frac{\tanh kh}{\tanh kh'} e^{i(kx - \omega t)} + (1 - r)g\frac{iCk}{\omega}(\tanh kh)e^{i(kx - \omega t)} = 0.
$$

Equivalently

$$
1 + r\frac{\tanh kh}{\tanh kh'} - \frac{(1 - r)gk}{\omega^2}\tanh kh = 0.
$$

One deduces that

$$
\omega^2 = \frac{(1 - r)gk\tanh kh\tanh kh'}{\tanh kh' + r\tanh kh},
$$

or equivalently

$$
\omega = (+, -)\sqrt{\frac{(1 - r)gk\tanh kh\tanh kh'}{\tanh kh' + r\tanh kh}}. \tag{1.15}
$$

In order to obtain the trajectories of a particle of the lower fluid, we call $(\tilde{X}, \tilde{Z})$ the perturbation of the particle at a given time around its mean position (X_0, Z_0). The

co-ordinates of the particle are give by

$$X = X_0 + \tilde{X}; \quad Z = Z_0 + \tilde{Z}.$$

By definition, one has

$$\frac{\partial \tilde{X}}{\partial t} = \frac{\partial \phi}{\partial x}|_{(X_0, Z_0)} \quad \text{and} \quad \frac{\partial \tilde{Z}}{\partial t} = \frac{\partial \phi}{\partial z}|_{(X_0, Z_0)}.$$

Therefore

$$\frac{\partial \tilde{X}}{\partial t} = -kC \frac{\cosh k(h + Z_0)}{\cosh kh} \sin(kX_0 - \omega t),$$

and

$$\frac{\partial \tilde{Z}}{\partial t} = kC \frac{\sinh k(h + Z_0)}{\cosh kh} \cos(kX_0 - \omega t).$$

Integrating the two previous equations with respect to t yields

$$\tilde{X} = -\frac{kC}{\omega} \frac{\cosh k(h + Z_0)}{\cosh kh} \cos(kX_0 - \omega t),$$

and

$$\tilde{Z} = -\frac{kC}{\omega} \frac{\sinh k(h + Z_0)}{\cosh kh} \sin(kX_0 - \omega t),$$

assuming that the mean value of $\tilde{X}$ and $\tilde{Z}$ are 0.

Thus

$$\frac{(X - X_0)^2}{(\cosh k(h + Z_0))^2} + \frac{(Z - Z_0)^2}{(\sinh k(h + Z_0))^2} = \left(\frac{kC}{\omega \cosh kh} \right)^2. \tag{1.16}$$

One deduces that the trajectories of the particles in the lower layer are elliptic.

Similarly, in order to obtain the trajectories of a particle in the upper layer, we call $(\tilde{X}', \tilde{Z}')$ the perturbations of the particle around its mean position (X_0', Z_0') . The co-ordinates of the particle can be written by

$$X' = X_0' + \tilde{X}'; \quad Z' = Z_0' + \tilde{Z}'.$$

By definition, one has

$$\frac{\partial \tilde{X}'}{\partial t} = \frac{\partial \tilde{\phi}'}{\partial x}|_{(X_0', Z_0')} \quad \text{and} \quad \frac{\partial \tilde{Z}'}{\partial t} = \frac{\partial \tilde{\phi}'}{\partial z}|_{(X_0', Z_0')}$$

Therefore

$$\frac{\partial \tilde{X}'}{\partial t} = Ck \frac{\cosh k(h' - Z_0') \tanh kh}{\sinh kh'} \sin(kX_0' - \omega t),$$

and

$$\frac{\partial \tilde{Z}'}{\partial t} = Ck \frac{\sinh k(h' - Z_0') \tanh kh}{\sinh kh'} \cos(kX_0' - \omega t).$$

Integrating the two previous equations with respect to t yields

$$\tilde{X}' = \frac{Ck}{\omega} \frac{\cosh k(h' - Z_0') \tanh kh}{\sinh kh'} \cos(kX_0' - \omega t),$$

and

$$\tilde{Z}' = -\frac{Ck}{\omega} \frac{\sinh k(h' - Z_0') \tanh kh}{\sinh kh'} \sin(kX_0' - \omega t),$$

assuming that the mean value of $\tilde{X}'$ and $\tilde{Z}'$ are 0.

One deduces that

$$\frac{(X' - X_0')^2}{(\cosh k(h' - Z_0'))^2} + \frac{(Z' - Z_0')^2}{(\sinh k(h' - Z_0'))^2} = \left(\frac{Ck \tanh kh}{\omega \sinh kh'}\right)^2. \qquad (1.17)$$

Thus, the trajectories of the particles of the upper layer are also elliptic.

For a particle at the interface, in the expressions (1.16) and (1.17), Z_0 and Z_0' will tend to 0 while X_0 and X_0' tend to the same value called X_I.

The expressions for the particles of the lower layer can be written as

$$\tilde{X} = -\frac{kC}{\omega} \cos(kX_I - \omega t),$$

and

$$\tilde{Z} = -\frac{kC}{\omega}(\tanh kh) \sin(kX_I - \omega t).$$

And the expressions for the particles of the upper layer are

$$\tilde{X}' = \frac{kC}{\omega} \frac{\tanh kh}{\tanh kh'} \cos(kX_I - \omega t),$$

and

$$\tilde{Z}' = -\frac{kC}{\omega}(\tanh kh) \sin(kX_I - \omega t).$$

Comparing these four expressions, one sees that at the interface one has $\tilde{Z} = \tilde{Z}'$ (as expected) but $\tilde{X} \neq \tilde{X}'$.

(a)   (b)
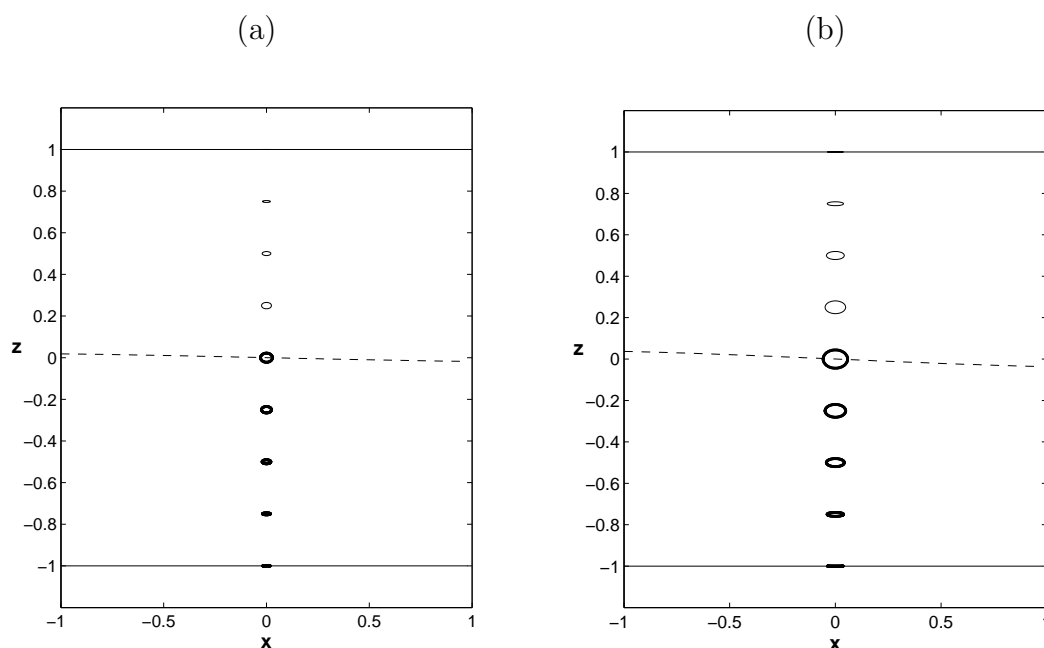
Figure 1.6: Trajectories of the particles of a two-layer fluid. They are described by equations (1.16), (1.17) and (1.15). The dashed curve represents the interface between the layers. The thick curves represent the trajectories of the particles of the lower layer. The thin curves represent the trajectories of the particles of the upper layer. The parameters are $h = 1\text{m}$, $h' = 1\text{m}$, $C = 0.008$, $k = 1\text{m}^{-1}$; (a) $r = 0.98$, $\omega = 0.27736\text{s}^{-1}$; (b) $r = 0.995$, $\omega = 0.13816\text{s}^{-1}$.

One concludes that the trajectories of the particles at the interface are not continuous. The particles follow the interface vertically but not tangentially.

Figure 1.6 shows the trajectories of the particles. One observes that more the difference between the density of the two layers are large, more the orbit of the trajectories of particles are large, by consequence more the amplitude of the interfacial waves are large.

Figure 1.7 shows also the trajectories of particles. The images (a) and (b) are for two different values of C while (c) and (d) show images corresponding to two different values of k. One observes that the orbit of the trajectories are right proportional to the value of C and k.
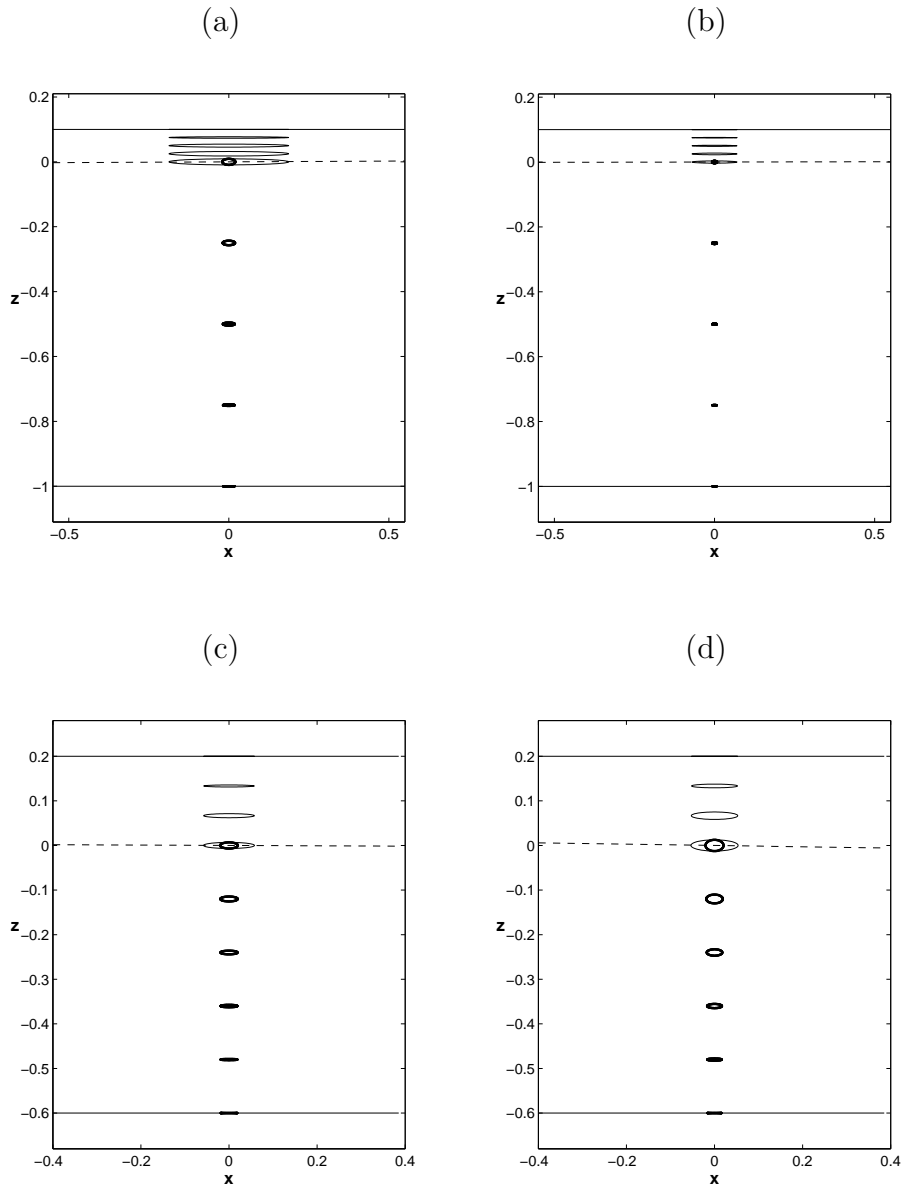
Figure 1.7: Trajectories of the particles of a two-layer fluid. They are described by equations (1.16), (1.17) and (1.15). The dashed curve represents the interface between the layers. The thick curves represent the trajectories of the particles of the lower layer. The thin curves represent the trajectories of the particles of the upper layer. The parameters for figures (a) and (b) are $h = 1\text{m}$, $h' = 0.1\text{m}$, $r = 0.85$, $k = 0.5\text{m}^{-1}$; (a) $C = 0.008$, $\omega = -0.19776\text{s}^{-1}$; (b) $C = 0.004$, $\omega = -0.197755\text{s}^{-1}$. The parameters for figures (c) and (d) are $h = 0.6\text{m}$, $h' = 0.2\text{m}$, $r = 0.9$, $C = 0.008$; (c) $k = 0.6\text{m}^{-1}$, $\omega = 0.23982\text{s}^{-1}$; (d) $k = 1.2\text{m}^{-1}$, $\omega = 0.46955\text{s}^{-1}$.

Chapter 2

Boussinesq equations and some extensions

In the nineteenth century, the study of water waves was of vital interest for application in naval architecture and for the knowledge of tided and floods. Notably in England and France, many researchers as Scott-Russell, Airy, Stokes, Lord Rayleigh, Lagrange, St. Venant, Boussinesq, etc, spent their studies on water wave of several kinds. In this chapter, we discuss the equations that Boussinesq established for model water waves and some extensions. The technique that Boussinesq used and the equations that he obtained are important contributions to modelling water waves.

Boussinesq equations were first derived by Boussinesq in the 1870s (see [8], [9]) to describe the two-way propagation of small amplitude and long-wave gravity waves on the surface of water in a channel. This model is restricted to the case where the bottom is flat, the fluid ideal, the flow irrotational and the vertical distribution of variables is parabolic or linear.

It is worth noting that 'small amplitude' ('long-wave') means that the wave amplitude (wavelength) is respectively small (large) compared to the water depth.

Many extensions of the classical Boussinesq equations have been obtained in order to extend the domain of validity or to improve the nonlinear and dispersive properties of the equations. Nowadays, one calls Boussinesq model all equation(s) resulting from studying small amplitude waves in a long-wave limit with the following assumptions: the flow is irrotational; the vertical distribution of variables is parabolic or linear, two-way propagation is allowed.

The main advantage of the Boussinesq models is the fact that they permit to model an n-dimensional ($n = 3$ or 2) physical phenomenon by an $(n - 1)$-dimensional problem. It is done by eliminating suitably the dependence of variables on the vertical direction.

In many laboratory studies or engineering applications, the full Euler equations appear more complex than is necessary for the modelling situation at hand. Consequently many approximate models adapted to restricted physical regimes have been derived. The Boussinesq models are a good choice to study small amplitude, long waves in shallow water, especially when the nonlinear and dispersive effects are of the same order of magnitude.

General waves cannot be properly described by the models of unidirectional waves such as Korteweg-de Vries equations. Models for two-way propagation like Boussinesq equations play an important role. They allow the study of the interaction between two or more waves, and the consideration of the reflected waves which appear when investigating the flow over an irregular topography.

Boussinesq equations take into account both nonlinearity and dispersion. It is well known that nonlinearity tends to steepen a given wave form during the course of its evolution, while dispersion has the opposite effect and tends to flatten steep free-surface gradients. One of the most striking manifestations of these two opposite effects lies in the possibility of the balance, which results in solitary waves.

2.1   Classical Boussinesq equations (1870s)

Boussinesq equations represent an approximation of the Euler equations for small amplitude water waves in shallow water. In Boussinesq (1871) [8], Boussinesq studied solitary waves in a channel on which he assumed that the movements are the same across the width. This allows to consider only the vertical plan, called (x, z). He also supposed that the flow is potential, the wave vanishes at infinity and the vertical distribution of the velocity vector field is obtained by a polynomial approximation.

In Boussinesq's model, an incompressible, inviscid fluid fills a channel from the flat bottom $z = 0$ up to the free surface $z = h + \eta(x, t)$. Herein, $\eta(x, t)$ is the displacement of the surface water from its undisturbed position h.

The system describing the motion of water wave that Boussinesq obtained is

$$\begin{cases} v_1 = \dfrac{\partial \eta}{\partial t} + u_1 \dfrac{\partial \eta}{\partial x} \\[2mm] g\eta + \dfrac{\partial \phi}{\partial t} + \dfrac{1}{2}(u_1^2 + v_1^2) = 0 \end{cases}, \tag{2.1}$$

where u_1, v_1 are respectively the horizontal and vertical velocities at the surface, g is the acceleration due to gravity and ϕ is the velocity potential.

Velocity potential ϕ is approximated by

$$\phi = -\int_x^\infty u_0 dx - \frac{1}{1.2}\frac{\partial u_0}{\partial x}z^2 + \frac{1}{1.2.3.4}\frac{\partial^3 u_0}{\partial x^3}z^4 - \frac{1}{1.2...5.6}\frac{\partial^5 u_0}{\partial x^5}z^6 + ...,$$

where u_0 is the horizontal velocity at the bottom.

Boussinesq supposed that the quantities u_0, η are very small and their derivatives with respect to x are smaller and smaller. This permits to neglect the small terms.

At the leading order, one has

$$v_1 = \frac{\partial \phi}{\partial z}\Big|_{z=h+\eta} = -\frac{\partial u_0}{\partial x}(h+\eta),$$

and

$$u_1 = \frac{\partial \phi}{\partial x}\Big|_{z=h+\eta} = u_0,$$

and

$$\phi_t|_{z=h+\eta} = -\int_x^\infty u_{0t}dx - \frac{1}{2}h^2 u_{0xt}.$$

Substituting these three expressions into (2.1) yields

$$\begin{cases} \dfrac{\partial \eta}{\partial t} + h\dfrac{\partial u_0}{\partial x} + (u_0\eta)_x = 0 \\[2mm] g\eta - \displaystyle\int_x^\infty u_{0t}dx - \dfrac{1}{2}h^2 u_{0xt} + \dfrac{1}{2}u_0^2 = 0 \end{cases},$$

where h is the water depth.

Differentiating the second equation of the previous system with respect to x, one obtains

$$\begin{cases} \eta_t + hu_{0x} + (u_0\eta)_x = 0 \\[2mm] g\eta_x + u_{0t} - \dfrac{1}{2}h^2 u_{0xxt} + u_0 u_{0x} = 0 \end{cases}. \tag{2.2}$$

Since the velocity potential ϕ can be evaluated at any water level, one can obtain the expression of the horizontal velocity $u = \dfrac{\partial \phi}{\partial x}$ everywhere along the water column. At water level $\theta = \frac{1}{\sqrt{3}} h$ one can take

$$u_\theta \approx u_0 - \frac{1}{6} h^2 u_{0xx}, \quad \text{or} \quad u_0 \approx u_\theta + \frac{1}{6} h^2 u_{\theta xx},$$

without changing the order of approximation.

Let $w = u_\theta$. System (2.2) becomes

$$\begin{cases} \eta_t + h w_x + (w\eta)_x = 0 \\[2mm] g\eta_x + w_t + w w_x - \frac{1}{3} h^2 w_{xxt} = 0 \end{cases}.$$

Using the following change of variables

$$x_{new} = \frac{x}{h} \quad t_{new} = \frac{c}{h} t, \quad \eta_{new} = \frac{1}{h}\eta, \quad w_{new} = \frac{w}{c}, \quad c = \sqrt{gh},$$

the previous system becomes (dropping the subscripts *new*)

$$\begin{cases} \eta_t + w_x + (w\eta)_x = 0 \\[2mm] \eta_x + w_t + w w_x - \frac{1}{3} w_{xxt} = 0 \end{cases}. \tag{2.3}$$

The system (2.3) is often considered as the classical Boussinesq equations (see Bona et al. (2002) [5]).

The classical Boussinesq model permits to study two-way wave propagation. Indeed, if one retains only the terms of the same order of η_t (see Boussinesq (1872) [9]) in (2.2) then

$$\begin{cases} \eta_t + h u_{0x} = 0 \\[2mm] g\eta_x + u_{0t} = 0 \end{cases}.$$

The previous system has solution

$$\eta = f(x - t\sqrt{gh}) + f_1(x + t\sqrt{gh}),$$

and

$$u_0 = \sqrt{\frac{g}{h}} \Big[f(x - t\sqrt{gh}) - f_1(x + t\sqrt{gh}) \Big].$$

At second order approximation, Boussinesq obtained the following well-known equation for bidirectional waves

$$\eta_{tt} = gh\eta_{xx} + \frac{3}{2}g(\eta^2)_{xx} + \frac{1}{3}gh^3\eta_{xxxx}. \tag{2.4}$$

If we restrict to waves propagating in one direction, for example to the right, at the lowest order (only two first terms are considered) the equation (2.4) will have solutions:

$$\eta = f(x - t\sqrt{gh}).$$

Therefore, the Boussinesq equation (2.4) can be factorized as

$$(\partial_t - \sqrt{gh}\partial_x)\Big(\eta_t + \frac{3}{2}\sqrt{\frac{g}{h}}\partial_x(\frac{2}{3}h\eta + \frac{1}{2}\eta^2 + \frac{h^3}{9}\eta_{xx})\Big) = 0. \tag{2.5}$$

2.2 Korteweg-de Vries equations

Under the supervision of Korteweg, de Vries has established during his thesis an equation to model water waves. The readers who are interested in the history of the KdV equation are invited to read Jager (2006) [32].

Boussinesq used a fixed coordinate system but Korteweg and de Vries chose the frame moving with the waves for their studies. The relation between the coordinates (ξ, τ) of the moving frame and the coordinates (x, t) of the fixed frame is given by

$$\xi = x - (\sqrt{gh} - \sqrt{\frac{g}{h}}\alpha)t, \qquad \tau = t,$$

where h is the depth water, g acceleration due to gravity and α an arbitrary constant. The equation of Korteweg and de Vries is given in the form

$$\eta_\tau + \frac{3}{2}\sqrt{\frac{g}{h}}\partial_\xi\Big(\frac{2}{3}\alpha\eta + \frac{1}{2}\eta^2 + \frac{1}{3}(\frac{1}{3}h^3 - \frac{Th}{\rho g})\eta_{\xi\xi}\Big) = 0, \tag{2.6}$$

where η is the displacement of the surface water from its undisturbed position and T surface tension.

If one ignores the surface tension T and takes $\alpha = h$ (the moving frame becomes the fixed frame), the one-way Boussinesq equation (2.5) recovers the KdV equation (2.6).

Using the following change of variables

$$\eta = \frac{2\alpha}{3}\eta_{new},$$

$$\xi = \frac{\sqrt{\frac{1}{2}(\frac{1}{3}h^3 - \frac{Th}{\rho g})}}{\sqrt{\alpha}}\xi_{new},$$

$$\tau = \frac{1}{\alpha}\sqrt{\frac{h}{g}}\frac{\sqrt{\frac{1}{2}(\frac{1}{3}h^3 - \frac{Th}{\rho g})}}{\sqrt{\alpha}}\tau_{new},$$

the KdV equation (2.6) can be written as (dropping the subscripts *new*)

$$\eta_\tau + \eta_\xi + \eta\eta_\xi + \eta_{\xi\xi\xi} = 0.$$

This equation is much more famous than the Boussinesq equations and appears in many physical contexts where wave motion is introduced. It possesses permanent solutions such as solitary waves, cnoidal waves.

It is worth noting that Boussinesq used the assumption that the wave vanishes at infinity, which is not necessary in the theory of Korteweg and de Vries. However, Korteweg and de Vries assumed that the waves are periodic.

2.3   Some extensions of the classical Boussinesq equations

2.3.1   Higher-order generalization of the Boussinesq equations

Bona et al. (2002) [5] derived a four-parameter family of Boussinesq systems from the two dimensional Euler equations for free-surface flow. In this study, it is supposed that

$$\alpha = \frac{A}{\ell} \ll 1, \quad \beta = \frac{h^2}{\ell^2} \ll 1, \quad S_t = \frac{\alpha}{\beta} \approx 1,$$

where A is the amplitude, ℓ is the wavelength and h is the water depth.
The first order approximations in the small parameters α and β are

$$\begin{cases} \eta_t + w_x + (w\eta)_x + aw_{xxx} - b\eta_{xxt} = 0 \\ \\ w_t + \eta_x + ww_x + c\eta_{xxx} - dw_{xxt} = 0 \end{cases}, \tag{2.7}$$

where a, b, c, d are parameters given by

$$a = \frac{1}{2}\left(\theta^2 - \frac{1}{3}\right)\lambda, \quad b = \frac{1}{2}\left(\theta^2 - \frac{1}{3}\right)(1 - \lambda),$$

$$c = \frac{1}{2}(1 - \theta^2)\mu, \quad d = \frac{1}{2}(1 - \theta^2)(1 - \mu).$$

Here λ, μ are real arbitrary parameters, $\theta \in [0,1]$ specifies the horizontal velocity represented by w.

At second order in the small parameters α and β, they obtained

$$\begin{cases} \eta_t - b\eta_{xxt} + b_1\eta_{xxxxt} = -w_x - (\eta w)_x - aw_{xxx} \\ \qquad\qquad +b(\eta w)_{xxx} - \left(a + b - \frac{1}{3}\right)(\eta w_{xx})_x - a_1 w_{xxxxx} \\ w_t - dw_{xxt} + d_1 w_{xxxxt} = -\eta_x - c\eta_{xxx} - ww_x - c(ww_x)_{xx} - (\eta\eta_{xx})_x \\ \qquad\qquad +(c + d - 1)w_x w_{xx} + (c + d)ww_{xxx} - c_1\eta_{xxxxx} \end{cases}, \tag{2.8}$$

with a, b, c, d given above and a_1, b_1, c_1, d_1 given by

$$\begin{aligned} a_1 &= -\frac{1}{4}\left(\theta^2 - \frac{1}{3}\right)^2(1 - \lambda) + \frac{5}{24}\left(\theta^2 - \frac{1}{5}\right)^2\lambda_1, \\ b_1 &= -\frac{5}{24}\left(\theta^2 - \frac{1}{5}\right)^2(1 - \lambda_1), \\ c_1 &= \frac{5}{24}(1 - \theta^2)\left(\theta^2 - \frac{1}{5}\right)(1 - \mu_1), \\ d_1 &= -\frac{1}{4}(1 - \theta^2)^2\mu - \frac{5}{24}(1 - \theta^2)\left(\theta^2 - \frac{1}{5}\right)\mu_1. \end{aligned}$$

Here λ_1, μ_1 are arbitrary parameters.

Exact travelling-wave solutions as well as exact solitary-wave solutions of many classes of (2.7) have been found by Chen (1997) [11]. Several classes of (2.7)

have been well studied in the literature, such as the Kaup system ($\theta^2 = 1$, $\lambda = 1$, μ *arbitrary*), the coupled KdV system ($\theta^2 = 2/3$, $\lambda = 1$, $\mu = 1$), etc. In the case

$$\theta^2 = \frac{1}{3}, \ \lambda \ arbitrary, \ \mu = 0$$

the system (2.7) recovers the classical Boussinesq equations. The BBM system ($\theta^2 = 2/3$, $\lambda = 0$, $\mu = 0$) was studied numerically by Bona & Chen (1998) [4].

The Boussinesq models given in (2.7) (or (2.8)) are formally equivalent but they may have rather different mathematical properties.

2.3.2 Arbitrary bathymetry

The classical Boussinesq model has a wide range of potential applicability. But the assumption that the bottom must be flat limits strongly its domain of application. Work has been done in order to improve this situation. A recent review is given by Dutykh & Dias (2007) [23].

In 1967, Peregrine obtained a three dimensional system applicable to irregular topography. This system is known as standard Boussinesq equations. It is written in physical variables as follows:

$$\begin{cases} \eta_t + \nabla \cdot [(h+\eta)\bar{\mathbf{u}}] = 0 \\ \bar{\mathbf{u}}_\mathbf{t} + g\nabla\eta + (\bar{\mathbf{u}} \cdot \nabla)\bar{\mathbf{u}} + \dfrac{h^2}{6}\nabla(\nabla \cdot \bar{\mathbf{u}}_t) - \dfrac{h}{2}\nabla[\nabla \cdot (h\bar{\mathbf{u}}_\mathbf{t})] = 0 \end{cases},$$

where $\bar{\mathbf{u}} = (u, v)$ is the mean horizontal velocity vector of the water column, η the displacement of the surface from its rest position, $h(x, y)$ the water depth and g the acceleration due to gravity.

In 1993 Nwogu established a three dimensional system which is also applicable to arbitrary bathymetry but the domain of application is larger than that of standard Boussinesq equations. In physical variables, it is written as

$$\begin{cases} \eta_t + \nabla \cdot [(h+\eta)\mathbf{u}_\theta] + \nabla \cdot \left[(\dfrac{z_\theta^2}{2} - \dfrac{h^2}{6})h\nabla(\nabla \cdot \mathbf{u}_\theta) + (z_\theta + \dfrac{h}{2})h\nabla[\nabla \cdot (h\mathbf{u}_\theta)]\right] = 0 \\ \mathbf{u}_{\theta t} + g\nabla\eta + (\mathbf{u}_\theta \cdot \nabla)\mathbf{u}_\theta + \left[\dfrac{z_\theta^2}{2}\nabla(\nabla \cdot \mathbf{u}_{\theta t}) + z_\theta\nabla[\nabla \cdot (h\mathbf{u}_{\theta t})]\right] = 0 \end{cases},$$

where $\mathbf{u}_\theta = (u_\theta, v_\theta)$ is the horizontal velocity vector at the water level z_θ; η, h and g are defined as in the Peregrine system. In this model, it is supposed that the vertical velocity varies linearly with respect to the vertical coordinate.

2.3.3   Two-layer fluid, extended KdV equation, extended Boussinesq equations

The procedure to obtain the KdV equation, as well as Boussinesq equations for water waves has been also applied to model the waves at the interface of two superposed fluids. In most cases, the nonlinearity is quadratic. However, when the square of the thickness ratio is close to the density ratio, the coefficients of the quadratic nonlinearities become small and the cubic nonlinearities must be considered. A KdV equation with both quadratic and cubic nonlinear terms is usually called 'extended' KdV (eKdV) equation. Sometimes the terminology 'modified KdV equation' or 'Gardner equation' is also used.

When dealing with interfacial waves with rigid boundaries in the framework of the full Euler equations, the amplitude of the central core is bounded by the configuration. In the case of solitary waves, it is known that when the wave speed approaches a critical value the solution reaches a maximum amplitude while becoming indefinitely wider; these waves are often called 'table-top' waves. In the limit as the width of the central core becomes infinite, the wave becomes a front (see Dias & Vanden-Broeck (2003) [19]). Such behavior is conveniently modelled by an extended Korteweg–de Vries (eKdV) equation.

Considering the two-layer fluid configuration described in section 1.2 for the case $\rho' \approx \rho$, the extended KdV equation is written as (see Grimshaw et al. (1997) [29])

$$\eta_t + c_1\eta_x + c_2\eta\eta_x + c_3\eta^2\eta_x + c_4\eta_{xxx} = 0,$$

where η is the displacement of the interface from its undisturbed position and c_i are coefficients given by

$$c_1 = \sqrt{\frac{g(\rho - \rho')}{\rho}\frac{hh'}{h + h'}},$$

$$c_2 = \frac{3c_1}{2}\frac{h' - h}{hh'},$$

$$c_3 = -\frac{3c_1}{8h^2h'^2}(h^2 + h'^2 + 6hh'),$$

$$c_4 = \frac{c_1hh'}{6}.$$

Here h and h' are respectively the depth of the lower and upper layer, ρ and ρ' respectively the density of the lower and upper layer, g acceleration due to gravity.

The steady version of the extended KdV equation for interfacial waves proposed by Dias & Vanden-Broeck (2004) [20] is

$$\frac{1}{6}b\eta_{xxx} + \frac{3}{2}a\eta\eta_x - \frac{3}{4}c\eta^2\eta_x - (F - F_{bif})\eta_x = 0,$$

where

$$F = \frac{U}{\sqrt{gh}},$$

$$F_{bif} = \sqrt{\frac{H(1-r)}{H+r}},$$

$$a = \frac{2(H - \sqrt{r})}{\sqrt{r}(1 + \sqrt{r})}F_{bif},$$

$$b = (1 - \sqrt{r} + r)F_{bif},$$

$$c = \frac{4}{\sqrt{r}}F_{bif}.$$

Here U is the velocity of the uniform flow in two layers, r the density ratio between the upper and the lower layer, H the depth ratio between the upper and the lower layer.

A similar equation was obtained by Choi et al. (1996) [12] by using asymptotic expansions.

A Boussinesq system with both quadratic and cubic nonlinear terms is called 'extended' Boussinesq system. An extended Boussinesq system can be derived from the Hamiltonian formulation obtained by Craig et al. (2005) [16]. In this work, a Hamiltonian perturbation theory was applied to obtain the Boussinesq system correct up to order β^2. In physical variables, this system is written as

$$\begin{cases} \eta_t = -\dfrac{hh'}{\rho'h + \rho h'}u_{Ix} - \dfrac{1}{3}\dfrac{(hh')^2(\rho'h' + \rho h)}{(\rho'h + \rho h')^2}u_{Ixxx} \\ \qquad\quad -\dfrac{\rho h'^2 - \rho'h^2}{(\rho'h + \rho h')^2}(\eta u_I)_x + \dfrac{\rho\rho'(h + h')^2}{(\rho'h + \rho h')^3}(\eta^2 u_I)_x \quad, \qquad (2.9) \\ u_{It} = -g(\rho - \rho')\eta_x - \dfrac{1}{2}\dfrac{\rho h'^2 - \rho'h^2}{(\rho'h + \rho h')^2}(u_I^2)_x - \dfrac{\rho\rho'(h + h')^2}{(\rho'h + \rho h')^3}(\eta u_I^2)_x \end{cases}$$

where $u_I = \rho u - \rho'u'$ is a combination of horizontal velocities at the interface.

In the work presented in chapter 4 a set of extended Boussinesq systems will be derived. The system (2.9) is a special case of it. The 'table top' solitary wave solutions to these extended Boussinesq systems will be studied in detail in chapter 5 in order to answer the questions: what are their properties and how do they interact?

Chapter 3

Modelling for interfacial waves by using a perturbation method

In this chapter one uses a perturbation method to derive a model for interfacial waves appearing at the interface of two superposed fluids. The bottom as well as the upper boundary are assumed to be flat and rigid. A sketch is given in Figure 3.1. The analysis is restricted to two-dimensional flows. In other words, there is only one horizontal direction, x^*, in addition to the vertical direction, z^*. The interface is described by $z^* = \eta^*(x^*, t^*)$. The bottom layer $\Omega_{t^*} = \{(x^*, z^*) : x^* \in \mathbb{R}, -h < z^* < \eta^*(x^*, t^*)\}$ and the upper layer $\Omega'_{t^*} = \{(x^*, z^*) : x^* \in \mathbb{R}, \eta^*(x^*, t^*) < z^* < h'\}$ are filled with inviscid, incompressible fluids, with densities ρ and ρ' respectively. Let (u^*, v^*) and (u'^*, v'^*) represent the velocity in (x^*, z^*) coordinate. All quantities related to the upper layer will be denoted with a prime and all physical variables will be denoted with a star.

In addition the flows are assumed to be irrotational. Only stable configurations with $\rho > \rho'$ are considered.

One introduces the dimensionless density ratio r as well as the depth ratio H:

$$r = \frac{\rho'}{\rho}, \quad H = \frac{h'}{h}.$$

Obviously r takes values between 0 and 1, the case $r \approx 0$ corresponding to water
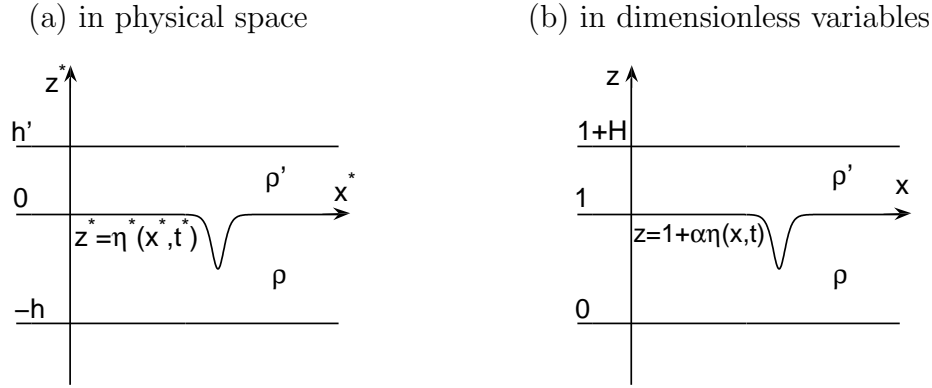
(a) in physical space   (b) in dimensionless variables

Figure 3.1: Sketch of solitary waves propagating at the interface between two fluid layers with different densities ρ' and ρ. The roof and the bottom of the fluid domain are flat and rigid boundaries, located respectively at $z^* = h'$ and $z^* = -h$. (a) Sketch of a solitary wave of depression in physical space; (b) Sketch of a solitary wave of depression in dimensionless coordinates, with the thickness h of the bottom layer taken as unit length and the long wave speed c as unit velocity. The dimensionless number H is equal to h'/h.

waves [1] while the case $r \approx 1$ corresponds to two fluids with almost the same density such as an upper, warmer layer extending down to the interface with a colder, more saline layer. The depth ratio takes theoretical values between 0 and ∞ but values $H \ll 1$ or $H \gg 1$ should be avoided in the framework of our weakly nonlinear analysis.

3.1   Governing equations

One starts with the Euler equations for the two-layer fluid configuration mentioned above:

$$u_{t^*}^* + u^* u_{x^*}^* + w^* u_{z^*}^* = \frac{-p_{x^*}^*}{\rho} \quad \text{for} \ -h < z^* < \eta^*(x^*, t^*), \tag{3.1}$$

$$u_{t^*}'^* + u'^* u_{x^*}'^* + w'^* w_{z^*}'^* = \frac{-p_{x^*}'^*}{\rho'} \quad \text{for} \ \eta^*(x^*, t^*) < z^* < h', \tag{3.2}$$

---

[1] In a recent paper, Kataoka (2006) [33] showed that when H is near unity, the stability of solitary waves changes drastically for small density ratios r. Therefore one must be careful in evaluating the stability of air-water solitary waves. In other words, there may be differences between $r = 0$ and the true value $r = 0.0013$.

$$w_{t*}^* + u^* w_{x*}^* + w^* u_{z*}^* = -\frac{p_{z*}^*}{\rho} - g \quad \text{for } -h < z^* < \eta^*(x^*, t^*), \tag{3.3}$$

$$w_{t*}^{'*} + u^{'*} w_{x*}^{'*} + w^{'*} w_{z*}^{'*} = -\frac{p_{z*}^{'*}}{\rho'} - g \quad \text{for } \eta^*(x^*, t^*) < z^* < h', \tag{3.4}$$

where p and p' are respectively the pressure of the lower and the upper fluid.

The continuity equations in each layer are

$$u_{x*}^* + w_{z*}^* = 0 \quad \text{for } -h < z^* < \eta^*(x^*, t^*), \tag{3.5}$$
$$u_x^{'*} + w_{z*}^{'*} = 0 \quad \text{for } \eta^*(x^*, t^*) < z^* < h'. \tag{3.6}$$

The boundary of the system $\{\Omega_{t*}, \Omega'_{t*}\}$ has two parts: the flat bottom $z^* = -h$ and the flat roof $z^* = h'$. The impermeability conditions along these rigid boundaries give

$$w^* = 0 \quad \text{at } z = -h, \tag{3.7}$$
$$w^{'*} = 0 \quad \text{at } z = h'. \tag{3.8}$$

The kinematic and dynamic conditions along the interface are

$$\eta_{t*}^* + u^* \eta_{x*}^* = w^* \quad \text{at } z^* = \eta^*, \tag{3.9}$$
$$\eta_{t*}^* + u^{'*} \eta_{x*}^* = w^{'*} \quad \text{at } z^* = \eta^*, \tag{3.10}$$

$$p^* = p'^* \quad \text{at } z^* = \eta^*. \tag{3.11}$$

The flows are assumed to be irrotational. Therefore

$$u_{z*}^* - w_{x*}^* = 0 \quad \text{for } -h < z^* < \eta^*(x^*, t^*), \tag{3.12}$$
$$u_{z*}^{'*} - w_{x*}^{'*} = 0 \quad \text{for } \eta^*(x^*, t^*) < z^* < h'. \tag{3.13}$$

3.2 Equation in the limit of long waves of small amplitude

Let us consider herein waves whose typical amplitude, A, is small compared to the depth of the bottom layer h, and whose typical wavelength, ℓ, is large compared

to the depth of the bottom layer [2]. Let us define the three following dimensionless numbers, with their characteristic magnitude:

$$\alpha = \frac{A}{h} \ll 1, \quad \beta = \frac{h^2}{\ell^2} \ll 1, \quad S_t = \frac{\alpha}{\beta} = \frac{A\ell^2}{h^3} \approx 1.$$

Here S_t is the Stokes number. α small means that the wave amplitude is small compared to the depth. β small means that the depth is small compared to the wavelength.

Using the following scaling

$$x^* = \ell x, \quad z^* = h(z - 1), \quad \eta^* = A\eta, \quad t^* = \ell t / c_0$$

$$u^* = \alpha c_0 u, \quad u'^* = \alpha c_0 u', \quad w^* = \alpha \sqrt{\beta} c_0 w, \quad w'^* = \alpha \sqrt{\beta} c_0 w',$$

$$p^* = -\rho g z^* + \rho g A p, \quad p'^* = -\rho' g z^* + \rho g A p',$$

where $c_0 = \sqrt{gh}$, equations (3.1)-(3.13) become

for the lower layer

$$
\begin{cases}
u_t + \alpha u u_x + \beta w u_z = -p_x \quad \text{for } 0 < z < 1 + \alpha\eta, \\[2mm]
\beta\Big(w_t + \alpha(u w_x + w w_z)\Big) = -p_z \quad \text{for } 0 < z < 1 + \alpha\eta, \\[2mm]
u_x + w_z = 0 \quad \text{for } 0 < z < 1 + \alpha\eta, \\[2mm]
w = 0 \quad \text{at } z = 0, \\[2mm]
w = \eta_t + \alpha u \eta_x \quad \text{at } z = 1 + \alpha\eta, \\[2mm]
(1 - r)\eta = p - p' \quad \text{at } z = 1 + \alpha\eta, \\[2mm]
u_z - \beta w_x = 0 \quad \text{for } 0 < z < 1 + \alpha\eta,
\end{cases}
\tag{3.14}
$$

---

[2]There is some arbitrariness in this choice since there are two fluid depths in the problem. One could has also chosen the depth of the roof layer as reference depth. In fact, one implicitly makes the assumption that the ratio of liquid depths is neither too small nor too large, without going into mathematical details. Models valid for arbitrary depth ratio have been derived for example by Choi & Camassa (1999) [13].

and for the upper layer

$$
\begin{cases}
u'_t + \alpha u' u'_x + \beta w' u'_z = -\dfrac{p'_x}{r} \quad \text{for } 1 + \alpha\eta < z < 1 + H, \\[2mm]
\beta\left(w'_t + \alpha(u' w'_x + w' w'_z)\right) = -\dfrac{p'_z}{r} \quad \text{for } 1 + \alpha\eta < z < 1 + H, \\[2mm]
u'_x + w'_z = 0 \quad \text{for } 1 + \alpha\eta < z < 1 + H, \\[2mm]
w' = 0 \quad \text{at } z = 1 + H, \\[2mm]
w' = \eta_t + \alpha u' \eta_x \quad \text{at } z = 1 + \alpha\eta, \\[2mm]
(1 - r)\eta = p - p' \quad \text{at } z = 1 + \alpha\eta, \\[2mm]
u'_z - \beta w'_x = 0 \quad \text{for } 1 + \alpha\eta < z < 1 + H.
\end{cases}
\tag{3.15}
$$

From now on one assumes that $\alpha = \beta$.

Applying Taylor expansions in terms of the small quantity $\alpha\eta$ to the interface boundary condition, one has:

for the bottom layer

$$
\begin{cases}
u_t + \alpha(u u_x + w u_z) = -p_x \quad \text{in } 0 < z < 1 + \alpha\eta, \\[2mm]
\alpha w_t + \alpha^2(u w_x + w w_z) = -p_z \quad \text{in } 0 < z < 1 + \alpha\eta, \\[2mm]
u_x + w_z = 0 \quad \text{in } 0 < z < 1 + \alpha\eta, \\[2mm]
w = 0 \quad \text{on } z = 0, \\[2mm]
w + \alpha\eta w_z + \dfrac{\alpha^2\eta^2}{2} w_{zz} = \eta_t + \alpha u \eta_x + \alpha^2 u_z \eta \eta_x \quad \text{on } z = 1, \\[2mm]
(r - 1)\eta + p - p' + \alpha\eta(p_z - p'_z) + \dfrac{\alpha^2\eta^2}{2}(p_{zz} - p'_{zz}) = 0 \quad \text{on } z = 1, \\[2mm]
u_z - \alpha w_x = 0 \quad \text{in } 0 < z < 1 + \alpha\eta,
\end{cases}
\tag{3.16}
$$

and for the upper layer

$$
\begin{cases}
u'_t + \alpha(u'u'_x + w'u'_z) = -\dfrac{p'_x}{r} \quad \text{in } 1 + \alpha\eta < z < 1 + H, \\[2mm]
\alpha w'_t + \alpha^2(u'w'_x + w'w'_z) = -\dfrac{p'_z}{r} \quad \text{in } 1 + \alpha\eta < z < 1 + H, \\[2mm]
u'_x + w'_z = 0 \quad \text{in } 1 + \alpha\eta < z < 1 + H, \\[2mm]
w' = 0 \quad \text{on } z = 1 + H, \\[2mm]
w' + \alpha\eta w'_z + \dfrac{\alpha^2\eta^2}{2} w'_{zz} = \eta_t + \alpha u'\eta_x + \alpha^2 u'_z \eta\eta_x \quad \text{on } z = 1, \\[2mm]
(r-1)\eta + p - p' + \alpha\eta(p_z - p'_z) + \dfrac{\alpha^2\eta^2}{2}(p_{zz} - p'_{zz}) = 0 \quad \text{on } z = 1, \\[2mm]
u'_z - \alpha w'_x = 0 \quad \text{in } 1 + \alpha\eta < z < 1 + H.
\end{cases}
\tag{3.17}
$$

Since one uses a perturbation method, the variables are expanded in powers of α:

$$
\begin{aligned}
u &= u_0 + \alpha u_1 + \alpha^2 u_2 + ..., \\
w &= w_0 + \alpha w_1 + \alpha^2 w_2 + ..., \\
p &= p_0 + \alpha p_1 + \alpha^2 p_2 + ..., \\
\eta &= \eta_0 + \alpha\eta_1 + \alpha^2\eta_2 + ...,
\end{aligned}
$$

$$
\begin{aligned}
u' &= u'_0 + \alpha u'_1 + \alpha^2 u'_2 + ..., \\
w' &= w'_0 + \alpha w'_1 + \alpha^2 w'_2 + ..., \\
p' &= p'_0 + \alpha p'_1 + \alpha^2 p'_2 + ...
\end{aligned}
$$

One will study the systems corresponding to each order of approximation such as $O(1)$, $O(\alpha)$, $O(\alpha^2)$ and then, one must combine the results in order to have the final equations in terms of the initial variables u, u' and η.

At order $O(1)$, one has the following 13 equations

$$
\begin{aligned}
u_{0t} &= -p_{0x} \quad \text{in } 0 < z < 1 + \alpha\eta, & (3.18) \\
p_{0z} &= 0 \quad \text{in } 0 < z < 1 + \alpha\eta, & (3.19) \\
u_{0x} + w_{0z} &= 0 \quad \text{in } 0 < z < 1 + \alpha\eta, & (3.20)
\end{aligned}
$$

$$
\begin{aligned}
w_0 &= 0 \quad \text{on } z = 0, & (3.21) \\
w_0 &= \eta_{0t} \quad \text{on } z = 1, & (3.22) \\
(r-1)\eta_0 + (p_0 - p_0') &= 0 \quad \text{on } z = 1, & (3.23) \\
u_{0z} &= 0 \quad \text{in } 0 < z < 1 + \alpha\eta, & (3.24) \\
u_{0t}' &= -\frac{p_{0x}'}{r} \quad \text{in } 1 + \alpha\eta < z < 1 + H, & (3.25) \\
p_{0z}' &= 0 \quad \text{in } 1 + \alpha\eta < z < 1 + H, & (3.26) \\
u_{0x}' + w_{0z}' &= 0 \quad \text{in } 1 + \alpha\eta < z < 1 + H, & (3.27) \\
w_0' &= 0 \quad \text{on } z = 1 + H, & (3.28) \\
w_0' &= \eta_{0t} \quad \text{on } z = 1, & (3.29) \\
u_{0z}' &= 0 \quad \text{in } 1 + \alpha\eta < z < 1 + H. & (3.30)
\end{aligned}
$$

It follows from (3.24) and (3.30) that u_0 and u_0' are independent of z. Similarly, it follows from (3.19) and (3.26) that p_0 and p_0' are also independent of z.

Taking the derivative of (3.23) with respect to x, one has

$$
p_{0x} - p_{0x}' = (1 - r)\eta_{0x} \quad \text{at } z = 1
$$

Since both the left hand side and the right hand side of the previous equation contain terms that are independent of z, one can consider that this equation is true for all values of z. Similarly, in some expressions below, one will not specify that they are obtained at the interface $z = 1$.

Substituting (3.18) and (3.25) into the previous equation leads to

$$
-u_{0t} + r u_{0t}' = (1 - r)\eta_{0x}.
$$

Taking the derivative of this equation with respect to x leads to

$$
-u_{0xt} + r u_{0xt}' = (1 - r)\eta_{0xx}. \tag{3.31}
$$

Integrating equation (3.20) with respect to z, one has

$$
w_0 = -z u_{0x} + A(x, t),
$$

where $A(x, t)$ is an arbitrary function of x and t.

Applying (3.21) to the previous equation, one obtains $A(x, t) = 0$. Therefore

$$
w_0 = -z u_{0x}.
$$

Consequently, one deduces from equation (3.22) that

$$u_{0x} = -\eta_{0t}.$$

Taking the derivative of this equation with respect to t, one has

$$u_{0xt} = -\eta_{0tt}. \tag{3.32}$$

By using the same procedure, one wishes to represent u'_{0xt} by η'_{0tt}.

Integrating equation (3.27) with respect to z, one has

$$w'_0 = -zu'_{0x} + B(x,t),$$

where $B(x,t)$ is an arbitrary function of x and t.

Applying (3.28) to the previous equation, one obtains $B(x,t) = (1+H)u'_{0x}$. Therefore

$$w'_0 = (-z + 1 + H)u'_{0x}.$$

Consequently, one deduces from (3.29) that

$$u'_{0x} = \frac{1}{H}\eta_{0t}.$$

Taking the derivative of this equation with respect to t yields

$$u'_{0xt} = \frac{1}{H}\eta_{0tt}. \tag{3.33}$$

Substituting (3.32) and (3.33) into (3.31) one obtains

$$\eta_{0tt} - \frac{1-r}{1 + \frac{r}{H}}\eta_{0xx} = 0. \tag{3.34}$$

The following expressions summarize some of the results obtained so far, which will be useful later on:

$$
\begin{aligned}
u_{0x} &= -\eta_{0t} \quad \text{in } 0 < z < 1 + \alpha\eta, \\
w_{0z} &= \eta_{0t} \quad \text{in } 0 < z < 1 + \alpha\eta, \\
w_0 &= z\eta_{0t} \quad \text{in } 0 < z < 1 + \alpha\eta, \\
u'_{0x} &= \frac{1}{H}\eta_{0t} \quad \text{in } 1 + \alpha\eta < z < 1 + H, \\
w'_{0z} &= -\frac{1}{H}\eta_{0t} \quad \text{in } 1 + \alpha\eta < z < 1 + H, \\
w'_0 &= \frac{-z + 1 + H}{H}\eta_{0t} \quad \text{in } 1 + \alpha\eta < z < 1 + H.
\end{aligned}
\tag{3.35}
$$

At order $O(\alpha)$, one has the following 13 equations (the expressions inside the big brackets are obtained by using (3.35):

$$
\begin{align}
u_{1t} + u_0 u_{0x} &= -p_{1x} \quad \text{in } 0 < z < 1 + \alpha\eta, \tag{3.36} \\
&= \left(u_{1t} - u_0\eta_{0t} \right) \\
w_{0t} &= -p_{1z} \quad \text{in } 0 < z < 1 + \alpha\eta, \tag{3.37} \\
u_{1x} + w_{1z} &= 0 \quad \text{in } 0 < z < 1 + \alpha\eta, \tag{3.38} \\
w_1 &= 0 \quad \text{on } z = 0, \tag{3.39} \\
w_1 + \eta_0 w_{0z} &= \eta_{1t} + u_0\eta_{0x} \quad \text{on } z = 1, \tag{3.40} \\
&= \left(w_1 + \eta_0\eta_{0t} \right) \\
(r-1)\eta_1 + p_1 - p_1' &= 0 \quad \text{on } z = 1, \tag{3.41} \\
u_{1z} &= w_{0x} \quad \text{in } 0 < z < 1 + \alpha\eta, \tag{3.42} \\
&= \left(z\eta_{0xt} \right) \\
u_{1t}' + u_0' u_{0x}' &= -\frac{p_{1x}'}{r} \quad \text{in } 1 + \alpha\eta < z < 1 + H, \tag{3.43} \\
&= \left(u_{1t}' + \frac{1}{H}u_0'\eta_{0t} \right) \\
w_{0t}' &= -\frac{p_{1z}'}{r} \quad \text{in } 1 + \alpha\eta < z < 1 + H, \tag{3.44} \\
u_{1x}' + w_{1z}' &= 0 \quad \text{in } 1 + \alpha\eta < z < 1 + H, \tag{3.45} \\
w_1' &= 0 \quad \text{on } z = 1 + H, \tag{3.46} \\
w_1' + \eta_0 w_{0z}' &= \eta_{1t} + u_0'\eta_{0x} \quad \text{on } z = 1, \tag{3.47} \\
&= \left(w_1' - \frac{1}{H}\eta_0\eta_{0t} \right) \\
u_{1z}' &= w_{0x}' \quad \text{in } 1 + \alpha\eta < z < 1 + H \tag{3.48} \\
&= \left(\frac{-z + 1 + H}{H}\eta_{0xt} \right).
\end{align}
$$

Taking the derivative of equation (3.41) twice with respect to x, one has

$$(r-1)\eta_{1xx} = -p_{1xx} + p_{1xx}' \quad \text{at } z = 1.$$

Taking the derivative of (3.36) and (3.43) with respect to x and then substituting them into the previous equation, one obtains

$$(r-1)\eta_{1xx} = u_{1xt} - r u_{1xt}' - (u_0\eta_{0t} + \frac{r}{H}u_0'\eta_{0t})_x \quad \text{at } z = 1. \tag{3.49}$$

Taking the derivative of (3.38) with respect to z, one has

$$\begin{aligned} w_{1zz} &= -u_{1xz} \\ &= -z\eta_{0xxt} \text{ (using (3.42))}. \end{aligned}$$

Integrating twice this equation with respect to z, one has

$$w_1 = -\frac{z^3}{6}\eta_{0xxt} + zC(x,t) + D(x,t),$$

where $C(x,t)$ and $D(x,t)$ are arbitrary functions of x and t.
Inserting the previous equation into (3.39) yields $D(x,t) = 0$. Therefore

$$w_1 = -\frac{z^3}{6}\eta_{0xxt} + zC(x,t). \tag{3.50}$$

Applying the previous equation to (3.40), one has

$$-\eta_0\eta_{0t} + \eta_{1t} + u_0\eta_{0x} = -\frac{1}{6}\eta_{0xxt} + C(x,t),$$

and one deduces that

$$C(x,t) = \frac{1}{6}\eta_{0xxt} - \eta_0\eta_{0t} + \eta_{1t} + u_0\eta_{0x}.$$

Substituting the expression of $C(x,t)$ into (3.50), one has

$$w_1 = (-\frac{z^3}{6} + \frac{z}{6})\eta_{0xxt} - z(\eta_0\eta_{0t} - \eta_{1t} - u_0\eta_{0x}). \tag{3.51}$$

Taking the derivative of (3.38) with respect to t and then using (3.51), one has

$$\begin{aligned} u_{1xt} &= -w_{1zt} \\ &= (\frac{z^2}{2} - \frac{1}{6})\eta_{0xxtt} + (\eta_0\eta_{0t})_t - \eta_{1tt} - (u_0\eta_{0x})_t. \end{aligned} \tag{3.52}$$

Let us now use the same arguments for u'_{1xt}.

Taking the derivative of (3.45) with respect to z, one has

$$\begin{aligned} w'_{1zz} &= -u'_{1xz} \\ &= \frac{z - (1+H)}{H}\eta_{0xxt} \text{ (using (3.48))}. \end{aligned}$$

Integrating twice this equation with respect to z gives

$$w_1' = \left(\frac{z^3}{6H} - z^2\frac{1+H}{2H}\right)\eta_{0xxt} + zE(x,t) + F(x,t),$$

where $E(x,t)$ and $F(x,t)$ are arbitrary functions of x and t.

Applying the previous equation to (3.46), one obtains

$$F(x,t) = \frac{(1+H)^3}{3H}\eta_{0xxt} - (1+H)E(x,t).$$

Therefore

$$w_1' = \left(\frac{z^3}{6H} - z^2\frac{1+H}{2H} + \frac{(1+H)^3}{3H}\right)\eta_{0xxt} + (z-1-H)E(x,t). \qquad (3.53)$$

Applying (3.53) to (3.47), one has

$$E(x,t) = \frac{2H^2 + 6H + 3}{6H}\eta_{0xxt} - \frac{1}{H^2}\eta_0\eta_{0t} - \frac{1}{H}\eta_{1t} - \frac{1}{H}u_0'\eta_{0x}.$$

Substituting the expression of $E(x,t)$ into (3.53), one has

$$\begin{aligned}
w_1' &= \left(\frac{z^3}{6H} - z^2\frac{1+H}{2H} + z\frac{2H^2+6H+3}{6H} - \frac{2H^2+3H+1}{6H}\right)\eta_{0xxt} \\
&\quad - \frac{z-1-H}{H^2}(\eta_0\eta_{0t} + H\eta_{1t} + Hu_0'\eta_{0x}).
\end{aligned} \qquad (3.54)$$

Taking the derivative of (3.45) with respect to t and then using (3.54), one has

$$\begin{aligned}
-u_{1xt}' &= \left(\frac{z^2}{2H} - z\frac{1+H}{H} + \frac{2H^2+6H+3}{6H}\right)\eta_{0xxtt} \\
&\quad - \frac{1}{H^2}(\eta_0\eta_{0t})_t - \frac{1}{H}\eta_{1tt} - \frac{1}{H}(u_0'\eta_{0x})_t
\end{aligned} \qquad (3.55)$$

Substituting (3.52) and (3.55) into (3.49), one obtains

$$\begin{aligned}
&\eta_{1tt} - \frac{1-r}{1+\frac{r}{H}}\eta_{1xx} - \frac{\frac{rH+1}{3}}{1+\frac{r}{H}}\eta_{0xxtt} + \frac{\frac{r}{H^2}-1}{1+\frac{r}{H}}(\eta_0\eta_{0t})_t \\
&+ \frac{1}{1+\frac{r}{H}}(u_0\eta_{0x} + \frac{r}{H}u_0'\eta_{0x})_t + \frac{1}{1+\frac{r}{H}}(u_0\eta_{0t} + \frac{r}{H}u_0'\eta_{0t})_x = 0 \text{ on } z=1. (3.56)
\end{aligned}$$

Let us now summarize some of the results obtained at orders $O(1)$ and $O(\alpha)$:

$$
\begin{aligned}
u_{1z} = w_{0x} &= z\eta_{0xt} \quad \text{in } 0 < z < 1 + \alpha\eta, \\
p_{1z} = -w_{0t} &= -z\eta_{0tt} \quad \text{in } 0 < z < 1 + \alpha\eta, \\
w_{1z} &= -u_{1x} \quad \text{in } 0 < z < 1 + \alpha\eta, \\
u'_{1z} = w'_{0x} &= \frac{-z+1+H}{H}\eta_{0xt} \quad \text{in } 1 + \alpha\eta < z < 1 + H, \\
p'_{1z} = -rw'_{0t} &= -r\frac{-z+1+H}{H}\eta_{0tt} \quad \text{in } 1 + \alpha\eta < z < 1 + H, \\
w'_{1z} &= -u'_{1x} \quad \text{in } 1 + \alpha\eta < z < 1 + H.
\end{aligned}
\tag{3.57}
$$

At order $O(\alpha^2)$ one has the following 13 equations (the expressions inside the big brackets are obtained by using the previous results written in (3.35) and (3.57))

$$
\begin{aligned}
u_{2t} + (u_0 u_1)_x + w_0 u_{1z} &= -p_{2x} \quad \text{in } 0 < z < 1 + \alpha\eta, &(3.58) \\
&= \left(u_{2t} + (u_0 u_1)_x + z^2 \eta_{0t}\eta_{0xt} \right) \\
w_{1t} + u_0 w_{0x} &= -p_{2z} \quad \text{in } 0 < z < 1 + \alpha\eta, &(3.59) \\
u_{2x} + w_{2z} &= 0 \quad \text{in } 0 < z < 1 + \alpha\eta, &(3.60) \\
w_2 &= 0 \quad \text{on } z = 0, &(3.61) \\
-\eta_1 w_{0z} - \eta_0 w_{1z} + \eta_{2t} + u_0 \eta_{1x} + u_1 \eta_{0x} &= w_2 \quad \text{on } z = 1, &(3.62) \\
\left(-\eta_1 \eta_{0t} + \eta_0 u_{1x} + \eta_{2t} + u_0 \eta_{1x} + u_1 \eta_{0x} \right) &= \\
(r-1)\eta_2 + (p_2 - p'_2) + \eta_0(p_{1z} - p'_{1z}) &= 0 \quad \text{on } z = 1, &(3.63) \\
\left((r-1)\eta_2 + (p_2 - p'_2) - (1-r)\eta_0 \eta_{0tt} \right) &= \\
u_{2z} - w_{1x} &= 0 \quad \text{in } 0 < z < 1 + \alpha\eta, &(3.64) \\
u'_{2t} + (u'_0 u'_1)_x + w'_0 u'_{1z} &= -\frac{p'_{2x}}{r} \quad \text{in } 1 + \alpha\eta < z < 1 + H, \\
\left(u'_{2t} + (u'_0 u'_1)_x + (\frac{-z+1+H}{H})^2 \eta_{0t}\eta_{0xt} \right) &= &(3.65) \\
w'_{1t} + u'_0 w'_{0x} &= -\frac{p'_{2z}}{r} \quad \text{in } 1 + \alpha\eta < z < 1 + H, \\
\left(w'_{1t} + \frac{-z+1+H}{H}u'_0 \eta_{0xt} - \frac{-z+1+H}{H^2}\eta_{0t}^2 \right) &= &(3.66) \\
u'_{2x} + w'_{2z} &= 0 \text{ in } 1 + \alpha\eta < z < 1 + H, &(3.67) \\
w'_2 &= 0 \quad \text{on } z = 1 + H, &(3.68) \\
\eta_1 w'_{0z} - \eta_0 w'_{1z} + \eta_{2t} + u'_0 \eta_{1x} + u'_1 \eta_{0x} &= w'_2 \quad \text{on } z = 1, &(3.69)
\end{aligned}
$$

$$\left(-\frac{1}{H}\eta_1\eta_{0t} + \eta_0 u'_{1x} + \eta_{2t} + u'_0\eta_{1x} + u'_1\eta_{0x}\right) =$$

$$u'_{2z} - w'_{1x} = 0 \text{ in } 1 + \alpha\eta < z < 1 + H. \quad (3.70)$$

Taking the derivation of equation (3.63) with respect to x, one has

$$(r-1)\eta_{2x} = (-p_2 + p'_2)_x + (1-r)(\eta_0\eta_{0tt})_x \quad \text{on } z = 1.$$

Substituting (3.58) and (3.65) into the previous equation, one has

$$(r-1)\eta_{2x} = u_{2t} - ru'_{2t} + (u_0u_1 - ru'_0u'_1)_x$$
$$+(1-r)\eta_{0t}\eta_{0xt} + (1-r)(\eta_0\eta_{0tt})_x \quad \text{on } z = 1.$$

Taking the derivation of the previous equation with respect to x, one has

$$(r-1)\eta_{2xx} = u_{2xt} - ru'_{2xt} + (u_0u_1 - ru'_0u'_1)_{xx}$$
$$+(1-r)(\eta_{0t}\eta_{0xt})_x + (1-r)(\eta_0\eta_{0tt})_{xx} \quad \text{on } z = 1. \quad (3.71)$$

Taking the derivation of (3.60) with respect to z gives

$$w_{2zz} = -u_{2xz}$$
$$= -w_{1xx} \text{ (using (3.64))}.$$

Taking the derivation of (3.51) twice with respect to x and then substituting into the previous equation, one obtains

$$w_{2zz} = (\frac{z^3}{6} - \frac{z}{6})\eta_{0xxxxt} + z(\eta_0\eta_{0t} - \eta_{1t} - u_0\eta_{0x})_{xx}.$$

Integrating this equation twice with respect to z gives

$$w_2 = (\frac{z^5}{120} - \frac{z^3}{36})\eta_{0xxxxt} + \frac{z^3}{6}(\eta_0\eta_{0t} - \eta_{1t} - u_0\eta_{0x})_{xx}$$
$$+zG(x,t) + J(x,t), \quad (3.72)$$

where $G(x,t)$ and $J(x,t)$ are arbitrary functions of x and t.

Applying (3.72) to (3.61) yields

$$J(x,t) = 0.$$

Applying (3.72) to (3.62) yields

$$-\frac{7}{360}\eta_{0xxxxt} + \frac{1}{6}(\eta_0\eta_{0t} - \eta_{1t} - u_0\eta_{0x})_{xx} + G(x,t)$$
$$= -\eta_1\eta_{0t} + \eta_0 u_{1x} + \eta_{2t} + u_0\eta_{1x} + u_1\eta_{0x}.$$

Consequently

$$G(x,t) = \frac{7}{360}\eta_{0xxxxt} - \frac{1}{6}(\eta_0\eta_{0t} - \eta_{1t} - u_0\eta_{0x})_{xx}$$
$$- \eta_1\eta_{0t} + \eta_0 u_{1x} + \eta_{2t} + u_0\eta_{1x} + u_1\eta_{0x}.$$

Substituting the expressions of $G(x,t)$ and $J(x,t)$ into (3.72) yields the expression for w_2. Taking the derivative of this expression twice with respect to z and t and using (3.60), one has

$$u_{2xt} = \frac{1}{45}\eta_{0xxxxtt} - \frac{1}{3}(\eta_0\eta_{0t} - \eta_{1t} - u_0\eta_{0x})_{xxt}$$
$$+(\eta_1\eta_{0t})_t - (\eta_0 u_{1x})_t - \eta_{2tt} - (u_0\eta_{1x})_t - (u_1\eta_{0x})_t, \quad \text{on } z = 1. \quad (3.73)$$

Using the same arguments, one looks for the expression of u'_{2xt}.

Taking the derivative of (3.67) with respect to z, one has

$$w'_{2zz} = -u'_{2xz}$$
$$= -w'_{1xx} \text{ (using (3.70))}.$$

Taking the derivative of equation (3.54) twice with respect to x and then substituting into the previous equation, one obtains

$$-w'_{2zz} = \left(\frac{z^3}{6H} - z^2\frac{1+H}{2H} + z\frac{2H^2+6H+3}{6H} - \frac{2H^2+3H+1}{6H}\right)\eta_{0xxxxt}$$
$$- \frac{z-1-H}{H^2}(\eta_0\eta_{0t} + H\eta_{1t} + Hu'_0\eta_{0x})_{xx}.$$

Integrating this equation twice with respect to z, one has

$$-w'_2 = \left(\frac{z^5}{120H} - z^4\frac{1+H}{24H} + z^3\frac{2H^2+6H+3}{36H} - z^2\frac{2H^2+3H+1}{12H}\right)\eta_{0xxxxt}$$
$$- \left(\frac{z^3}{6H^2} - z^2\frac{1+H}{2H^2}\right)(\eta_0\eta_{0t} + H\eta_{1t} + Hu'_0\eta_{0x})_{xx} + zI(x,t) + K(x,t),$$

where $I(x,t)$ and $K(x,t)$ are arbitrary functions of x and t.

Applying the previous equation to (3.68), one obtains

$$K(x,t) = -\frac{2H^5 - 15H^3 - 25H^2 - 15H - 3}{90H}\eta_{0xxxxt}$$
$$-\frac{(1+H)^3}{3H^2}(\eta_0\eta_{0t} + H\eta_{1t} + Hu_0'\eta_{0x})_{xx} - (1+H)I(x,t).$$

Substituting the value of $K(x,t)$ into the expression of w_2', one obtains

$$-w_2' = \left(\frac{z^5}{120H} - z^4\frac{1+H}{24H} + z^3\frac{2H^2 + 6H + 3}{36H} - z^2\frac{2H^2 + 3H + 1}{12H}\right.$$
$$\left. -\frac{2H^5 - 15H^3 - 25H^2 - 15H - 3}{90H}\right)\eta_{0xxxxt} \qquad (3.74)$$
$$-\left(\frac{z^3}{6H^2} - z^2\frac{1+H}{2H^2} + \frac{(1+H)^3}{3H^2}\right)(\eta_0\eta_{0t} + H\eta_{1t} + Hu_0'\eta_{0x})_{xx}$$
$$+(z - 1 - H)I(x,t).$$

Applying the previous equation to (3.69), one obtains

$$I(x,t) = -\frac{8H^4 - 60H^2 - 60H - 15}{360H}\eta_{0xxxxt}$$
$$-\frac{2H^2 + 6H + 3}{6H^2}(\eta_0\eta_{0t} + H\eta_{1t} + Hu_0'\eta_{0x})_{xx}$$
$$+\frac{1}{H}\eta_0u_{1x}' + \frac{1}{H^2}\eta_1\eta_{0t} + \frac{1}{H}\eta_{2t} + \frac{1}{H}u_0'\eta_{1x} + \frac{1}{H}u_1'\eta_{0x}.$$

Substituting the expression of $I(x,t)$ into (3.74), one obtains the expression of w_2'. Taking the deriving twice of it with respect to z and t, then using the derivative with respect to x of (3.67), one has

$$u_{2xt}' = -\frac{H^3}{45}\eta_{0xxxxtt} - \frac{1}{3}(\eta_0\eta_{0t} + H\eta_{1t} + Hu_0'\eta_{0x})_{xxt}$$
$$+\frac{1}{H}(\eta_0u_{1x}')_t + \frac{1}{H^2}(\eta_1\eta_{0t})_t + \frac{1}{H}\eta_{2tt} + \frac{1}{H}(u_0'\eta_{1x})_t + \frac{1}{H}(u_1'\eta_{0x})_t$$
$$\text{on } z = 1. \qquad (3.75)$$

Substituting (3.73) and (3.75) into (3.71), one has

$$\eta_{2tt} - \frac{1-r}{1+\frac{r}{H}}\eta_{2xx} - \frac{1}{1+\frac{r}{H}}(u_0u_1 - ru_0'u_1')_{xx} - \frac{1-r}{1+\frac{r}{H}}(\eta_{0t}\eta_{0xt})_x$$

$$-\frac{\frac{1+rH}{3}}{1+\frac{r}{H}}\eta_{1xxtt} + \frac{\frac{r}{H^2}-1}{1+\frac{r}{H}}(\eta_1\eta_{0t})_t \tag{3.76}$$

$$+\frac{1}{1+\frac{r}{H}}(u_0\eta_{1x} + \frac{r}{H}u_0'\eta_{1x})_t + \frac{1}{1+\frac{r}{H}}(u_1\eta_0 + \frac{r}{H}u_1'\eta_0)_{xt}$$

$$-\frac{\frac{1}{45}+\frac{rH^3}{45}}{1+\frac{r}{H}}\eta_{0xxxxtt} + \frac{\frac{1-r}{3}}{1+\frac{r}{H}}(\eta_0\eta_{0t})_{xxt} - \frac{1-r}{1+\frac{r}{H}}(\eta_0\eta_{0tt})_{xx}$$

$$-\frac{\frac{1}{3}}{1+\frac{r}{H}}(u_0\eta_{0x} + rHu_0'\eta_{0x})_{xxt} \quad = \quad 0 \quad \text{on } z = 1.$$

After solving the problem at orders $O(1)$, $O(\alpha)$ and $O(\alpha^2)$, it is now possible to combine the results in order to obtain an equation in terms of the initial variables.

Combining equations (3.34) with α times equation (3.56) and α^2 times equation (3.76), one has:

$$\eta_{tt} - \frac{1-r}{1+\frac{r}{H}}\eta_{xx} + \frac{\alpha}{1+\frac{r}{H}}(u_0\eta_{0t} + \frac{r}{H}u_0'\eta_{0t})_x \tag{3.77}$$

$$-\frac{\alpha^2}{1+\frac{r}{H}}(u_0u_1 - ru_0'u_1')_{xx} - \frac{\alpha^2(1-r)}{1+\frac{r}{H}}(\eta_{0t}\eta_{0xt})_x - \frac{\alpha^2(1-r)}{1+\frac{r}{H}}(\eta_0\eta_{0tt})_{xx}$$

$$+\frac{\alpha}{1+\frac{r}{H}}(u_0\eta_{0x} + \frac{r}{H}u_0'\eta_{0x} + \alpha u_0\eta_{1x} + \alpha\frac{r}{H}u_0'\eta_{1x})_t + \alpha\frac{\frac{r}{H^2}-1}{1+\frac{r}{H}}(\eta_0\eta_{0t} + \alpha\eta_1\eta_{0t})_t$$

$$+\frac{\alpha^2}{1+\frac{r}{H}}(u_1\eta_0 + \frac{r}{H}u_1'\eta_0)_{xt} - \alpha\frac{\frac{1+rH}{3}}{1+\frac{r}{H}}\eta_{0xxtt} - \alpha^2\frac{\frac{1+rH}{3}}{1+\frac{r}{H}}\eta_{1xxtt}$$

$$-\frac{\frac{\alpha^2}{45}+\frac{\alpha^2rH^3}{45}}{1+\frac{r}{H}}\eta_{0xxxxtt} + \alpha^2\frac{\frac{1-r}{3}}{1+\frac{r}{H}}(\eta_0\eta_{0t})_{xxt} - \frac{\alpha^2}{1+\frac{r}{H}}(\frac{1}{3}u_0\eta_{0x} + \frac{rH}{3}u_0'\eta_{0x})_{xxt} = 0$$

$$\text{on } z = 1.$$

Combining (3.32) with α times (3.52) and α^2 times (3.73), then integrating the result with respect to t yields

$$u_x = -\eta_t + \alpha\left(\frac{1}{3}\eta_{0xxt} + \eta_0\eta_{0t} - u_0\eta_{0x}\right)$$

$$+\alpha^2\left(\frac{1}{45}\eta_{0xxxxt} - \frac{1}{3}(\eta_0\eta_{0t} - \eta_{1t} - u_0\eta_{0x})_{xx}\right) \tag{3.78}$$

$$+\eta_1\eta_{0t} - \eta_0u_{1x} - u_0\eta_{1x} - u_1\eta_{0x}\right) \quad \text{on } z = 1.$$

Similarly, combining (3.33) with α times (3.55) and α^2 times (3.75) and then inte-

grating the result with respect to t yield

$$u'_x = \frac{1}{H}\eta_t + \alpha\left(-\frac{H}{3}\eta_{0xxt} + \frac{1}{H^2}\eta_0\eta_{0t} + \frac{1}{H}u'_0\eta_{0x}\right) \tag{3.79}$$
$$+\alpha^2\left(-\frac{H^3}{45}\eta_{0xxxxt} - \frac{1}{3}(\eta_0\eta_{0t} + H\eta_{1t} + Hu'_0\eta_{0x})_{xx} + \frac{1}{H}\eta_0u'_{1x}\right.$$
$$\left.+\frac{1}{H^2}\eta_1\eta_{0t} + \frac{1}{H}u'_0\eta_{1x} + \frac{1}{H}u'_1\eta_{0x}\right) \qquad \text{on } z = 1.$$

Equations (3.77)–(3.79) contain a part of the decomposition of u as u_0, u_1; a part of the decomposition of u' as u'_0, u'_1 and a part of the decomposition of η as η_0, η_1. It is shown in Appendix A how to go back from the variables u_0, u_1, u'_0, u'_1, η_0 and η_1 to u, u' and η. One obtains the following equations for modelling the waves at the interface.

$$\eta_{tt} - \frac{1-r}{1+\frac{r}{H}}\eta_{xx} - \frac{\alpha}{1+\frac{r}{H}}(uu_x - ru'u'_x)_x + \frac{\alpha}{1+\frac{r}{H}}(u\eta + \frac{r}{H}u'\eta)_{xt}$$
$$+\frac{\frac{1}{3}\alpha}{1+\frac{r}{H}}(u - rH^2u')_{xxxt} - \frac{\alpha^2}{1+\frac{r}{H}}(u_xu_{xx} - rH^2u'_xu'_{xx})_x \tag{3.80}$$
$$+\frac{\alpha^2}{1+\frac{r}{H}}(\eta u_{xt} + rH\eta u'_{xt})_{xx} + \frac{\frac{2}{15}\alpha^2}{1+\frac{r}{H}}(u - rH^4u')_{xxxxxt} = 0,$$

$$u_x = -\eta_t + \alpha\frac{1}{3}\eta_{xxt} - \alpha(u\eta)_x + \alpha^2\frac{1}{45}\eta_{xxxxt} - \alpha^2\frac{1}{3}(\eta\eta_t - u\eta_x)_{xx}, \tag{3.81}$$

$$u'_x = \frac{1}{H}\eta_t - \alpha\frac{H}{3}\eta_{xxt} + \alpha\frac{1}{H}(\eta u')_x - \alpha^2\frac{H^3}{45}\eta_{xxxxt} - \alpha^2\frac{1}{3}(\eta\eta_t + Hu'\eta_x)_{xx}. \tag{3.82}$$

3.3 Remarks

The limit $r = 0$ and $H = 1$ corresponds to a one layer fluid. The equation (3.80) recovers the model (3.39) proposed by Daripa (2006) [17] (when surface tension is ignored and α is equal to β) for modelling water waves.

The combination of equation (3.34) and α times equation (3.56) for a one layer fluid recovers the model (3.41) proposed by Johnson (1997) [31] for water waves, which is correct up to order $O(\alpha)$.

Note that, the system of three equations (3.80)–(3.82) is written with horizontal velocities at the interface. It is not appropriate for numerical simulations, as explained at the end of section 4.3. However, from this system, one can obtain other systems written with arbitrary horizontal velocities, which can be studied numerically. The technique to do this will be shown in the next chapter.

In the next chapter, we will use another method to model the problem at hand. A system of three equations free of the assumption $\alpha = \beta$ will be obtained. This system is written with horizontal velocities at the bottom and at the roof. We will demonstrate that it is formally equivalent to system (3.80)–(3.82) in the case $\alpha = \beta$.

Chapter 4

Boussinesq systems for interfacial waves

In this chapter, an asymptotic expansion method will be used to derive two model systems for interfacial waves of the configuration described at the beginning of chapter 3. The first model system contains quadratic nonlinear terms. The second one contains both quadratic and cubic nonlinear terms. It corresponds to the case where the square of thickness ratio is close to the density ratio. Comparison between the Boussinesq system with quadratic nonlinear terms and the system of three equations obtained in the previous chapter will be also established.

4.1 Governing equations

In this section, the origin of the systems of partial differential equations that will be derived at the end of this chapter is explained. The methods are standard, but to my knowledge some of these equations are derived for the first time.

As the flows are assumed to be irrotational, one is dealing with potential flows. Velocity potentials $\phi^* = \phi^*((x^*, z^*), t^*)$ in Ω_{t^*} and $\phi^{*'} = \phi^{*'}((x^*, z^*), t^*)$ in Ω'_{t^*} are introduced, so that the velocity vectors $\mathbf{v}^*$ and $\mathbf{v}^{*'}$ are given by

$$\mathbf{v}^* = \nabla \phi^*, \tag{4.1}$$

$$\mathbf{v}^{*'} = \nabla \phi^{*'}. \tag{4.2}$$

Writing the continuity equations in each layer leads to

$$\phi^*_{x^*x^*} + \phi^*_{z^*z^*} = 0 \quad \text{for} \quad -h < z^* < \eta^*(x^*, t^*), \tag{4.3}$$
$$\phi^{*\prime}_{x^*x^*} + \phi^{*\prime}_{z^*z^*} = 0 \quad \text{for} \quad \eta^*(x^*, t^*) < z^* < h'. \tag{4.4}$$

The boundary of the system $\{\Omega_{t^*}, \Omega'_{t^*}\}$ has two parts: the flat bottom $z^* = -h$ and the flat roof $z^* = h'$. The impermeability conditions along these rigid boundaries give

$$\phi^*_{z^*} = 0 \quad \text{at} \quad z^* = -h, \tag{4.5}$$
$$\phi^{*\prime}_{z^*} = 0 \quad \text{at} \quad z^* = h'. \tag{4.6}$$

The kinematic conditions along the interface, namely $D(\eta^* - z^*)/Dt^* = 0$, give

$$\eta^*_{t^*} = \phi^*_{z^*} - \phi^*_x \eta^*_x \quad \text{at} \quad z^* = \eta^*(x^*, t^*), \tag{4.7}$$
$$\eta^*_{t^*} = \phi^{*\prime}_{z^*} - \phi^{*\prime}_x \eta^*_x \quad \text{at} \quad z^* = \eta^*(x^*, t^*). \tag{4.8}$$

The dynamic boundary condition imposed on the interface, namely the continuity of pressure since surface tension effects are neglected, gives

$$\rho \left(\frac{\partial \phi^*}{\partial t^*} + \frac{1}{2} |\nabla \phi^*|^2 + g z^* \right) = \rho' \left(\frac{\partial \phi^{*\prime}}{\partial t^*} + \frac{1}{2} |\nabla \phi^{*\prime}|^2 + g z^* \right) \quad \text{at} \quad z^* = \eta^*(x^*, t^*), \tag{4.9}$$

where g is the acceleration due to gravity.

The system of seven equations (4.3)–(4.9) represents the starting model for the study of wave propagation at the interface between two fluids. Combined with initial conditions or periodicity conditions, it is the classical interfacial wave problem, which has been studied for more than a century. A nice feature of this formulation is that the pressures in both layers have been removed. In some cases, it is advantageous to keep the pressures in the equations. For example, Bridges & Donaldson (2007) [10] in their study of the criticality of two-layer flows provide an appendix on the inclusion of the lid pressure in the calculation of uniform flows. In the next sections, we will derive simplified models based on certain additional assumptions on wave amplitude, wavelength and fluid depth.
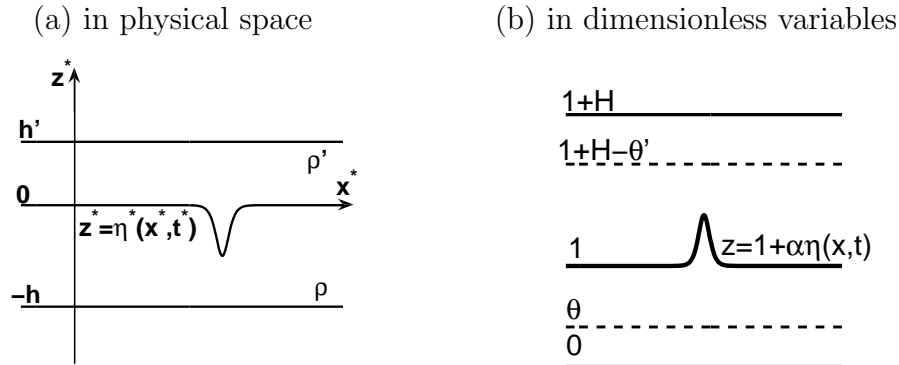
Figure 4.1: Sketch of solitary waves propagating at the interface between two fluid layers with different densities ρ' and ρ. The roof and the bottom of the fluid domain are flat and rigid boundaries, located respectively at $z^* = h'$ and $z^* = -h$. (a) Sketch of a solitary wave of depression in physical space; (b) Sketch of a solitary wave of elevation in dimensionless coordinates, with the thickness h of the bottom layer taken as unit length and the long wave speed c as unit velocity. The dashed lines represent arbitrary fluid levels θ and $1 + H - \theta'$ in each layer. The dimensionless number H is equal to h'/h.

4.2   System of three equations in the limit of long, weakly dispersive waves

The derivation follows closely that of Bona et al. (2002) [5] for a single layer. Let introduce two small parameters

$$\alpha = \frac{A}{h} \ll 1, \quad \beta = \frac{h^2}{\ell^2} \ll 1$$

as well as Stokes number

$$S_t = \frac{\alpha}{\beta} = \frac{A\ell^2}{h^3} \approx 1,$$

where A is typical amplitude, ℓ is typical wavelength and h is the depth of the bottom layer. As mention in section 3.2 one can chose the depth of the roof layer as reference depth. The assumption that the ratio of liquid depths is neither too small nor too large is also made.

The procedure is most transparent when working with the variables scaled in such a way that the dependent quantities appearing in the problem are all of order one, while the assumptions about small amplitude and long wavelength appear explicitly

connected with small parameters in the equations of motion. Such consideration leads to the scaled, dimensionless variables

$$x^* = \ell x, \quad z^* = h(z-1), \quad \eta^* = A\eta, \quad t^* = \ell t/c_0, \quad \phi^* = gA\ell\phi/c_0, \quad \phi^{*'} = gA\ell\phi'/c_0, \tag{4.10}$$

where $c_0 = \sqrt{gh}$. The speed c_0, which represents the long wave speed in the limit $r \to 0$, is not necessarily the most natural choice for interfacial waves. The natural choice would be to take

$$c_0 = \sqrt{gh}\sqrt{\frac{1-r}{1+r/H}},$$

which is the speed of long waves in the configuration shown in Figure 4.1. It does not matter for the asymptotic expansions to be performed later.

In these new variables, the set of equations (4.3)–(4.9) becomes after reordering

$$\beta\phi_{xx} + \phi_{zz} = 0 \quad \text{in } 0 < z < 1+\alpha\eta, \tag{4.11}$$

$$\phi_z = 0 \quad \text{on } z = 0, \tag{4.12}$$

$$\eta_t + \alpha\phi_x\eta_x - \frac{1}{\beta}\phi_z = 0 \quad \text{on } z = 1+\alpha\eta, \tag{4.13}$$

$$\beta\phi'_{xx} + \phi'_{zz} = 0 \quad \text{in } 1+\alpha\eta < z < 1+H, \tag{4.14}$$

$$\phi'_z = 0 \quad \text{on } z = 1+H, \tag{4.15}$$

$$\eta_t + \alpha\phi'_x\eta_x - \frac{1}{\beta}\phi'_z = 0 \quad \text{on } z = 1+\alpha\eta, \tag{4.16}$$

$$\left(\eta + \phi_t + \frac{1}{2}\alpha\phi_x^2 + \frac{1}{2}\frac{\alpha}{\beta}\phi_z^2\right) = r\left(\eta + \phi'_t + \frac{1}{2}\alpha\phi'^2_x + \frac{1}{2}\frac{\alpha}{\beta}\phi'^2_z\right) \quad \text{on } z = 1+\alpha\eta. \tag{4.17}$$

One represents the potential ϕ as a formal expansion

$$\phi((x,z),t) = \sum_{m=0}^{\infty} f_m(x,t)z^m. \tag{4.18}$$

Demanding that ϕ formally satisfy Laplace's equation (4.11) leads to

$$\beta\sum_{m=0}^{\infty}\left(f_m(x,t)\right)_{xx}z^m + \sum_{m=2}^{\infty} m(m-1)f_m(x,t)z^{m-2} = 0.$$

One deduces from the previous equation the recurrence relation

$$(m+2)(m+1)f_{m+2}(x,t) = -\beta\left(f_m(x,t)\right)_{xx}, \quad \forall m = 0, 1, 2, \ldots. \tag{4.19}$$

Let $F(x,t) = f_0(x,t)$ denote the velocity potential at the bottom $z = 0$ and use (4.19) repeatedly to obtain

$$f_{2k}(x,t) = \frac{(-1)^k \beta^k}{(2k)!} \frac{\partial^{2k} F(x,t)}{\partial x^{2k}}, \quad \forall k = 0, 1, 2, \ldots,$$

$$f_{2k+1}(x,t) = \frac{(-1)^k \beta^k}{(2k+1)!} \frac{\partial^{2k} f_1(x,t)}{\partial x^{2k}}, \quad \forall k = 0, 1, 2, \ldots. \tag{4.20}$$

Inserting (4.18) into the boundary condition (4.12) yields

$$f_1(x,t) + \sum_{m=2}^{\infty} m f_m(x,t) z^{m-1} = 0 \quad \text{on } z = 0.$$

It results

$$f_1(x,t) = 0.$$

Consequently, it follows from (4.20) that

$$f_{2k+1}(x,t) = 0, \quad \forall k = 0, 1, 2, \ldots$$

Therefore

$$\phi(x, z, t) = \sum_{k=0}^{\infty} \frac{(-1)^k \beta^k}{(2k)!} \frac{\partial^{2k} F(x,t)}{\partial x^{2k}} z^{2k}.$$

The following expressions show some partial derivatives with respect to time or space of ϕ at the interface, which are useful later on.

$$\begin{aligned}
\phi_x|_{z=1+\alpha\eta} &= \sum_{k=0}^{\infty} \frac{(-1)^k \beta^k}{(2k)!} \frac{\partial^{2k+1} F(x,t)}{\partial x^{2k+1}} z^{2k}|_{z=1+\alpha\eta} \\
&= \frac{\partial F}{\partial x} + \left[-\frac{1}{2}\beta \frac{\partial^3 F}{\partial x^3}(1+\alpha\eta)^2 \right] + O(\beta^2) \\
&= \frac{\partial F}{\partial x} - \frac{1}{2}\beta \frac{\partial^3 F}{\partial x^3} + O(\beta^2),
\end{aligned} \tag{4.21}$$

$$\begin{aligned}
\phi_t|_{z=1+\alpha\eta} &= \sum_{k=0}^{\infty} \frac{(-1)^k \beta^k}{(2k)!} \frac{\partial^{2k+1} F(x,t)}{\partial x^{2k} \partial t} z^{2k}|_{z=1+\alpha\eta} \\
&= \frac{\partial F}{\partial t} + \left[-\frac{1}{2}\beta \frac{\partial^3 F}{\partial x^2 \partial t}(1+\alpha\eta)^2 \right] + \left[\frac{1}{24}\beta^2 \frac{\partial^5 F}{\partial x^4 \partial t}(1+\alpha\eta)^4 \right] + O(\beta^3) \\
&= \frac{\partial F}{\partial t} - \frac{1}{2}\beta \frac{\partial^3 F}{\partial x^2 \partial t} - \alpha\beta\eta \frac{\partial^3 F}{\partial x^2 \partial t} + \frac{1}{24}\beta^2 \frac{\partial^5 F}{\partial x^4 \partial t} + O(\beta^3),
\end{aligned} \tag{4.22}$$

$$\phi_z|_{z=1+\alpha\eta} = \sum_{k=0}^{\infty} \frac{(-1)^{k+1}\beta^{k+1}}{(2k+1)!} \frac{\partial^{2k+2} F(x,t)}{\partial x^{2k+2}} z^{2k+1}|_{z=1+\alpha\eta}$$

$$= -\beta\frac{\partial^2 F}{\partial x^2}(1+\alpha\eta) + \left[\frac{1}{6}\beta^2\frac{\partial^4 F}{\partial x^4}(1+\alpha\eta)^3\right] \tag{4.23}$$

$$+ \left[-\frac{1}{120}\beta^3\frac{\partial^6 F}{\partial x^6}(1+\alpha\eta)^5\right] + O(\beta^4)$$

$$= -\beta\frac{\partial^2 F}{\partial x^2} - \alpha\beta\eta\frac{\partial^2 F}{\partial x^2} + \frac{1}{6}\beta^2\frac{\partial^4 F}{\partial x^4} + \frac{1}{2}\alpha\beta^2\eta\frac{\partial^4 F}{\partial x^4} - \frac{1}{120}\beta^3\frac{\partial^6 F}{\partial x^6} + O(\beta^4).$$

Substituting (4.21) and (4.23) into (4.13) yields

$$\eta_t + \alpha\eta_x\left(\frac{\partial F}{\partial x} - \frac{1}{2}\beta\frac{\partial^3 F}{\partial x^3}\right)$$

$$-\frac{1}{\beta}\left(-\beta\frac{\partial^2 F}{\partial x^2} - \alpha\beta\eta\frac{\partial^2 F}{\partial x^2} + \frac{1}{6}\beta^2\frac{\partial^4 F}{\partial x^4} + \frac{1}{2}\alpha\beta^2\eta\frac{\partial^4 F}{\partial x^4} - \frac{1}{120}\beta^3\frac{\partial^6 F}{\partial x^6}\right) + O(\beta^3) = 0.$$

Let call $\partial F(x,t)/\partial x = u(x,t)$; $u(x,t)$ is the horizontal velocity at the bottom. The previous equation can be written in the form

$$\eta_t + \alpha\eta_x u - \frac{1}{2}\alpha\beta\eta_x u_{xx} + u_x + \alpha\eta u_x$$

$$-\frac{1}{6}\beta u_{xxx} - \frac{1}{2}\alpha\beta\eta u_{xxx} + \frac{1}{120}\beta^2 u_{xxxxx} + O(\beta^3) = 0.$$

or equivalently

$$\eta_t + u_x + \alpha(u\eta)_x - \frac{1}{6}\beta u_{xxx} - \frac{1}{2}\alpha\beta\eta_x u_{xx}$$

$$-\frac{1}{2}\alpha\beta\eta u_{xxx} + \frac{1}{120}\beta^2 u_{xxxxx} + O(\beta^3) = 0. \tag{4.24}$$

Similarly, one presents the potential ϕ' as a formal expansion

$$\phi'(x,z,t) = \sum_{m=0}^{\infty} f'_m(x,t)(1+H-z)^m. \tag{4.25}$$

Demanding that ϕ' formally satisfy Laplace's equation (4.14) leads to

$$\beta\sum_{m=0}^{\infty}\left(f'_m(x,t)\right)_{xx}(1+H-z)^m + \sum_{m=2}^{\infty} m(m-1)f'_m(x,t)(1+H-z)^{m-2} = 0.$$

One deduces from the previous equation the recurrence relation

$$(m+2)(m+1)f'_{m+2}(x,t) = -\beta\Big(f'_m(x,t)\Big)_{xx}, \quad \forall m = 0,1,2,... \tag{4.26}$$

Let $F'(x,t) = f'_0(x,t)$ denote the velocity potential at the roof $z = 1 + H$ and use (4.26) repeatedly to obtain

$$f'_{2k}(x,t) = \frac{(-1)^k \beta^k}{2k!} \frac{\partial^{2k} F'(x,t)}{\partial x^{2k}}, \quad \forall k = 0,1,2,...$$

$$f'_{2k+1}(x,t) = \frac{(-1)^k \beta^k}{(2k+1)!} \frac{\partial^{2k} f'_1(x,t)}{\partial x^{2k}}, \quad \forall k = 0,1,2,.... \tag{4.27}$$

Inserting (4.25) into the boundary condition (4.15) implies that

$$f'_1(x,t) = 0.$$

Consequently, it follows from (4.27) that

$$f'_{2k+1}(x,t) = 0, \quad \forall k = 0,1,2,\ldots,$$

Therefore

$$\phi'((x,z),t) = \sum_{k=0}^{\infty} \frac{(-1)^k \beta^k}{(2k)!} \frac{\partial^{2k} F'(x,t)}{\partial x^{2k}} (1+H-z)^{2k}.$$

The following expressions show some derivatives of ϕ' with respect to time or space at the interface. They will be useful later on

$$\begin{aligned}
\phi'_x|_{z=1+\alpha\eta} &= \sum_{k=0}^{\infty} \frac{(-1)^k \beta^k}{(2k)!} \frac{\partial^{2k+1} F'(x,t)}{\partial x^{2k+1}} (1+H-z)^{2k}|_{z=1+\alpha\eta} \\
&= \frac{\partial F'}{\partial x} + \left[-\frac{1}{2}\beta \frac{\partial^3 F'}{\partial x^3}(H-\alpha\eta)^2 \right] + O(\beta^2) \\
&= \frac{\partial F'}{\partial x} - \frac{1}{2}\beta H^2 \frac{\partial^3 F'}{\partial x^3} + O(\beta^2),
\end{aligned} \tag{4.28}$$

$$\begin{aligned}
\phi'_t|_{z=1+\alpha\eta} &= \sum_{k=0}^{\infty} \frac{(-1)^k \beta^k}{(2k)!} \frac{\partial^{2k+1} F'(x,t)}{\partial x^{2k}\partial t} (1+H-z)^{2k}|_{z=1+\alpha\eta} \\
&= \frac{\partial F'}{\partial t} + \left[-\frac{1}{2}\beta \frac{\partial^3 F'}{\partial^2 x \partial t}(H-\alpha\eta)^2 \right] + \left[\frac{1}{24}\beta^2 \frac{\partial^5 F'}{\partial x^4 \partial t}(H-\alpha\eta)^4 \right] + O(\beta^3) \\
&= \frac{\partial F'}{\partial t} - \frac{1}{2}\beta H^2 \frac{\partial^3 F'}{\partial x^2 \partial t} + \alpha\beta H\eta \frac{\partial^3 F'}{\partial x^2 \partial t} \\
&\quad + \frac{1}{24}\beta^2 H^4 \frac{\partial^5 F'}{\partial x^4 \partial t} + O(\beta^3),
\end{aligned} \tag{4.29}$$

$$\phi'_z|_{z=1+\alpha\eta} = \sum_{k=0}^{\infty} \frac{(-1)^k \beta^{k+1}}{(2k+1)!} \frac{\partial^{2k+2} F'(x,t)}{\partial x^{2k+2}} (1 + H - z)^{2k+1}|_{z=1+\alpha\eta}$$

$$= \beta \frac{\partial^2 F'}{\partial x^2}(H - \alpha\eta) + \left[-\frac{\beta^2}{6} \frac{\partial^4 F'}{\partial x^4}(H - \alpha\eta)^3 \right]$$

$$+ \left[\frac{\beta^3}{120} \frac{\partial^6 F'}{\partial x^6}(H - \alpha\eta)^5 \right] + O(\beta^4)$$

$$= \beta H \frac{\partial^2 F'}{\partial x^2} - \alpha\beta\eta \frac{\partial^2 F'}{\partial x^2} - \frac{1}{6}\beta^2 H^3 \frac{\partial^4 F'}{\partial x^4} + \frac{1}{2}\alpha\beta^2 H^2 \eta \frac{\partial^4 F'}{\partial x^4}$$

$$+ \frac{1}{120}\beta^3 H^5 \frac{\partial^6 F'}{\partial x^6} + O(\beta^4). \tag{4.30}$$

Substituting (4.28) and (4.30) into (4.16), one obtain

$$\eta_t + \alpha\eta_x \left(\frac{\partial F'}{\partial x} - \frac{1}{2}\beta H^2 \frac{\partial^3 F'}{\partial x^3} \right) - \frac{1}{\beta} \left(\beta H \frac{\partial^2 F'}{\partial x^2} - \alpha\beta\eta \frac{\partial^2 F'}{\partial x^2} \right.$$

$$\left. -\frac{1}{6}\beta^2 H^3 \frac{\partial^4 F}{\partial x^4} + \frac{1}{2}\alpha\beta^2 H^2 \eta \frac{\partial^4 F'}{\partial x^4} + \frac{1}{120}\beta^3 H^5 \frac{\partial^6 F'}{\partial x^6} \right) + O(\beta^3) = 0.$$

Let call $\partial F'(x,t)/\partial x = u'(x,t)$; $u'(x,t)$ is the horizontal velocity at the roof. The previous equation can be written in the form

$$\eta_t + \alpha\eta_x u' - \frac{1}{2}\alpha\beta H^2 \eta_x u'_{xx} - Hu'_x + \alpha\eta u'_x + \frac{1}{6}\beta H^3 u'_{xxx}$$

$$-\frac{1}{2}\alpha\beta H^2 \eta u'_{xxx} - \frac{1}{120}\beta^2 H^5 u'_{xxxxx} + O(\beta^3) = 0,$$

or equivalently

$$\eta_t - Hu'_x + \alpha(u'\eta)_x + \frac{1}{6}\beta H^3 u'_{xxx} \tag{4.31}$$

$$-\frac{1}{2}\alpha\beta H^2 \eta_x u'_{xx} - \frac{1}{2}\alpha\beta H^2 \eta u'_{xxx} - \frac{1}{120}\beta^2 H^5 u'_{xxxxx} + O(\beta^3) = 0.$$

It is important at this stage that $H = O(1)$.

Substituting the partial derivatives of ϕ and ϕ' with respect to t, x, z into the dynamic condition (4.17) yields

$$(1 - r)\eta + \left(\frac{\partial F}{\partial t} - \frac{1}{2}\beta \frac{\partial^3 F}{\partial x^2 \partial t} - \alpha\beta\eta \frac{\partial^3 F}{\partial x^2 \partial t} + \frac{1}{24}\beta^2 \frac{\partial^5 F}{\partial x^4 \partial t} \right)$$

$$-r\Big(\frac{\partial F'}{\partial t} - \frac{1}{2}\beta H^2 \frac{\partial^3 F'}{\partial x^2 \partial t} + \alpha\beta H\eta \frac{\partial^3 F'}{\partial x^2 \partial t} + \frac{1}{24}\beta^2 H^4 \frac{\partial^5 F'}{\partial x^4 \partial t}\Big)$$
$$+\frac{\alpha}{2}\Big(\frac{\partial F}{\partial x} - \frac{1}{2}\beta \frac{\partial^3 F}{\partial x^3}\Big)^2 - r\frac{\alpha}{2}\Big(\frac{\partial F'}{\partial x} - \frac{1}{2}\beta H^2 \frac{\partial^3 F'}{\partial x^3}\Big)^2$$
$$+\frac{1}{2}\frac{\alpha}{\beta}\Big(-\beta\frac{\partial^2 F}{\partial x^2}\Big)^2 - \frac{1}{2}r\frac{\alpha}{\beta}\Big(\beta H\frac{\partial^2 F'}{\partial x^2}\Big)^2 + O(\beta^3) \;\; = \;\; 0.$$

Using u and u' instead of $\dfrac{\partial F}{\partial x}$ and $\dfrac{\partial F'}{\partial x}$, the previous equation becomes

$$(1-r)\eta + \frac{\partial F}{\partial t} - r\frac{\partial F'}{\partial t} - \frac{1}{2}\beta u_{xt} + \frac{1}{2}\beta r H^2 u'_{xt}$$
$$-\alpha\beta\eta u_{xt} - \alpha\beta r H\eta u'_{xt} + \frac{1}{24}\beta^2 u_{xxxt} - \frac{1}{24}\beta^2 r H^4 u'_{xxxt} + \frac{1}{2}\alpha(u^2 - \beta u u_{xx})$$
$$-\frac{1}{2}\alpha r(u'^2 - \beta H^2 u' u'_{xx}) + \frac{1}{2}\alpha\beta(u_x^2 - r H^2 u_x'^2) + O(\beta^3) = 0.$$

Taking the derivative with respect to x of this equation, one obtains

$$(1-r)\eta_x + u_t - ru'_t + \alpha(uu_x - ru'u'_x) - \frac{1}{2}\beta u_{xxt} + \frac{1}{2}\beta r H^2 u'_{xxt} \qquad (4.32)$$
$$-\alpha\beta(\eta u_{xt})_x - \alpha\beta r H(\eta u'_{xt})_x + \frac{1}{24}\beta^2 u_{xxxxt} - \frac{1}{24}\beta^2 r H^4 u'_{xxxxt}$$
$$-\frac{1}{2}\alpha\beta(uu_{xx} - rH^2 u'u'_{xx})_x + \alpha\beta(u_x u_{xx} - rH^2 u'_x u'_{xx}) + O(\beta^3) = 0.$$

The three equations (4.24), (4.31) and (4.32) provide a Boussinesq system of equations describing waves at the interface $\eta(x,t)$ between two fluid layers based on the horizontal velocities u and u' along the bottom and the roof, respectively. It is correct up to second order in α, β. In the limit when $r \to 0$ and $H \to 1$, (4.24) and (4.32) recover the model equations (2.19) and (2.20) obtained by Bona et al. (2002) [5] for water waves.

We can derive a class of systems which are formally equivalent to the system we have just derived. This will be accomplished by considering changes in the dependent variables and by making use of lower-order relations in higher-order terms. Toward this goal, begin by letting $w(x,t)$ be the scaled horizontal velocity corresponding to the physical depth $(1-\theta)h$ below the unperturbed interface, and $w'(x,t)$ be the scaled horizontal velocity corresponding to the physical depth $(H-\theta')h$ above the unperturbed interface. The ranges for the parameters θ and θ' are $0 \le \theta \le 1$

and $0 \leq \theta' \leq H$. Note that $(\theta, \theta') = (0,0)$ leads to $w = u$ and $w' = u'$, while $(\theta, \theta') = (1, H)$ leads to both velocities evaluated along the interface. A formal use of Taylor's formula with remainder shows that

$$
\begin{aligned}
w = \phi_x|_{z=\theta} &= \left(F_x - \frac{1}{2}\beta z^2 F_{xxx} + \frac{1}{24}\beta^2 z^4 F_{xxxxx} \right)|_{z=\theta} + O(\beta^3) \\
&= F_x - \frac{1}{2}\beta \theta^2 F_{xxx} + \frac{1}{24}\beta^2 \theta^4 F_{xxxxx} + O(\beta^3) \\
&= u - \frac{1}{2}\beta \theta^2 u_{xx} + \frac{1}{24}\beta^2 \theta^4 u_{xxxx} + O(\beta^3)
\end{aligned}
$$

as $\beta \to 0$. In Fourier space, the latter relationship may be written as

$$
\hat{w} = \left(1 + \frac{1}{2}\beta \theta^2 k^2 + \frac{1}{24}\beta^2 \theta^4 k^4 \right)\hat{u} + O(\beta^3).
$$

Inverting the positive Fourier multiplier yields

$$
\begin{aligned}
\hat{u} &= \left(1 + \frac{1}{2}\beta \theta^2 k^2 + \frac{1}{24}\beta^2 \theta^4 k^4 \right)^{-1}\hat{w} + O(\beta^3) \\
&= \left(1 - \frac{1}{2}\beta \theta^2 k^2 + \frac{5}{24}\beta^2 \theta^4 k^4 \right)\hat{w} + O(\beta^3)
\end{aligned}
$$

as $\beta \to 0$. Thus there appears the relationship

$$
u = w + \frac{1}{2}\beta \theta^2 w_{xx} + \frac{5}{24}\beta^2 \theta^4 w_{xxxx} + O(\beta^3). \tag{4.33}
$$

Similarly

$$
\begin{aligned}
w' &= \phi'_x|_{z=1+H-\theta'} \\
&= \left(F'_x - \frac{1}{2}\beta F'_{xxx}(1+H-z)^2 + \frac{1}{24}\beta^2 F'_{xxxxx}(1+H-z)^4 \right)|_{z=1+H-\theta'} + O(\beta^3) \\
&= F'_x - \frac{1}{2}\beta \theta'^2 F'_{xxx} + \frac{1}{24}\beta^2 \theta'^4 F'_{xxxxx} + O(\beta^3) \\
&= u' - \frac{1}{2}\beta \theta'^2 u'_{xx} + \frac{1}{24}\beta^2 \theta'^4 u'_{xxxx} + O(\beta^3)
\end{aligned}
$$

and

$$
\hat{w}' = \left(1 + \frac{1}{2}\beta \theta'^2 k^2 + \frac{1}{24}\beta^2 \theta'^4 k^4 \right)\hat{u}' + O(\beta^3).
$$

Inverting the positive Fourier multiplier yields

$$
\begin{aligned}
\hat{u}' &= \left(1 + \frac{1}{2}\beta \theta'^2 k^2 + \frac{1}{24}\beta^2 \theta'^4 k^4 \right)^{-1}\hat{w}' + O(\beta^3) \\
&= \left(1 - \frac{1}{2}\beta \theta'^2 k^2 + \frac{5}{24}\beta^2 \theta'^4 k^4 \right)\hat{w}' + O(\beta^3)
\end{aligned}
$$

and thus the relationship

$$u' = w' + \frac{1}{2}\beta\theta'^2 w'_{xx} + \frac{5}{24}\beta^2\theta'^4 w'_{xxxx} + O(\beta^3). \tag{4.34}$$

Substituting (4.33) into (4.24) yields

$$\eta_t + \left(w_x + \frac{1}{2}\beta\theta^2 w_{xxx} + \frac{5}{24}\beta^2\theta^4 w_{xxxxx}\right)$$
$$+\alpha\left(\left(w + \frac{1}{2}\beta\theta^2 w_{xx}\right)\eta\right)_x - \frac{1}{6}\beta\left(w_{xxx} + \frac{1}{2}\beta\theta^2 w_{xxxxx}\right)$$
$$-\frac{1}{2}\alpha\beta\eta_x w_{xx} - \frac{1}{2}\alpha\beta\eta w_{xxx} + \frac{1}{120}\beta^2 w_{xxxxx} + O(\beta^3) = 0,$$

or equivalently

$$\eta_t + w_x + \alpha(w\eta)_x + \frac{1}{2}\beta\left(\theta^2 - \frac{1}{3}\right)w_{xxx}$$
$$+\frac{1}{2}\alpha\beta(\theta^2 - 1)(\eta w_{xx})_x + \frac{5}{24}\beta^2\left(\theta^2 - \frac{1}{5}\right)^2 w_{xxxxx} + O(\beta^3) = 0. \tag{4.35}$$

Substituting (4.34) into (4.31) yields

$$\eta_t - H\left(w'_x + \frac{1}{2}\beta\theta'^2 w'_{xxx} + \frac{5}{24}\beta^2\theta'^4 w'_{xxxxx}\right)$$
$$+\alpha\left(\left(w' + \frac{1}{2}\beta\theta'^2 w'_{xx}\right)\eta\right)_x + \frac{1}{6}\beta H^3\left(w'_{xxx} + \frac{1}{2}\beta\theta'^2 w'_{xxxxx}\right)$$
$$-\frac{1}{2}\alpha\beta H^2\eta_x w'_{xx} - \frac{1}{2}\alpha\beta H^2\eta w'_{xxx} - \frac{1}{120}\beta^2 H^5 w'_{xxxxx} + O(\beta^3) = 0,$$

or equivalently

$$\eta_t - Hw'_x + \alpha(w'\eta)_x - \frac{1}{2}\beta H\left(\theta'^2 - \frac{1}{3}H^2\right)w'_{xxx}$$
$$+\frac{1}{2}\alpha\beta\left(\theta'^2 - H^2\right)(\eta w'_{xx})_x - \frac{5}{24}\beta^2 H\left(\theta'^2 - \frac{1}{5}H^2\right)^2 w'_{xxxxx} + O(\beta^3) \quad = \quad 0. \tag{4.36}$$

Substituting (4.33) and (4.34) into (4.32) yields

$$(1-r)\eta_x + \left(w_t + \frac{1}{2}\beta\theta^2 w_{xxt} + \frac{5}{24}\beta^2\theta^4 w_{xxxxt}\right)$$

$$-r\left(w'_t + \frac{1}{2}\beta\theta'^2 w'_{xxt} + \frac{5}{24}\beta^2\theta'^4 w'_{xxxxt}\right)$$

$$+\alpha\left((w + \frac{1}{2}\beta\theta^2 w_{xx})(w_x + \frac{1}{2}\beta\theta^2 w_{xxx}) - r(w' + \frac{1}{2}\beta\theta'^2 w'_{xx})(w'_x + \frac{1}{2}\beta\theta'^2 w'_{xxx})\right)$$

$$-\frac{1}{2}\beta\left(w_{xxt} + \frac{1}{2}\beta\theta^2 w_{xxxxt}\right) + \frac{1}{2}\beta r H^2\left(w'_{xxt} + \frac{1}{2}\beta\theta'^2 w'_{xxxxt}\right)$$

$$-\alpha\beta(\eta w_{xt})_x - \alpha\beta r H(\eta w'_{xt})_x + \frac{1}{24}\beta^2 w_{xxxxt} - \frac{1}{24}\beta^2 r H^4 w'_{xxxxt}$$

$$-\frac{1}{2}\alpha\beta(ww_{xx} - rH^2 w'w'_{xx})_x + \alpha\beta(w_x w_{xx} - rH^2 w'_x w'_{xx}) + O(\beta^3) \quad = \quad 0$$

or equivalently

$$(1-r)\eta_x + w_t - rw'_t + \alpha(ww_x - rw'w'_x) + \frac{1}{2}\beta\left[(\theta^2 - 1)w - r(\theta'^2 - H^2)w'\right]_{xxt}$$

$$+\frac{1}{24}\beta^2\left[(\theta^2 - 1)(5\theta^2 - 1)w - r(\theta'^2 - H^2)(5\theta'^2 - H^2)w'\right]_{xxxxt} \qquad (4.37)$$

$$-\alpha\beta\left[(\eta w_{xt})_x + rH(\eta w'_{xt})_x\right] + \frac{1}{2}\alpha\beta\left[(\theta^2 - 1)ww_{xxx} - r(\theta'^2 - H^2)w'w'_{xxx}\right]$$

$$+\frac{1}{2}\alpha\beta\left[(\theta^2 + 1)w_x w_{xx} - r(\theta'^2 + H^2)w'_x w'_{xx}\right] + O(\beta^3) \quad = \quad 0.$$

The system of three equations (4.35)–(4.37) is formally equivalent to the system of three equations (4.24), (4.31) and (4.32) but it allows one to choose the fluid levels θ and θ' as reference for the horizontal velocities. Among all these systems that model the same physical problem one can select those with the best dispersion relations. Neglecting terms of $O(\alpha^2, \beta^2, \alpha\beta)$, the system (4.35)–(4.37) reduces to

$$\begin{cases} \eta_t + w_x + \alpha(w\eta)_x + \frac{1}{2}\beta\left(\theta^2 - \frac{1}{3}\right)w_{xxx} = 0 \\[2mm] \eta_t - Hw'_x + \alpha(w'\eta)_x - \frac{1}{2}\beta H\left(\theta'^2 - \frac{1}{3}H^2\right)w'_{xxx} = 0 \\[2mm] (1-r)\eta_x + w_t - rw'_t + \alpha(ww_x - rw'w'_x) + \frac{1}{2}\beta\left[(\theta^2 - 1)w - r(\theta'^2 - H^2)w'\right]_{xxt} = 0. \end{cases}$$
$$(4.38)$$

In order to find the dispersion relation of this system, one looks for solution η, w,

w' proportional to $\exp(ikx - i\omega t)$ of the linearized system

$$
\begin{cases}
\eta_t + w_x + \dfrac{1}{2}\beta\left(\theta^2 - \dfrac{1}{3}\right)w_{xxx} = 0 \\[2mm]
\eta_t - Hw'_x - \dfrac{1}{2}\beta H\left(\theta'^2 - \dfrac{1}{3}H^2\right)w'_{xxx} = 0 \\[2mm]
(1-r)\eta_x + w_t - rw'_t + \dfrac{1}{2}\beta\left[(\theta^2-1)w - r(\theta'^2 - H^2)w'\right]_{xxt} = 0.
\end{cases}
\tag{4.39}
$$

In appendix B, after several calculations, one obtains the dispersion relation of system (4.39). In dimensionless variables

$$
\frac{\omega^2}{k^2} = \frac{H(1-r)\left(1 - \frac{\beta(\theta^2-\frac{1}{3})k^2}{2}\right)\left(1 - \frac{\beta(\theta'^2-\frac{1}{3}H^2)k^2}{2}\right)}{H\left(1 - \frac{\beta(\theta^2-1)k^2}{2}\right)\left(1 - \frac{\beta(\theta'^2-\frac{1}{3}H^2)k^2}{2}\right) + r\left(1 - \frac{\beta(\theta^2-\frac{1}{3})k^2}{2}\right)\left(1 - \frac{\beta(\theta'^2-H^2)k^2}{2}\right)},
\tag{4.40}
$$

and in physical variables

$$
\frac{\omega^2}{k^2} = \frac{ghH(1-r)\left(1 - \frac{h^2(\theta^2-\frac{1}{3})k^2}{2}\right)\left(1 - \frac{h^2(\theta'^2-\frac{1}{3}H^2)k^2}{2}\right)}{H\left(1 - \frac{h^2(\theta^2-1)k^2}{2}\right)\left(1 - \frac{h^2(\theta'^2-\frac{1}{3}H^2)k^2}{2}\right) + r\left(1 - \frac{h^2(\theta^2-\frac{1}{3})k^2}{2}\right)\left(1 - \frac{h^2(\theta'^2-H^2)k^2}{2}\right)}.
\tag{4.41}
$$

When w and w' are velocities at the bottom and at the top ($\theta = \theta' = 0$), one has

$$
\frac{\omega^2}{k^2} = gh\frac{H(1-r)\left(1 + \frac{1}{6}h^2k^2\right)\left(1 + \frac{1}{6}H^2h^2k^2\right)}{H\left(1 + \frac{1}{2}h^2k^2\right)\left(1 + \frac{1}{6}H^2h^2k^2\right) + r\left(1 + \frac{1}{6}h^2k^2\right)\left(1 + \frac{1}{2}H^2h^2k^2\right)}
\tag{4.42}
$$

The formulation (4.40) or (4.41) is also the dispersion relation of the system (4.35)–(4.37)

In figure 4.2 two cases of the dispersion relation for Boussinesq system (4.38) are plotted in comparison with the dispersion relation for the linearized interfacial wave equations, without the long wave assumption.

Note that the dotted curve cuts the k axis. It means that the system (4.38), as well as system (4.35)–(4.37), written with horizontal velocities at the interface are not appropriate for numerical simulation. At the end of section 4.4 we will discuss more about the possible choices of the reference fluid levels θ and θ' which ensure that $\dfrac{\omega^2}{k^2}$ takes positive values for all k.
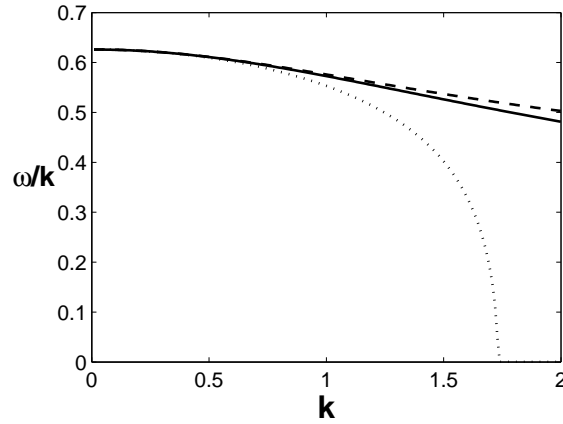
Figure 4.2: Dispersion relation (4.41) for the right-running wave solution to the Boussinesq system (4.38) with $r = 0.9$, $H = 0.6$; dashed curve: horizontal velocities at the bottom and the roof ($\theta = \theta' = 0$); dotted curve: horizontal velocities at the interface ($\theta = 1$, $\theta' = H$). The thick curve represents the dispersion relation for the linearized interfacial wave equations, without the long wave assumption (see for example Dias & Vanden-Broeck (2004) [20], see also (1.15)).

4.3 Comparison system (3.80)–(3.82) with system (4.35)–(4.37)

System (3.80)–(3.82) is written with horizontal velocities u, u' at the interface while system (4.35)–(4.37) can be applied to horizontal velocities at any fluid levels. Moreover, system (3.80)–(3.82) was established by assuming that $\alpha = \beta$ while the derivation of system (4.35)–(4.37) asks only $\alpha = O(\beta)$. In order to compare these two systems, one will write system (4.35)–(4.37) with the horizontal velocities at the interface and $\alpha = \beta$. It is worth pointing out that, unlike in section 4.2, one uses here u and u' to denote the horizontal velocities at the interface of respectively the lower and upper layer.

System (4.35)–(4.37) written for the horizontal velocities at the interface ($\theta = 1$

and $\theta' = H$), up to order α^2 is

$$
\begin{cases}
\eta_t + u_x + \alpha(u\eta)_x + \dfrac{1}{3}\alpha u_{xxx} + \dfrac{2}{15}\alpha^2 u_{xxxxx} = 0 \\[2mm]
\eta_t - Hu'_x + \alpha(u'\eta)_x - \dfrac{1}{3}\alpha H^3 u'_{xxx} - \dfrac{2H^5}{15}\alpha^2 u'_{xxxxx} = 0 \\[2mm]
(1-r)\eta_x + u_t - ru'_t + \alpha(uu_x - ru'u'_x) - \alpha^2(\eta u_{xt} + rH\eta u'_{xt})_x \\[2mm]
\hspace{4cm} + \alpha^2(u_x u_{xx} - rH^2 u'_x u'_{xx}) = 0.
\end{cases}
\tag{4.43}
$$

Adding H times the first equation to r times the second equation of system (4.43) yields

$$
(r+H)\eta_t + H(u - ru')_x + \alpha(Hu\eta + ru'\eta)_x
$$
$$
+\frac{1}{3}\alpha H(u - rH^2 u')_{xxx} + \frac{2}{15}\alpha^2 H(u - rH^4 u')_{xxxxx} = 0.
$$

Taking the derivative with respect to time of the previous equation, one has

$$
(r+H)\eta_{tt} + H(u - ru')_{xt} + \alpha(Hu\eta + ru'\eta)_{xt}
$$
$$
+\frac{1}{3}\alpha H(u - rH^2 u')_{xxxt} + \frac{2}{15}\alpha^2 H(u - rH^4 u')_{xxxxxt} = 0.
$$

Equivalently

$$
\eta_{tt} + \frac{1}{1 + \frac{r}{H}}(u - ru')_{xt} + \frac{\alpha}{1 + \frac{r}{H}}\left(u\eta + \frac{r}{H}u'\eta\right)_{xt}
$$
$$
+\frac{\frac{1}{3}\alpha}{1 + \frac{r}{H}}(u - rH^2 u')_{xxxt} + \frac{\frac{2}{15}\alpha^2}{1 + \frac{r}{H}}(u - rH^4 u')_{xxxxxt} = 0.
\tag{4.44}
$$

Taking the derivative with respect to x of the third equation of system (4.43), one has

$$
(1-r)\eta_{xx} + (u - ru')_{xt} + \alpha(uu_x - ru'u'_x)_x
$$
$$
-\alpha^2(\eta u_{xt} + rH\eta u'_{xt})_{xx} + \alpha^2(u_x u_{xx} - rH^2 u'_x u'_{xx})_x = 0.
$$

Dividing the previous equation by $\left(1 + \frac{r}{H}\right)$ yields

$$
\frac{1-r}{1 + \frac{r}{H}}\eta_{xx} + \frac{1}{1 + \frac{r}{H}}(u - ru')_{xt} + \frac{\alpha}{1 + \frac{r}{H}}(uu_x - ru'u'_x)_x
$$
$$
-\frac{\alpha^2}{1 + \frac{r}{H}}(\eta u_{xt} + rH\eta u'_{xt})_{xx} + \frac{\alpha^2}{1 + \frac{r}{H}}(u_x u_{xx} - rH^2 u'_x u'_{xx})_x = 0.
\tag{4.45}
$$

Deducing side by side (4.44) to (4.45), one has

$$\eta_{tt} - \frac{1-r}{1+\frac{r}{H}}\eta_{xx} - \frac{\alpha}{1+\frac{r}{H}}(uu_x - ru'u'_x)_x + \frac{\alpha}{1+\frac{r}{H}}\left(u\eta + \frac{r}{H}u'\eta\right)_{xt}$$

$$+\frac{\frac{1}{3}\alpha}{1+\frac{r}{H}}(u - rH^2u')_{xxxt} - \frac{\alpha^2}{1+\frac{r}{H}}(u_xu_{xx} - rH^2u'_xu'_{xx})_x \qquad (4.46)$$

$$+\frac{\alpha^2}{1+\frac{r}{H}}(\eta u_{xt} + rH\eta u'_{xt})_{xx} + \frac{\frac{2}{15}\alpha^2}{1+\frac{r}{H}}(u - rH^4u')_{xxxxxt} = 0.$$

This equation is exactly equation (3.80).

From the first equation of (4.43), one has

$$u_x = -\eta_t - \alpha(u\eta)_x - \frac{1}{3}\alpha u_{xxx} - \frac{2}{15}\alpha^2 u_{xxxxx}. \qquad (4.47)$$

Up to order α, equation (4.47) can be written as

$$u_x = -\eta_t - \alpha(u\eta)_x - \frac{1}{3}\alpha u_{xxx}$$

Substituting the previous equation into (4.47), one has

$$u_x = -\eta_t - \alpha(u\eta)_x - \frac{1}{3}\alpha\left(-\eta_t - \alpha(u\eta)_x - \frac{1}{3}\alpha u_{xxx}\right)_{xx} - \alpha^2\frac{2}{15}u_{xxxxx}.$$

Equivalently

$$u_x = -\eta_t - \alpha(u\eta)_x + \frac{1}{3}\alpha\eta_{xxt} + \frac{1}{3}\alpha^2(u_x\eta + u\eta_x)_{xx} - \alpha^2\frac{1}{45}u_{xxxxx}.$$

Up to order O(1), (4.47) can be written as $u_x = -\eta_t$. Substituting it into term in α^2 of the previous equation, one obtains

$$u_x = -\eta_t - \alpha(u\eta)_x + \frac{1}{3}\alpha\eta_{xxt} - \frac{1}{3}\alpha^2(\eta\eta_t - u\eta_x)_{xx} + \alpha^2\frac{1}{45}\eta_{xxxxt}. \qquad (4.48)$$

This is exactly equation (3.81).

Similarly, from the second equation of (4.43), one has

$$u'_x = \frac{1}{H}\eta_t + \alpha\frac{1}{H}(u'\eta)_x - \alpha\frac{H^2}{3}u'_{xxx} - \alpha^2\frac{2H^4}{15}u'_{xxxxx}. \qquad (4.49)$$

Up to order α, equation (4.49) can be written as

$$u'_x = \frac{1}{H}\eta_t + \alpha\frac{1}{H}(u'\eta)_x - \alpha\frac{H^2}{3}u'_{xxx}.$$

Substituting the previous equation into (4.49), one has

$$\begin{aligned}
u'_x &= \frac{1}{H}\eta_t + \alpha\frac{1}{H}(u'\eta)_x \\
&\quad -\alpha\frac{H^2}{3}\left(\frac{1}{H}\eta_t + \alpha\frac{1}{H}(u'\eta)_x - \alpha\frac{H^2}{3}u'_{xxx}\right)_{xx} - \alpha^2\frac{2H^4}{15}u'_{xxxxx}.
\end{aligned}$$

Equivalently

$$\begin{aligned}
u'_x &= \frac{1}{H}\eta_t + \alpha\frac{1}{H}(u'\eta)_x \\
&\quad -\alpha\frac{H}{3}\eta_{xxt} - \alpha^2\frac{H}{3}(u'_x\eta + u'\eta_x)_{xx} - \alpha^2\frac{H^4}{45}u'_{xxxxx}.
\end{aligned}$$

Up to order O(1), (4.49) can be written as $u'_x = \frac{1}{H}\eta_t$. Substituting into term in α^2 of the previous equation, one obtains

$$\begin{aligned}
u'_x &= \frac{1}{H}\eta_t + \alpha\frac{1}{H}(u'\eta)_x - \alpha\frac{H}{3}\eta_{xxt} \\
&\quad -\alpha^2\frac{1}{3}(\eta\eta_t + Hu'\eta_x)_{xx} - \alpha^2\frac{H^3}{45}\eta_{xxxxt}. \tag{4.50}
\end{aligned}$$

This equation is exactly equation (3.82).

The three equations (4.46), (4.48) and (4.50) show that one can obtain system (3.80)–(3.82) from system (4.35)–(4.37). The system (4.35)–(4.37) is more general than system (3.80)–(3.82) because it is free of the assumption $\alpha = \beta$ and it can be applied to horizontal velocities at any fluid levels.

As mentioned in section 4.2, the system (4.43) is not appropriate from the numerical point of view. Therefore the system of three equations (3.80)–(3.82) which is formally equivalent to it, is also not good for numerical simulation.

4.4   System of two equations

The systems obtained in the previous section are not appropriate for numerical computations. One would like to obtain a system of two evolution equations for

the variables η and $W = w - rw'$. In fact, Benjamin & Bridges (1997) [3] (see also Dias & Bridges (1994) [18], Craig at al. (2005) [16], Agafontsev et al. (2007) [1]) formulated the interfacial wave problem using Hamiltonian formalism and showed that the canonical variables for interfacial waves are $\eta^*(x^*, t^*)$ and $\rho\phi^*(x^*, \eta^*, t^*) - \rho'\phi^{*\prime}(x^*, \eta^*, t^*)$, where ϕ and ϕ' are respectively velocity potentials of the lower and upper layer.

At leading order, the first two equations of system (4.38) give

$$\begin{cases} \eta_t + w_x = 0, \\[2mm] \eta_t - Hw'_x = 0. \end{cases}$$

One deduces that

$$w_x = -Hw'_x.$$

One assumes that the fluids is at rest as $x \to \infty$. Integrating the previous equation with respect to x, the constant will take value 0. Therefore

$$w = -Hw'.$$

It leads to

$$w = \frac{H}{r+H}W + O(\beta), \quad w' = \frac{-1}{r+H}W + O(\beta). \tag{4.51}$$

Adding H times the first equation to r times the second equation of system (4.38) yields

$$(r+H)\eta_t + H(w - rw')_x + \alpha\left[(Hw + rw')\eta\right]_x$$
$$+ \frac{H}{2}\beta\left[\left(\theta^2 - \frac{1}{3}\right)w_{xxx} - r\left(\theta'^2 - \frac{1}{3}H^2\right)w'_{xxx}\right] = 0. \tag{4.52}$$

Up to order $O(\beta)$, the third and the fourth term of (4.52) can be written

$$\alpha\left[(Hw + rw')\eta\right]_x = \alpha\left[\left(\frac{H^2}{r+H}W - \frac{r}{r+H}W\right)\eta\right]_x$$
$$= \alpha\frac{H^2 - r}{r+H}(W\eta)_x,$$

and

$$\frac{1}{2}\beta H\left[(\theta^2 - \frac{1}{3})w_{xxx} - r\left(\theta'^2 - \frac{1}{3}H^2\right)w'_{xxx}\right]$$

$$= \frac{1}{2}\beta \frac{H^2(\theta^2 - \frac{1}{3}) + rH\left(\theta'^2 - \frac{1}{3}H^2\right)}{r + H} W_{xxx}$$

$$= \frac{1}{2}\beta \frac{H^2(\theta^2 - 1) + rH\left(\theta'^2 - H^2\right) + \frac{2}{3}H^2 + \frac{2}{3}rH^3}{r + H} W_{xxx}$$

$$= \beta\left(\frac{1}{2}\frac{H^2 S}{r + H} + \frac{1}{3}\frac{H^2(1 + rH)}{r + H}\right) W_{xxx},$$

where

$$S = (\theta^2 - 1) + \frac{r}{H}\left(\theta'^2 - H^2\right).$$

So that equation (4.52) becomes

$$(r + H)\eta_t + HW_x + \alpha\frac{H^2 - r}{r + H}(W\eta)_x + \beta\left(\frac{1}{2}\frac{H^2 S}{r + H} + \frac{1}{3}\frac{H^2(1 + rH)}{r + H}\right) W_{xxx} = 0.$$

Dividing this equation by $(r + H)$ yields

$$\eta_t = -\frac{H}{r + H}W_x - \alpha\frac{H^2 - r}{(r + H)^2}(W\eta)_x - \beta\left(\frac{1}{2}\frac{H^2 S}{(r + H)^2} + \frac{1}{3}\frac{H^2(1 + rH)}{(r + H)^2}\right) W_{xxx}.$$

In the third equation of system (4.38), the term in α can be written in the form

$$\alpha(ww_x - rw'w'_x) = \alpha\left(\frac{H^2}{(r + H)^2}WW_x - \frac{r}{(r + H)^2}WW_x\right)$$

$$= \alpha\frac{H^2 - r}{(r + H)^2}WW_x,$$

and the term in β can be written as

$$\frac{1}{2}\beta\left[(\theta^2 - 1)w - r(\theta'^2 - H^2)w'\right]_{xxt}$$

$$= \frac{1}{2}\beta\left((\theta^2 - 1)\frac{H}{r + H} - r(\theta'^2 - H^2)\frac{(-1)}{r + H}\right) W_{xxt}$$

$$= \frac{1}{2}\beta\frac{H(\theta^2 - 1) + r\left(\theta'^2 - H^2\right)}{r + H} W_{xxt}$$

$$= \frac{\beta}{2}\frac{HS}{r + H} W_{xxt}.$$

Then the third equation of system (4.38) becomes

$$(1 - r)\eta_x + W_t + \alpha\frac{H^2 - r}{(r + H)^2}WW_x + \frac{\beta}{2}\frac{HS}{r + H}W_{xxt} = 0,$$

or equivalently

$$W_t = -(1-r)\eta_x - \alpha \frac{H^2 - r}{(r+H)^2} W W_x - \frac{1}{2}\beta \frac{HS}{r+H} W_{xxt}.$$

The final system of two equations for interfacial waves in the limit of long, weakly dispersive waves, can be written in terms of the horizontal velocities at arbitrary fluid levels as (in dimensionless form)

$$\begin{cases} \eta_t = -\dfrac{H}{r+H} W_x - \alpha \dfrac{H^2 - r}{(r+H)^2} (W\eta)_x - \beta \left(\dfrac{1}{2}\dfrac{H^2 S}{(r+H)^2} + \dfrac{1}{3}\dfrac{H^2(1+rH)}{(r+H)^2} \right) W_{xxx} \\[3mm] W_t = -(1-r)\eta_x - \alpha \dfrac{H^2 - r}{(r+H)^2} W W_x - \dfrac{1}{2}\beta \dfrac{HS}{r+H} W_{xxt}, \end{cases}$$

(4.53)

or as (in physical variables)

$$\begin{cases} \eta^*_{t^*} = -h d_1 W^*_{x^*} - d_4 (W^*\eta^*)_{x^*} - h^3 d_2 W^*_{x^*x^*x^*}, \\[3mm] W^*_{t^*} = -g(1-r)\eta^*_{x^*} - d_4 W^* W^*_{x^*} - h^2 d_3 W^*_{x^*x^*t^*}, \end{cases}$$

(4.54)

where

$$d_1 = \frac{H}{r+H}, \quad d_2 = \frac{H^2}{2(r+H)^2}\left(S + \frac{2}{3}(1+rH) \right), \quad d_3 = \frac{1}{2}S d_1, \quad d_4 = \frac{H^2 - r}{(r+H)^2}.$$

(4.55)

Note that, the case $S = 0$ corresponding to the horizontal velocities at the interface, this system recovers system (1.1) that Craig et al. (2005) [16] obtained by using Hamiltonian method.

Another remark is: Choi & Camassa (1999) [13] also derived a system of two equations (see system (1.2)), but it is different from ours. In particular, their coefficient d_2 is equal to 0, and their equation for W_t possesses an extra quadratic term $\eta\eta_x$. The reason is that their 'W' is the mean horizontal velocity through the upper layer. The value of S which best approximates the Choi & Camassa equations is $S = -\frac{2}{3}(1 + rH)$. Indeed the coefficient d_2 then vanishes. This particular value for S can be explained as follows. The leading order correction to the horizontal velocity is given by

$$w(z) = u - \tfrac{1}{2}\beta z^2 u_{xx}.$$

The value of z, say $z = \theta$, for which the mean velocity

$$\overline{w} = \int_0^1 w(z)\, dz$$

is equal to $w(\theta)$ is given by $\theta = 1/\sqrt{3}$. Similarly, one finds $\theta' = (1/\sqrt{3})H$ for the upper layer. Therefore $S = -\frac{2}{3}(1 + rH)$.

Recall that the scaling (4.10) that led to our Boussinesq system can be written in the form

$$\frac{x^*}{h} = \frac{x}{\sqrt{\beta}}, \quad \frac{\eta^*}{h} = \alpha\eta, \quad \frac{t^*}{h/c_0} = \frac{t}{\sqrt{\beta}}, \quad \frac{W^*}{gh/c_0} = \alpha W$$

with $c_0 = \sqrt{gh}$, $\alpha \ll 1$, $\beta \ll 1$ and $\alpha = O(\beta)$.

Linearizing system (4.54) and looking for solutions (η^*, W^*) proportional to $\exp(ikx^* - i\omega t^*)$ leads to the dispersion relation

$$\frac{\omega^2}{k^2} = \frac{gh(1 - r)(d_1 - d_2k^2h^2)}{1 - d_3k^2h^2}.$$

Plots of the dispersion relation are given in the next section. Since $0 \leq \theta \leq 1$ and $0 \leq \theta' \leq H$, the definition of S implies that

$$-1 - rH \leq S \leq 0.$$

It follows that $d_3 \leq 0$ and therefore the denominator $1 - d_3h^2k^2$ is positive. In order to have well-posedness (that is ω^2/k^2 positive for all values of k), d_2 must be negative, which is the case if $S \leq -\frac{2}{3}(1 + rH)$. Finally the condition one wants to impose on S is that

$$-(1 + rH) \leq S \leq -\frac{2}{3}(1 + rH). \tag{4.56}$$

It is satisfied if one takes the horizontal velocities on the bottom and on the roof ($S = -(1 + rH)$) or the mean horizontal velocities in the lower and upper layers ($S = -\frac{2}{3}(1 + rH)$), but it is not if one takes the horizontal velocities along the interface ($S = 0$).

4.5   Extended Boussinesq system of two equations with cubic terms

In system (4.53), when $|H^2 - r|$ is small, the quadratic nonlinear terms become so small compared to other terms. In this case, one needs to go one step beyond and take into consideration the cubic terms. Again one would like to obtain a system of two equations for the variables η and $W = w - rw'$. One derives first a general system of two equations with cubic terms. Then one introduces a specific scaling

for the case where $|H^2 - r|$ is small. A lot of terms in the system drop out because they are of higher order.

The leading order terms lead to the same equation as before, namely $w = -Hw'$. And again

$$w = \frac{H}{r+H}W + O(\beta), \quad w' = \frac{-1}{r+H}W + O(\beta). \tag{4.57}$$

At the next order, the first two equations of (4.38) give

$$w_x + \alpha(w\eta)_x + \frac{1}{2}\beta\left(\theta^2 - \frac{1}{3}\right)w_{xxx} = -Hw'_x + \alpha(w'\eta)_x - \frac{1}{2}\beta H\left(\theta'^2 - \frac{1}{3}H^2\right)w'_{xxx}.$$

Integrating this equation with respect to x. As the fluids are assumed to be at rest when $x \to \infty$, the constant takes value 0. Therefore

$$w + \alpha w\eta + \frac{1}{2}\beta(\theta^2 - \frac{1}{3})w_{xx} = -Hw' + \alpha w'\eta - \frac{1}{2}\beta H\left(\theta'^2 - \frac{1}{3}H^2\right)w'_{xx}.$$

It is equivalent to

$$w = -Hw' + \alpha(w' - w)\eta - \frac{1}{2}\beta\left(H\left(\theta'^2 - \frac{1}{3}H^2\right)w'_{xx} + \left(\theta^2 - \frac{1}{3}\right)w_{xx}\right).$$

Dividing this equation by H, one obtains

$$w' = -\frac{1}{H}w + \alpha\frac{1}{H}(w' - w)\eta - \frac{1}{2H}\beta\left(H\left(\theta'^2 - \frac{1}{3}H^2\right)w'_{xx} + \left(\theta^2 - \frac{1}{3}\right)w_{xx}\right).$$

Applying (4.57) to terms containing α or β in the right hand side of the two previous equations, one has

$$w = -Hw' - \alpha\frac{1+H}{r+H}W\eta + \frac{1}{2}\beta H\frac{\left(\theta'^2 - \frac{1}{3}H^2\right) - \left(\theta^2 - \frac{1}{3}\right)}{r+H}W_{xx}, \tag{4.58}$$

and

$$w' = -\frac{w}{H} - \alpha\frac{1+H}{H(r+H)}W\eta + \frac{1}{2}\beta\frac{\left(\theta'^2 - \frac{1}{3}H^2\right) - \left(\theta^2 - \frac{1}{3}\right)}{r+H}W_{xx}. \tag{4.59}$$

In Appendix B, after several substitutions, one obtains the system of two equations (B-10) and (B-17). Switching back to the physical variables

$$x^* = \ell x, \quad \eta^* = A\eta, \quad t^* = \ell t/c_0, \quad W^* = gAW/c_0, \quad \text{with } c_0 = \sqrt{gh},$$

the system (B-10),(B-17) becomes

$$
(r+H)\eta_{t^*}^* + hHW_{x^*}^* + \frac{H^2-r}{r+H}(W^*\eta^*)_{x^*} + \frac{1}{2}h^3H\frac{H(\theta^2-\frac{1}{3})+r(\theta'^2-\frac{1}{3}H^2)}{r+H}W_{x^*x^*x^*}^*
$$
$$
-\frac{1}{h}\frac{r(1+H)^2}{(r+H)^2}(W^*\eta^{*2})_{x^*} + \frac{1}{2}h^2rH(1+H)\frac{(\theta'^2-\frac{1}{3}H^2)-(\theta^2-\frac{1}{3})}{(r+H)^2}(W^*\eta^*)_{x^*x^*x^*}
$$
$$
+\frac{1}{2}h^2\left(rH(1+H)\frac{(\theta'^2-\frac{1}{3}H^2)-(\theta^2-\frac{1}{3})}{(r+H)^2} + \frac{H^2(\theta^2-1)-r(\theta'^2-H^2)}{r+H}\right)(W_{x^*x^*}^*\eta^*)_{x^*}
$$
$$
-\frac{1}{4}h^5\left(\frac{rH^2\left((\theta'^2-\frac{1}{3}H^2)-(\theta^2-\frac{1}{3})\right)^2}{(r+H)^2} - \frac{5}{6}\frac{H^2(\theta^2-\frac{1}{5})^2+rH(\theta'^2-\frac{1}{5}H^2)^2}{r+H}\right)W_{x^*x^*x^*x^*x^*}^*
$$
$$
= 0,
$$

$$(4.60)$$

and

$$
g(1-r)\eta_{x^*}^* + W_{t^*}^* + \frac{H^2-r}{(r+H)^2}W^*W_{x^*}^* + \frac{1}{2}h^2\frac{H(\theta^2-1)+r(\theta'^2-H^2)}{r+H}W_{x^*x^*t^*}^*
$$
$$
-\frac{1}{h}\frac{r(1+H)^2}{(r+H)^3}(W^{*2}\eta^*)_{x^*} + \frac{1}{2}h^2rH(1+H)\frac{(\theta'^2-\frac{1}{3}H^2)-(\theta^2-\frac{1}{3})}{(r+H)^3}(W^*W_{x^*x^*}^*)_{x^*}
$$
$$
-h\frac{H(1-r)}{r+H}(\eta^*W_{x^*t^*}^*)_{x^*} + \frac{1}{2}h^2\frac{H^2(\theta^2-1)-r(\theta'^2-H^2)}{(r+H)^2}W^*W_{x^*x^*x^*}^*
$$
$$
+\frac{1}{2}h^2\frac{H^2(\theta^2+1)-r(\theta'^2+H^2)}{(r+H)^2}W_{x^*}^*W_{x^*x^*}^*
$$
$$
-\frac{1}{2}hrH(1+H)\frac{(\theta^2-1)-(\theta'^2-H^2)}{(r+H)^2}(W^*\eta^*)_{x^*x^*t^*}
$$
$$
+h^4\left(\frac{rH\left((\theta^2-1)-(\theta'^2-H^2)\right)\left((\theta'^2-\frac{1}{3}H^2)-(\theta^2-\frac{1}{3})\right)}{4(r+H)^2}\right.
$$
$$
\left.+\frac{H(\theta^2-1)(5\theta^2-1)+r(\theta'^2-H^2)(5\theta'^2-H^2)}{2(r+H)}\right)W_{x^*x^*x^*x^*t^*}^* = 0.
$$

$$(4.61)$$

The specific scaling for small values of $|H^2-r|$,

$$
\frac{x^*}{h} = \frac{x}{\beta}, \quad \frac{t^*}{h/c_0} = \frac{t}{\alpha}, \quad \frac{\eta^*}{h} = \alpha\eta, \quad \frac{W^*}{gh/c_0} = \alpha W, \quad H^2-r = \alpha\mathcal{C},
$$

with $c_0 = \sqrt{gh}$, $\alpha \ll 1$, $\beta \ll 1$, $\alpha = O(\beta)$, will lead to a new Boussinesq system with cubic terms. A lot of terms in (4.60)-(4.61) drop out (see appendix B) because they are of higher order. Going back to physical variables, the system of two equations

becomes

$$
\left\{
\begin{aligned}
\eta_{t^*}^* &= -h\frac{H}{r+H}W_{x^*}^* - h^3\left(\frac{1}{2}\frac{H^2 S}{(r+H)^2} + \frac{1}{3}\frac{H^2(1+rH)}{(r+H)^2}\right)W_{x^*x^*x^*}^* \\
&\quad - \frac{H^2-r}{(r+H)^2}(W^*\eta^*)_{x^*} + \frac{1}{h}\frac{r(1+H)^2}{(r+H)^3}(W^*\eta^{*2})_{x^*} \\
W_{t^*}^* &= -g(1-r)\eta_{x^*}^* - \frac{1}{2}h^2\frac{HS}{r+H}W_{x^*x^*t^*}^* \\
&\quad - \frac{H^2-r}{(r+H)^2}W^*W_{x^*}^* + \frac{1}{h}\frac{r(1+H)^2}{(r+H)^3}(W^{*2}\eta^*)_{x^*}.
\end{aligned}
\right.
\tag{4.62}
$$

This is the same system as (4.54) with two extra terms, the cubic terms. One will call it a system of extended Boussinesq equations (see also Craig et al. (2005) [16]). Linearizing (4.62) gives the same dispersion relation as before.

Note that, if we take the horizontal velocities at the interface, S will vanish. In this case, system (4.62) is exactly system (2.9) that Craig et al. (2005) [16] obtained by using Hamiltonian method. Therefore one can consider that our systems (4.54) and (4.62) are more general than the models that Craig et al. have obtained for small amplitude, long wave regime. This important remark reinforces the confidence to the judicious of our models which will be studied numerically in the next chapter.

Note that the value $S = 0$ does not belong to the interval that ensure the well-posedness of the problem (see (4.56)). Therefore, the systems (1.1) and (2.9) are not appropriate for the numerical simulation.

Chapter 5

Numerical studies

In this chapter, we study numerically the Boussinesq systems (4.54) and (4.62) obtained in the previous chapter. The propagation of solitary waves of both elevation and depression will be shown. The inelastic collision between two solitary waves of elevation or between two solitary waves of depression will be discussed in detail.

In order to do this, one needs to construct numerical schemes and impose initial conditions. The approximate solutions to Boussinesq systems at time 0 will be taken as initial conditions.

5.1 Boussinesq system with quadratic nonlinear terms

In order to integrate the Boussinesq system (4.54) numerically, one introduces a slightly different change of variables. The stars still denote the physical variables and no new notation is introduced for the dimensionless variables:

$$x = \frac{x^*}{h}, \quad \eta = \frac{\eta^*}{h}, \quad t = \frac{c}{h}t^*, \quad W = \frac{W^*}{c}, \quad \text{with} \quad c^2 = gh\frac{H(1-r)}{r+H}. \tag{5.1}$$

The system (4.54) then becomes

$$\begin{cases} \eta_t = -d_1 W_x - d_4(W\eta)_x - d_2 W_{xxx} \\ \\ W_t = -\dfrac{1}{d_1}\eta_x - d_4 W W_x - d_3 W_{xxt} \end{cases}. \tag{5.2}$$

81
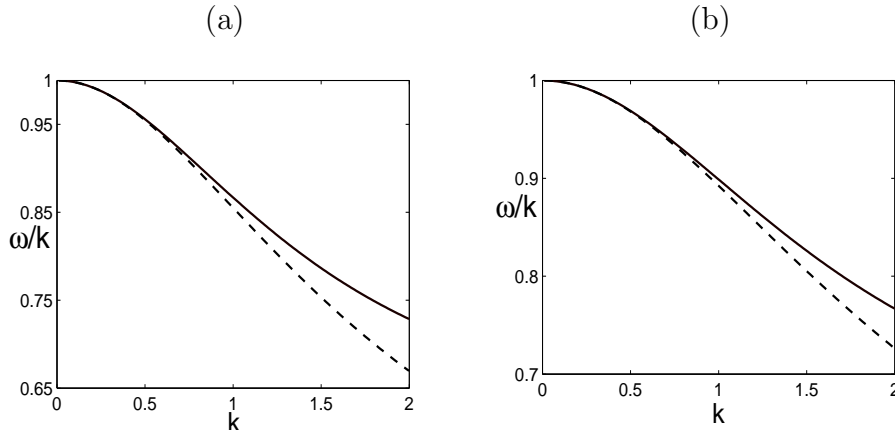
Figure 5.1: Dispersion relation (5.3) for the right-running wave solution to the Boussinesq system (5.2) with $S = -1 - rH$, $r = 0.9$: (a) $H = 1.2$, (b) $H = 0.8$. The dashed curves represent the dispersion relation for the linearized interfacial wave equations, without the long wave assumption (see for example Dias & Vanden-Broeck (2004) [20], see also (1.15)).

The dispersion relation of system (5.2) is

$$\frac{\omega^2}{k^2} = \frac{d_1 - d_2 k^2}{d_1(1 - d_3 k^2)}. \tag{5.3}$$

As $k \to 0$, $\dfrac{\omega^2}{k^2} \to 1$. As $k \to \infty$,

$$\frac{\omega^2}{k^2} \to \frac{d_2}{d_1 d_3} = 1 + \frac{2(1 + rH)}{3S}.$$

Typical plots of the dispersion relation (5.3) are given in Figure 5.1. Comparisons between the approximate and the exact dispersion relations, given by

$$\frac{\omega^2}{k^2} = \frac{\tanh k \tanh kH}{d_1 k(\tanh kH + r \tanh k)}$$

are also shown. A very good agreement is found for small k.

5.1.1   Numerical scheme

Taking the Fourier transform of the system (5.2) gives

$$
\begin{cases}
\hat{\eta}_t = -d_1(ik)\hat{W} - d_4(ik)\widehat{W\eta} - d_2(ik)^3\hat{W} \\
\hat{W}_t = -\dfrac{1}{d_1}(ik)\hat{\eta} - \dfrac{d_4}{2}(ik)\widehat{W^2} - d_3(ik)^2\hat{W}_t
\end{cases}.
$$

Equivalently

$$
\begin{cases}
\hat{\eta}_t = (d_2 k^2 - d_1)ik\hat{W} - d_4 ik\widehat{W\eta} \\
\hat{W}_t = -\dfrac{1}{d_1(1 - d_3 k^2)}ik\hat{\eta} - \dfrac{d_4}{2(1 - d_3 k^2)}ik\widehat{W^2}
\end{cases}.
$$

The system of differential equations (5.2) will be solved by a pseudo-spectral method in space with a number N of Fourier modes on a periodic domain of length L. For most applications, $N = 1024$ was found to be sufficient. The time integration is performed using the classical fourth-order explicit Runge–Kutta scheme. The time step Δt was optimized through a trial and error process and was found to have a dependence in $1/N$. In this chapter, Δt is used to denote the time steps in Fourier domain from $-\pi$ to π. The time step for the periodic domain L will be $L/(2 \times \pi) * \Delta t$.

5.1.2   Initial conditions

Since the main goal is to study the propagation and the collision of solitary waves, one first looks for solitary wave solutions of the system (5.2). As opposed to the KdV equation, there are no explicit solitary wave solutions of the Boussinesq system that are physically relevant. Therefore one must look for an approximate solitary wave solution to (5.2) as in Bona & Chen (1998) [4] (see also Dougalis & Mitsotakis (2004) [22] for the existence of solitary wave solutions). The leading-order terms give

$$
\eta_t = -d_1 W_x, \quad W_t = -\frac{1}{d_1}\eta_x.
$$

A solution representing a right-running wave is

$$
W(x - t) = \frac{1}{d_1}\eta(x - t).
$$

One then looks for solutions of system (5.2) in the form

$$W(x,t) = \frac{1}{d_1}\Big[\eta(x,t) + M(x,t)\Big],$$

where M is assumed to be small compared to η and W. Substituting the expression for W into (5.2) and neglecting higher-order terms yields

$$\begin{cases} \eta_t = -\eta_x - M_x - \dfrac{d_4}{d_1}(\eta^2)_x - \dfrac{d_2}{d_1}\eta_{xxx} \\[2mm] \eta_t = -\eta_x - M_t - \dfrac{1}{2}\dfrac{d_4}{d_1}(\eta^2)_x - d_3\eta_{xxt} \end{cases}. \tag{5.4}$$

Comparing the two equations of system (5.4), one has

$$M_x + \frac{d_4}{d_1}(\eta^2)_x + \frac{d_2}{d_1}\eta_{xxx} = M_t + \frac{1}{2}\frac{d_4}{d_1}(\eta^2)_x + d_3\eta_{xxt}.$$

Assume that the solitary wave goes to the right. Remark that, in (5.1), c is the phase velocity of system (4.54) up to order $O(1)$. Moreover, the horizontal velocity combination W is scaled by c, so that the waves will propagate with an approximate velocity of about 1 in the new variables. Since M is relatively small, one can consider that $M_t \approx -M_x$. Therefore, from the previous equation, one has

$$M_x = -\frac{1}{4}\frac{d_4}{d_1}(\eta^2)_x - \frac{1}{2}\frac{d_2}{d_1}\eta_{xxx} + \frac{1}{2}d_3\eta_{xxt}. \tag{5.5}$$

Substituting the expression for M_x into one of the equations of system (5.4) yields

$$\eta_t + \eta_x + \frac{3d_4}{4d_1}(\eta^2)_x + \frac{d_2}{2d_1}\eta_{xxx} + \frac{d_3}{2}\eta_{xxt} = 0. \tag{5.6}$$

This is essentially the model equation that was studied by Bona et al. (1981) [7].

Looking for solitary wave solutions of (5.6) in the form

$$\eta = \eta_0 \operatorname{sech}^2[\kappa(x + x_0 - Vt)] \tag{5.7}$$

leads to two equations for κ and V:

$$\begin{cases} -V + 1 + 2(d_2/d_1)\kappa^2 - 2d_3\kappa^2 V = 0 \\[2mm] d_4\eta_0 - 4d_2\kappa^2 + 4d_1 d_3\kappa^2 V = 0 \end{cases},$$

and x_0 can take arbitrary value.

Solving for κ^2 and V yields

$$\kappa^2 = \frac{d_4\eta_0}{4\left(d_2 - d_1d_3 - \frac{1}{2}d_3d_4\eta_0\right)}, \quad V = 1 + \frac{d_4\eta_0}{2d_1}.$$

One looks for M by integrating (5.5) with respect to x

$$M = -\frac{1}{4}\frac{d_4}{d_1}\eta^2 - \frac{1}{2}\frac{d_2}{d_1}\eta_{xx} + \frac{1}{2}d_3\eta_{xt} + C(t),$$

where $C(t)$ is an arbitrary function of t. Since the fluids are assumed to be at rest as $x \to \infty$, one has $M(\pm\infty, t) = 0$ and $\eta(\pm\infty, t) = 0$. Therefore $C(t) = 0$ and one obtains explicitly the following expression for M

$$M = -\frac{d_4}{4d_1}\eta^2 - \frac{d_2}{2d_1}\eta_{xx} + \frac{d_3}{2}\eta_{xt}.$$

For a given pair (r, H), one must only consider values of η_0 which are such that $\kappa^2 > 0$.

In addition, one has the condition (4.56) on S. The sign of d_4 depends on the relation between H^2 and r. Let us assume first that $H^2 > r$ so that $d_4 > 0$. In order for the condition $\kappa^2 > 0$ to be satisfied, one needs

$$\eta_0\left(d_2 - d_1d_3 - \frac{1}{2}d_3d_4\eta_0\right) > 0.$$

The values of η_0 for which the left-hand side of the inequality vanishes are

$$\eta_{01} = 0, \quad \eta_{02} = \frac{4H(r + H)(1 + rH)}{3(H^2 - r)S}.$$

Since $S < 0$ one has $\eta_{02} < 0$ and therefore $\eta_{02} < \eta_{01}$. The coefficient of η_0^2 in the inequality is positive. Consequently one must have

$$\eta_0 > \eta_{01} = 0 \quad \text{or} \quad \eta_0 < \eta_{02} = \frac{4H(r + H)(1 + rH)}{3(H^2 - r)S}.$$

This second branch is not acceptable since

$$\frac{4H(r + H)(1 + rH)}{3(H^2 - r)} > 1 + rH > -S > 0.$$

Therefore

$$\frac{4H(r+H)(1+rH)}{3(H^2-r)S} < -1,$$

which gives an amplitude larger than the depth of the lower layer!

Similarly, when $H^2 < r$ one has $d_4 < 0$. In order for the condition $\kappa^2 > 0$ to be satisfied, one needs

$$\eta_0\left(d_2 - d_1 d_3 - \frac{1}{2}d_3 d_4 \eta_0\right) < 0.$$

The values of η_0 for which the left-hand side of the inequality will vanish still are

$$\eta_{01} = 0, \quad \eta_{02} = \frac{4H(r+H)(1+rH)}{3(H^2-r)S}.$$

In this case $\eta_{02} > 0$, the coefficient of η_0^2 in the inequality is negative. Consequently one must have

$$\eta_0 < \eta_{01} = 0 \quad \text{or} \quad \eta_0 > \eta_{02} = \frac{4H(r+H)(1+rH)}{3(H^2-r)S}.$$

This second branch is not acceptable since

$$\frac{4H(r+H)(1+rH)}{3(H^2-r)S} = H\frac{4(r+H)}{3(r-H^2)}\frac{(1+rH)}{(-S)} > H\frac{4r}{3r}1 > H,$$

which gives an amplitude larger than the depth of the upper layer.
The summary of acceptable values for η_0 is given in the table below:

$H^2 - r > 0$	$0 < \eta_0 < H$
$H^2 - r < 0$	$-1 < \eta_0 < 0$

For a "thick" upper layer ($H^2 > r$), the solitary waves are of elevation, while they are of depression for a "thick" bottom layer ($H^2 < r$). The weakly nonlinear theory developed in this section does not provide any bounds on the amplitude of the solitary waves. We have added a physical constraint based on the fact that both layers are bounded by flat solid boundaries. It is well-known in the framework of full interfacial wave equations (see for example Laget & Dias (1997) [34]) that the rigid top and bottom provide natural bounds on the solitary wave amplitudes.

Different positions of the initial solitary wave along the horizontal axis can be obtained by varying the value of x_0. The initial condition for the left-running wave

can be constructed easily from the numerical point of view. If the pair $\eta_{initial}(x, 0)$ and $W_{initial}(x, 0)$ is an initial condition for right-running wave, the pair $\eta_{initial}(x, 0)$ and $-W_{initial}(x, 0)$ will be an initial solitary wave for a left-running wave. In other words, one needs only to change the direction of the propagation of wave. This simple technique can be explained theoretically as follows.

Using the above procedure for obtaining a right-running wave, a solution representing a left-running wave is

$$W(x + t) = -\frac{1}{d_1}\eta(x + t).$$

Instead of having (5.5) and (5.6), one will have

$$M_x = -\frac{1}{4}\frac{d_4}{d_1}(\eta^2)_x - \frac{1}{2}\frac{d_2}{d_1}\eta_{xxx} - \frac{1}{2}d_3\eta_{xxt}$$

and

$$-\eta_t + \eta_x + \frac{3d_4}{4d_1}(\eta^2)_x + \frac{d_2}{2d_1}\eta_{xxx} - \frac{d_3}{2}\eta_{xxt} = 0.$$

Looking for solitary wave solutions of the previous equation in the form

$$\eta = \eta_0\text{sech}^2[\kappa(x + x_0 + Vt)]$$

lead to the same values of κ and V for the right-running wave.

The difference between the formulations of η for a right-running wave and a left-running wave is not a problem, since the initial condition is applied at $t = 0$. Moreover this difference does not influence the value of M at $t = 0$. Consequently, one can keep the same expression for $W_{initial}$ and simply put the opposite sign ahead.

As the speed increases, the wave amplitude reaches a limit. In the next section, one extends the weakly nonlinear analysis to cubic terms so that this effect can be incorporated.

5.1.3   Numerical simulations

Once the approximate solitary wave (5.7) has been obtained, it is possible to make it cleaner by iterative filtering. This technique has been used by several authors, including Bona & Chen (1998) [4] and Bona et al. (2007) [6]. In order to study run-ups and phase shifts during collision of solitary waves, it is important to use clean

solitary waves for the initial conditions. On the other hand, in order to show only the qualitative behavior, it is not necessary. Therefore results in this Section are given for non-filtered solitary waves. Some results with filtered waves are described in the next section.

In this chapter, the parameter x_0 which determine the position of solitary wave in horizontal axis will take values in Fourier domain from $-\pi$ to π. The position of solitary wave in the periodic domain L will be $L/(2 \times \pi) \times x_0$

Figure 5.2 shows the propagation of an almost perfect right-running solitary wave of elevation. Even though all computations are performed with dimensionless variables, it is interesting to provide numerical applications for a configuration that could be realized in the laboratory (see Michallet & Barthélemy (1998) [35]). Keeping $r = 0.9$ as in the figure, one could take for example $h = 10$ cm, $h' = 11$ cm ($H = 1.1$). The solitary wave amplitude is 1 cm, its speed $c \approx 23.2$ cm/s, the length of the domain 51.2 m (a bit long!). The plots (b)–(e) would then correspond to snapshots at $t = 21.5$ s, $t = 68.9$ s, $t = 94.8$ s and $t = 163.7$ s.

Figure 5.3 shows the head-on collision of two almost perfect solitary waves of elevation of equal amplitude moving in opposite directions. As in the one-layer case, the solution rises to an amplitude slightly larger than the sum of the amplitudes of the two incident solitary waves. After the collision, two similar waves emerge and return to the form of two separated solitary waves. As a result of this collision, the centers of the two resulting solitary waves are slightly retarded from the trajectories of the incoming centers.

Figure 5.4 shows the head-on collision of two almost perfect solitary waves of depression of unequal amplitudes moving in opposite directions. The numerical simulations exhibit the same features that have been observed in the symmetric case.

Figure 5.5 shows the overtaking collision between two solitary waves of elevation of different amplitudes. A sequence of spatial profiles is shown. The larger one, which is faster, eventually passes the smaller one, which is slower. After the collision, two similar waves emerge and return to the form of two separated solitary waves. Again there is a phase shift after the interaction. The amplitude of the solution $\eta(x,t)$ never exceeds that of the larger solitary wave, nor does it dip below the amplitude

(a) $t = 0$

(b) $t = 50$

(c) $t = 160$

(d) $t = 220$

(e) $t = 380$

(f) evolution in time
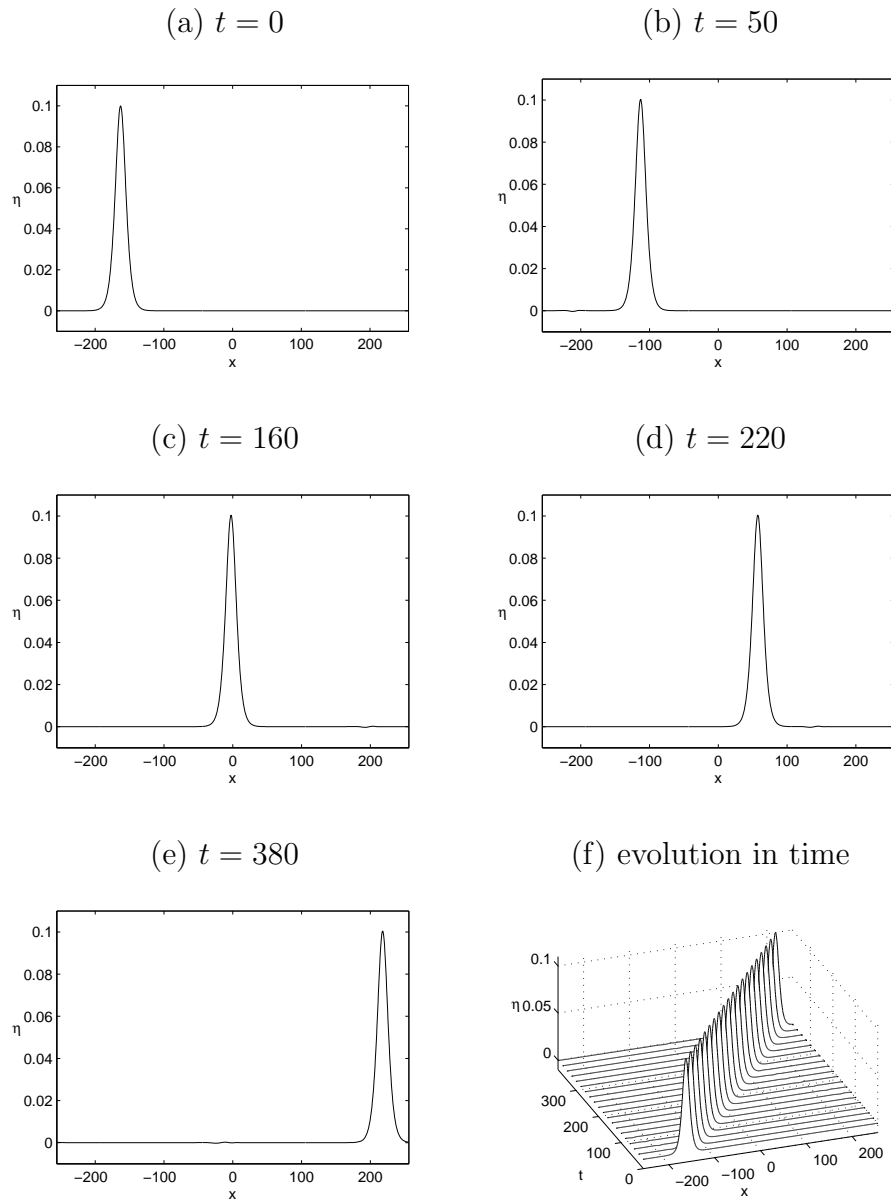
Figure 5.2: An approximate solitary wave propagating to the right. This is a solution to the system of quadratic Boussinesq equations (5.2), with parameters $H = 1.1$, $r = 0.9$, $L = 512$, $N = 1024$, $S = -1 - rH$, $\Delta t = 1/N$, $x_0 = 2$, $\eta_0 = 0.1$.

(a) $t = 0$

(b) $t = 40$

(c) $t = 161$

(d) $t = 170$

(e) $t = 250$

(f) evolution in time

Figure 5.3: Head-on collision of two approximate solitary waves of elevation of equal size. This is a solution to the system of quadratic Boussinesq equations (5.2), with parameters $H = 1.2$, $r = 0.8$, $L = 512$, $N = 1024$, $S = -1 - rH$, $\Delta t = 1/N$, $x_0 = 2$, $\eta_0^\ell = \eta_0^r = 0.1$, where the superscripts ℓ and r stand for left and right respectively.
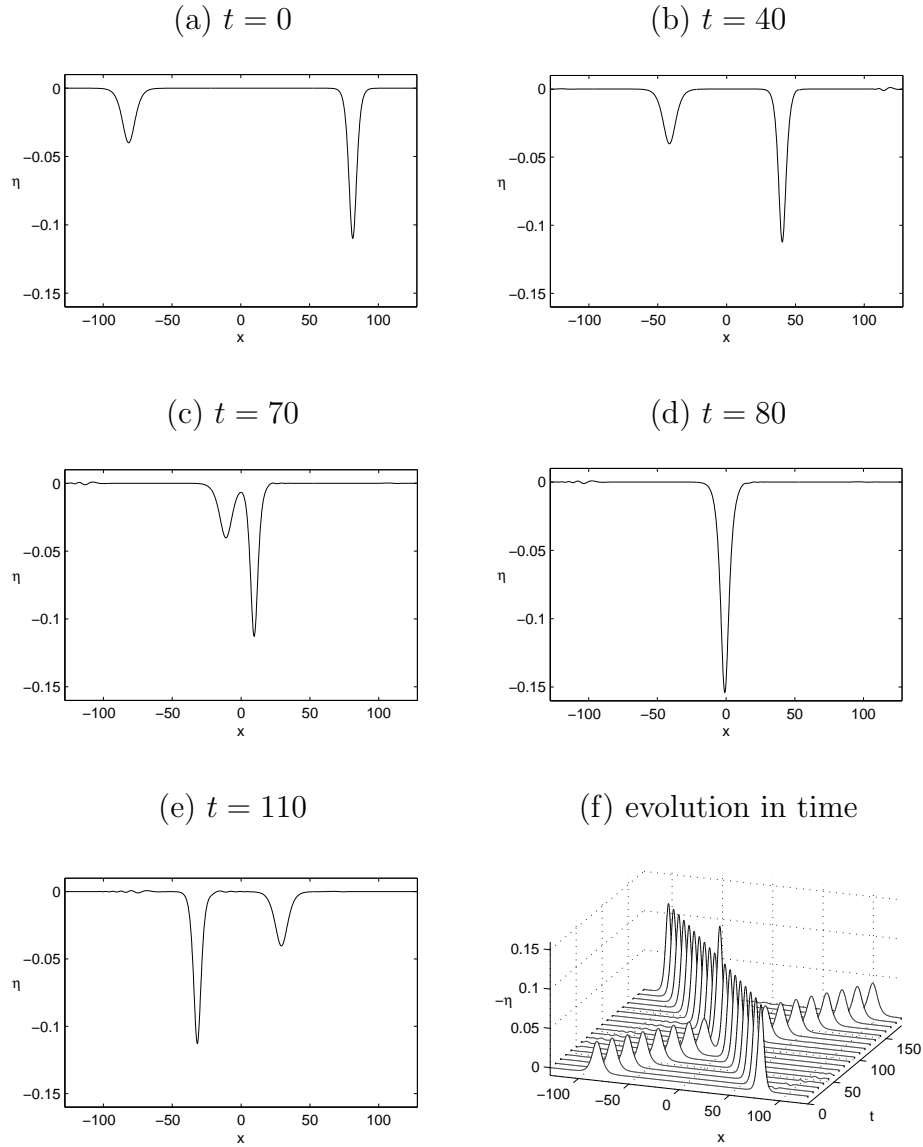
Figure 5.4: Head-on collision of two almost perfect solitary waves of depression of different sizes. This is a solution to the system of quadratic Boussinesq equations (5.2), with parameters $H = 0.6$, $r = 0.85$, $L = 256$, $N = 1024$, $S = -1 - rH$, $\Delta t = 1/N$, $x_0^\ell = 2$, $x^r = -2$, $\eta_0^\ell = -0.04$, $\eta_0^r = -0.11$, where the superscripts ℓ and r stand for left and right respectively. In plot (f), note that $-\eta(x,t)$ has been plotted for the sake of clarity.

Figure 5.5: Overtaking collision of two almost perfect solitary waves of elevation of different sizes. This is a solution to the system of quadratic Boussinesq equations (5.2), with parameters $H = 1.6$, $r = 0.95$, $L = 2^{14}$, $N = 2^{14}$, $S = -1 - rH$, $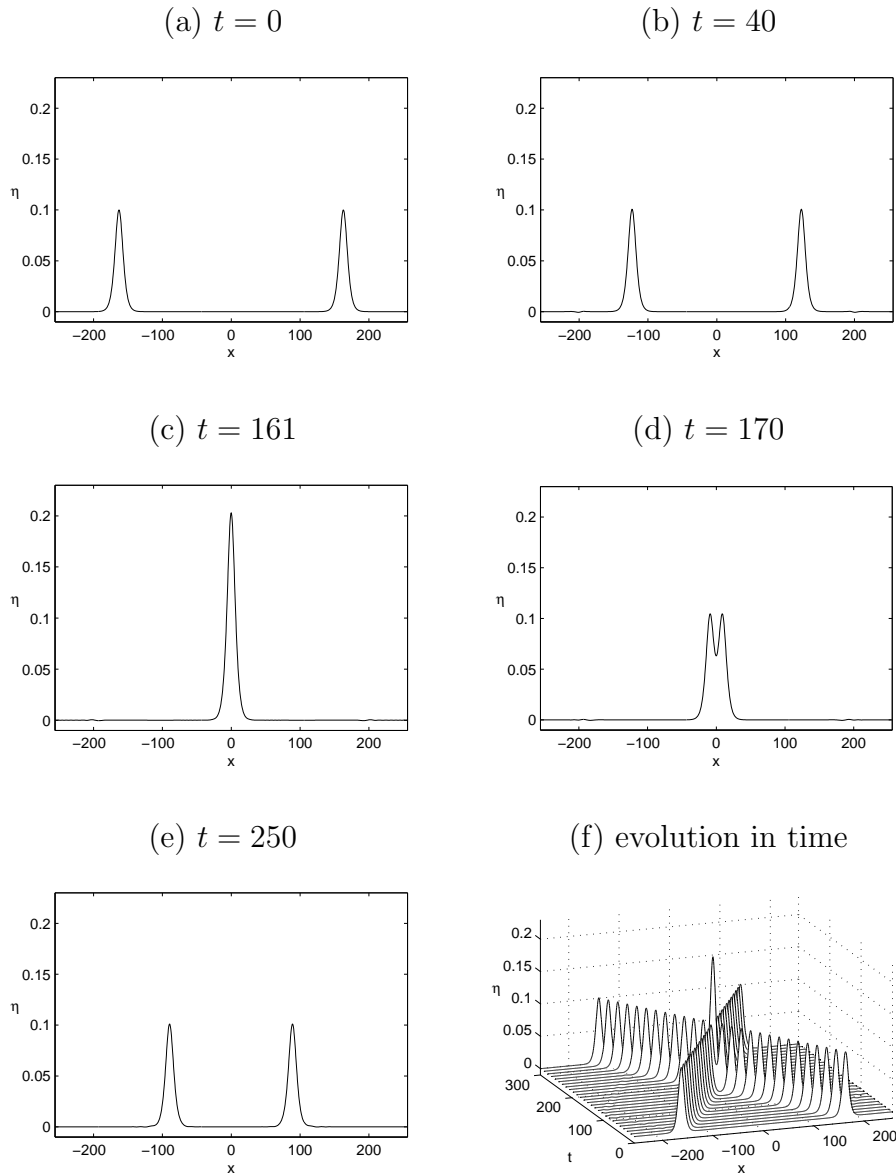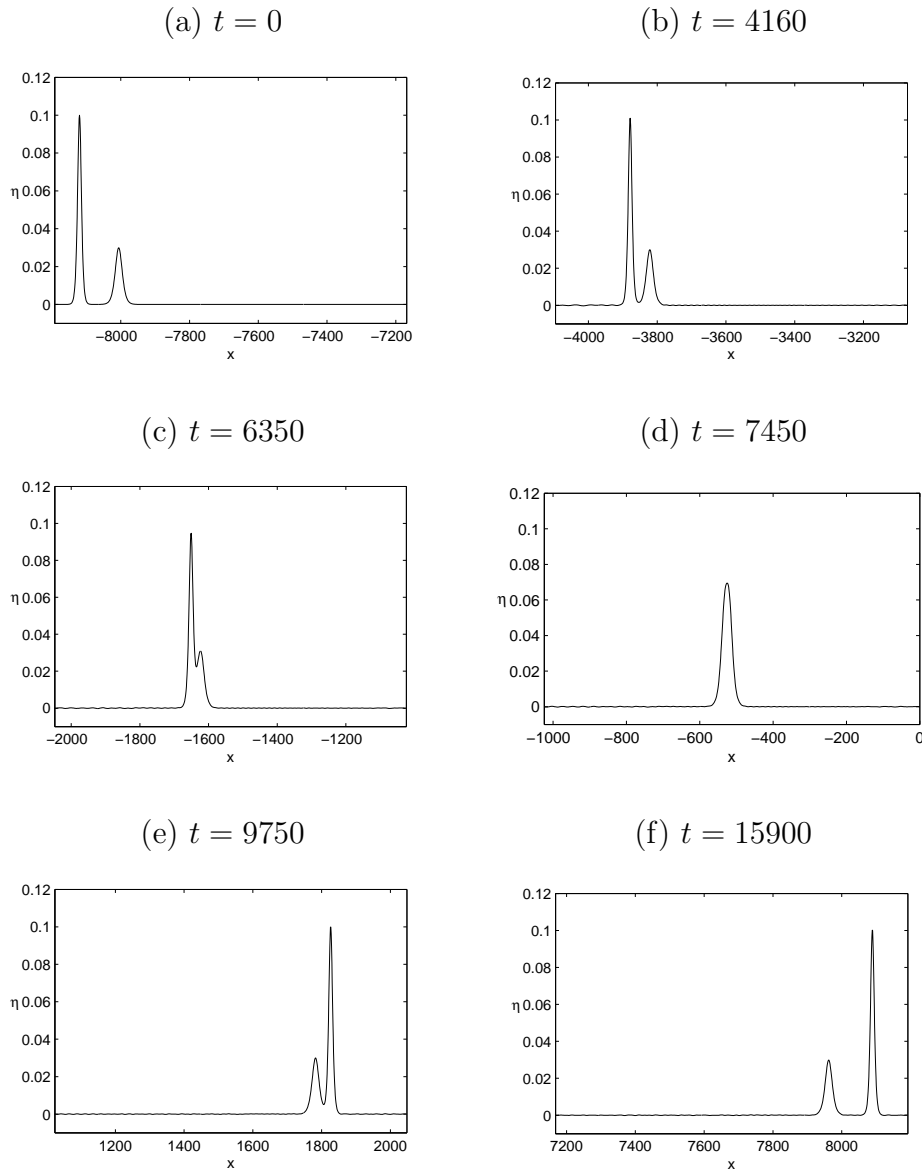\Delta t = 8/N$, $x_0^\ell = 2$, $x_0^r = 1.4$, $\eta_0^\ell = 0.1$, $\eta_0^r = 0.03$, where the superscripts ℓ and r stand for left and right respectively.

of the smaller.

5.1.4   Run-ups and phase shifts

In this section we provide accurate results on run-ups and phase shifts. The terminology 'run-up' denotes the fact that during the collision of two counter propagating solitary waves the wave amplitude increases beyond the sum of the two single wave amplitudes. Since run-ups and phase shifts are always very small, they must be computed with high accuracy. This is why it is important to clean the solitary waves obtained by the approximate expression (5.7). One proceeds as follows. One begins with an approximate solution, let it propagate across the domain, truncate the leading pulse, use it as new initial value by translating it to the left of the domain, let it propagate again and distance itself from the trailing dispersive tail, truncate again, and repeat the whole process over and over until a clean, at least to the eye, solitary wave is produced. Sometimes, after shifting the solitary wave backward, one puts a small part on the left of the domain equal to 0. The larger of this part is called ss, it will not be mentioned in all of the following iterative cleaning. Then we use this new filtered solution as initial guess to study the various collisions.

In order to improve the accuracy, one will choose the periodic domain larger than that of the previous numerical experiments and the number of Fourier modes is increased to $N = 2^{13}$. This change requires a computational time much longer than in the cases above. Fortunately, one can increase about 8 times the time step without lack of considerable precision. Some of the following numerical experiments use this possibility, others do not.

Figure 5.6 shows the effect of cleaning. Starting with a solitary wave of depression of amplitude

$$-\eta_{\min} = 0.11,$$

after 20 iterations of cleaning, one obtains a clean solitary wave of amplitude.

$$-\eta_{\min} = 0.112101.$$

As the amplitude reaches an asymptotic level after the iterative cleaning, the resulting wave will propagate in a perfectly stable manner. One can use these clean solutions for the following experiments to study quantitatively the head-on collision as well as overtaking collision between solitary waves with high precision. Note

(a)

(b)   (c)

(d)   (e)
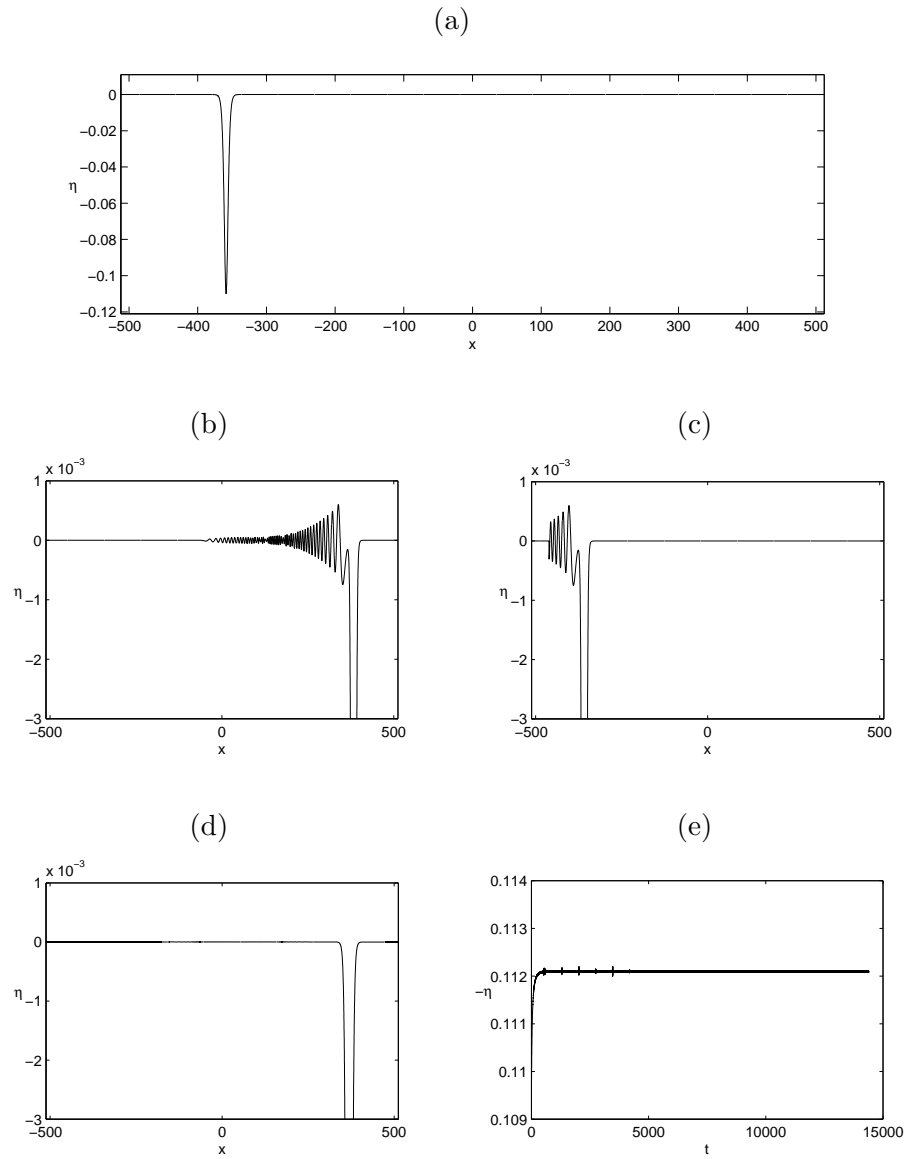
Figure 5.6: A solitary wave produced by iterative cleaning. This is a solution to the Boussinesq system (5.2) with parameters $H = 0.6$, $r = 0.85$, $L = 1024$, $N = 2^{13}$, $S = -1 - rH$, $\Delta t = 6/N$, $x_0 = 2.2$, $\eta_0 = -0.11$, $ss = 52$. (a) Profile of the initial solitary wave. (b) Profile of the approximate solitary waves (5.7) after one propagation across the domain. (c) Profile (b) after cleaning and translation to the left of the domain. (d) Profile (b) after 20 iterations of cleaning. (e) Evolution of maximum amplitude $-\eta_{\min}$ during 20 iterations of cleaning. The amplitude reaches an asymptotic level.

that, the smaller is the amplitude of the solitary waves, the more time one needs to repeat the iterative cleaning. The number of iterative cleanings required for the solitary waves of elevation and depression of equal amplitude are not always the same. This number depends also on how much the wave is shifted backward after each iteration of cleaning.

For solitary wave solutions to the Boussinesq system with quadratic nonlinearities (5.2), the behavior is the same as the behavior shown for example in Craig et al. (2006) [14]. In particular one obtains figures that look very similar to their Figure 2 for the phase shift resulting from the head-on collision of two solitary waves of equal height, to their Figure 4 for the time evolution of the maximum amplitude of the solution (it rises sharply to more than twice the elevation of the incident solitary waves, then descends to below this level after crest detachment, and finally relaxes back to almost its initial level) and to their Figure 12 for the asymmetric head-on collision of two solitary waves of different heights. However the quantitative of these phenomena are very small compared to what Craig et al. (2006) [14] have obtained, they can be observed only by a zoom in a very small scaling. Therefore, in the following studies, the phase shift will be described differently.

Figure 5.7 shows a head-on collision between two clean solitary waves of depression of equal amplitude. The amplitude of solitary waves before cleaning was $-\eta_{\min} = 0.08$.
After 20 iterations of cleaning ($x_0 = 2.2$ has been chosen), it reached

$$-\eta_{\min} = 0.081132.$$

The run-up during the collision is small:

$$-\eta_{\min} = 0.163961$$

at collision, which is slightly larger than

$$2 \times (0.081132) = 0.162264.$$

Both solitary waves shift backward after the collision.

Figure 5.8 shows a head-on collision between two clean solitary waves of different amplitudes. Starting the cleaning procedure with two solitary waves of amplitude

$$\eta_{\max} = 0.1 \quad \text{and} \quad \eta_{\max} = 0.08,$$

(a)

(b)   (c)

(d)   (e)
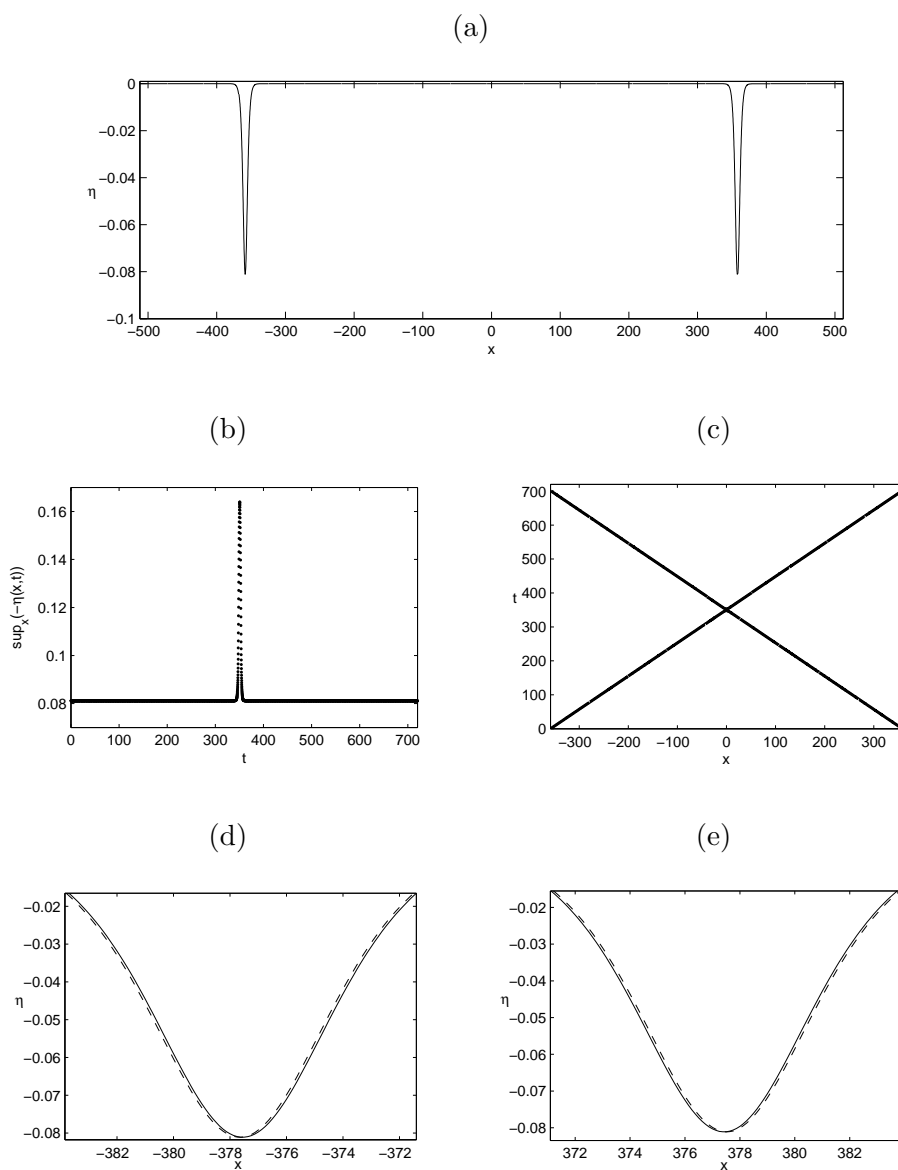
Figure 5.7:   A head-on collision between two solitary waves of depression of equal amplitude. This is a solution to the Boussinesq system (5.2) with parameters $H = 0.6$, $r = 0.85$, $L = 1024$, $N = 2^{13}$, $S = -1 - rH$, $\Delta t = 6/N$, $-\eta^l_{\min} = -\eta^r_{\min} = 0.081132$. (a) Initial profile. (b) Time evolution of the amplitude $-\eta_{\min}$. (c) Crest trajectory. (d) Phase shift of the left-running wave; dashed curve represents the left-running wave which propagates without collision. (e) Phase shift of the right-running wave; dashed curve represents the right-running wave which propagates without collision.

(a)

(b)   (c)

(d)   (e)

Figure 5.8: A head-on collision between two solitary waves of elevation of different heights. This is a solution to the Boussinesq system (5.2) with parameters $H = 1.8$, $r = 0.85$, $L = 1024$, $N = 2^{13}$, $S - 1 - rH$, $\Delta t = 6/N$, $\eta_{\max}^{l} = 0.101567$, $\eta_{\max}^{r} = 0.081011$. (a) Initial profile. (b) Time evolution of the amplitude $\eta_{\max}$. (c) Crest trajectory. (d) Phase shift of the left-running wave, dashed curve represents the left-running wave which propagates without collision. (e) Phase shift of the right-running wave, dashed curve represents the right-running wave which propagates without collision.

after 16 iterations, one obtains two waves of amplitude

$$\eta_{\max} = 0.101567 \quad \text{and} \quad \eta_{\max} = 0.081011,$$

respectively. Put these two resulting solitary waves at the ends of the domain and make them propagate in opposite directions. During the collision, the amplitude of the solution reaches

$$\eta_{\max} = 0.184505.$$

This is slightly larger than the sum of the amplitudes of the two incident solitary waves:

$$0.101567 + 0.081011 = 0.182578.$$

Similarly to the head-on collision between two solitary waves of equal amplitude, both solitary waves in this numerical experiment are retarded from their trajectories after the collision.

Figure 5.9 shows the overtaking collision between two solitary waves of elevation of different heights. Two solitary waves of amplitudes

$$\eta_{\max} = 0.101 \quad \text{and} \quad \eta_{\max} = 0.030$$

have been obtained respectively from two solitary waves of amplitudes $\eta_{\max} = 0.1$ and $\eta_{\max} = 0.03$ after 30 and 60 iterations of cleaning. The solitary wave with smaller amplitude (the shorter wave) was put in front of the solitary wave of larger amplitude (the higher wave). As the higher wave moves faster than the shorter one, it passes the small one after a moment and the overtaking collision takes place. During this collision the amplitude of the solution $\eta(x,t)$ never exceeds that of the higher solitary wave, nor does it dip below the amplitude of the shorter.

After the overtaking collision, the solitary wave of higher amplitude shifts forward while the shorter one shifts backward. In this case, one observes that the distance that the shorter wave shifts is larger.

Image (b) is similar to Figure 18 obtained by Craig et al. (2006) [14].
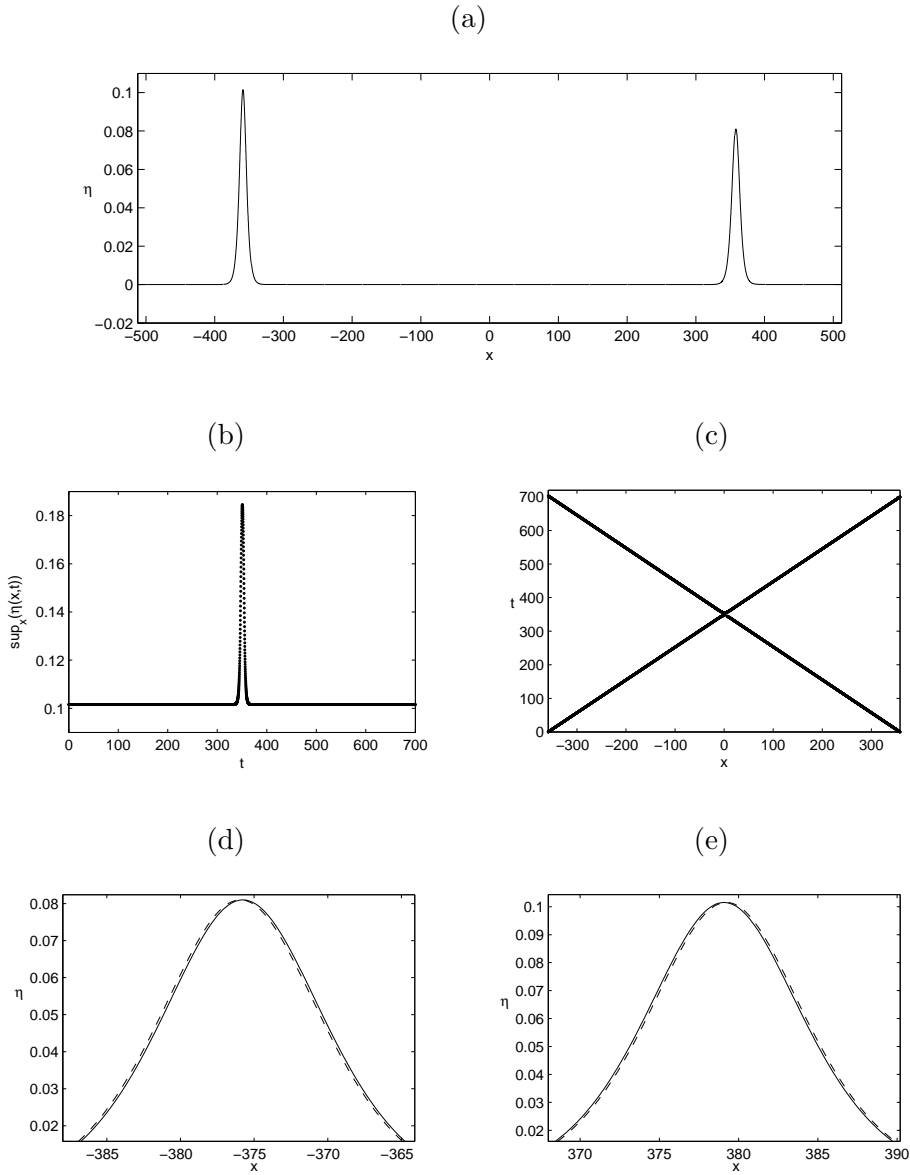
(a)

(b)

(c)
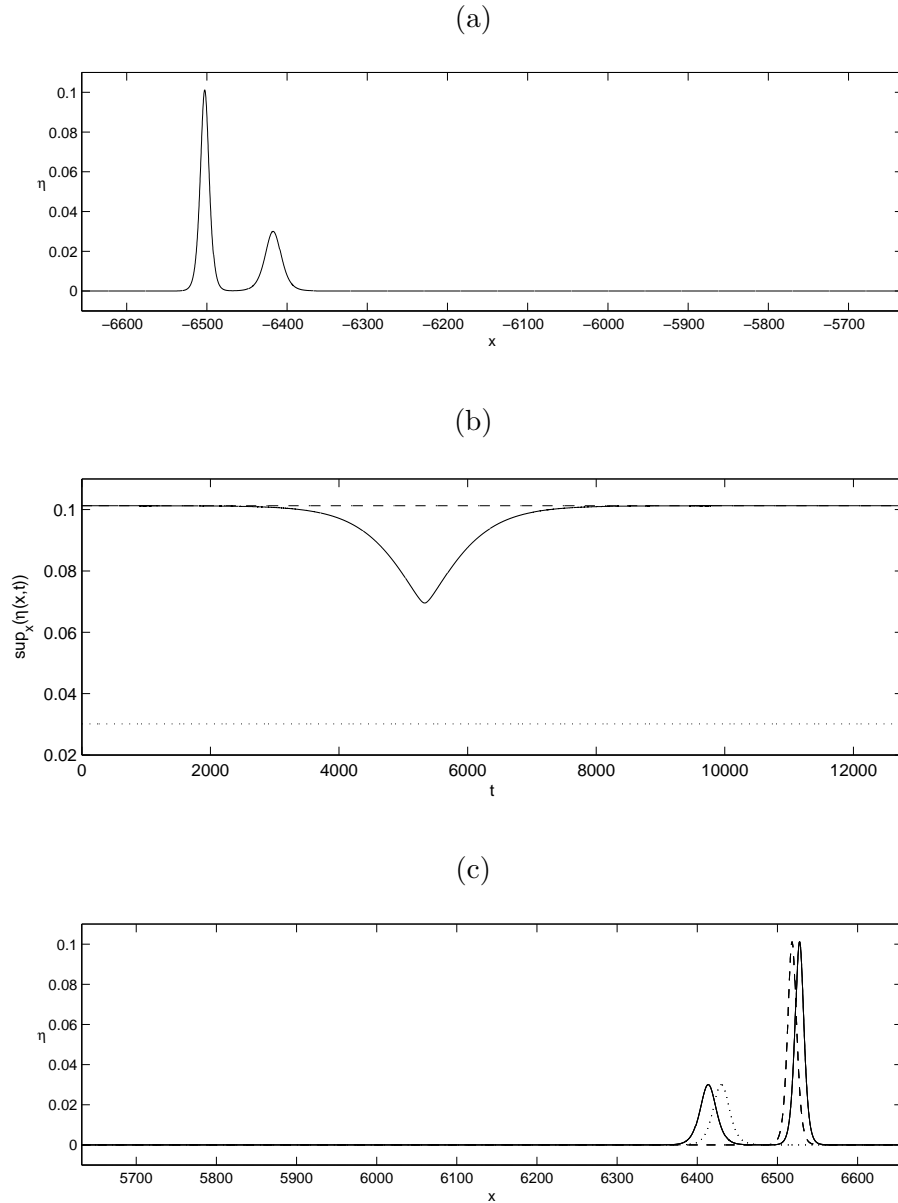
Figure 5.9: Overtaking collision between two solitary waves of elevation of different heights. This is a solution to the Boussinesq system (5.2) with parameters $H = 1.6$, $r = 0.95$, $L = 1024 \times 13$, $N = 2^{13} \times 13$, $S - 1 - rH$, $\Delta t = 6/N$, $\eta^{\ell}_{\max} = 0.101$, $\eta^{r}_{\max} = 0.030$. (a) Initial profile. (b) Evolution in time of the amplitude $\eta_{\max}$; dashed and dotted lines represent respectively the evolution in time of the amplitudes of the higher and the shorter waves without overtaking collision. (c) Phase shift; dashed and dotted lines represent respectively the profile of the higher and the shorter waves without overtaking collision.

5.2 Extended Boussinesq system with cubic non-linear terms

In order to integrate numerically the extended Boussinesq system (4.62), one introduces a slightly different change of variables. The stars still denote the physical variables and no new notation is introduced for the dimensionless variables:

$$x = \frac{x^*}{h}, \quad \eta = \frac{\eta^*}{h}, \quad t = \frac{c}{h}t^*, \quad W = \frac{W^*}{c}, \quad \text{with} \quad c^2 = \frac{ghh'(\rho - \rho')}{\rho'h + \rho h'} = \frac{ghH(1-r)}{r+H}.$$

Using the same coefficients as in (4.55), one rewrites system (4.62) with the new variables as

$$\begin{cases} \eta_t & = & -d_1 W_x - d_2 W_{xxx} - d_4 (W\eta)_x + d_5 (W\eta^2)_x \\[2mm] W_t & = & -\dfrac{1}{d_1}\eta_x - d_3 W_{xxt} - d_4 W W_x + d_5 (W^2\eta)_x \end{cases} \tag{5.8}$$

where the new coefficient d_5 is equal to

$$d_5 = \frac{r(1+H)^2}{(r+H)^3}.$$

5.2.1 Numerical scheme for the extended Boussinesq system

Taking the Fourier transform of the system (5.8) gives

$$\begin{cases} \hat{\eta}_t & = & -d_1 ik\hat{W} - d_2 (ik)^3 \hat{W} - d_4 ik\widehat{(W\eta)} + d_5 ik\widehat{(W\eta^2)} \\[2mm] \hat{W}_t & = & -\dfrac{1}{d_1} ik\hat{\eta} - d_3 (ik)^2 \hat{W}_t - \dfrac{d_4}{2} ik\widehat{(W^2)} + d_5 ik\widehat{(W^2\eta)} \end{cases}.$$

Equivalently

$$\begin{cases} \hat{\eta}_t & = & (d_2 k^2 - d_1)ik\hat{W} - d_4 ik\widehat{(W\eta)} + d_5 ik\widehat{(W\eta^2)} \\[2mm] (1 - d_3 k^2)\hat{W}_t & = & -\dfrac{1}{d_1} ik\hat{\eta} - \dfrac{d_4}{2} ik\widehat{(W^2)} + d_5 ik\widehat{(W^2\eta)} \end{cases}.$$

The system of differential equations (5.8) will be integrated numerically by using the method described in section 5.1.1. However, the solitary wave solutions to

the extended Boussinesq system are relatively larger compared to that solution to Boussinesq system with quadratic nonlinear terms. Therefore, one needs to extend the periodic domain. For most applications we will use $L = 4096$. For qualitative studies, $N = 1024$ will usually be taken and for quantitative studies $N = 2^{13}$ will be used more frequently. The time step Δt was optimized through a trial and error process and found to have a dependence in $1/N$ (in Fourier domain from $-\pi$ to π).

5.2.2   Initial solutions for the extended Boussinesq system

Again, one looks for approximate solitary wave solutions to (5.8). As before one looks for solutions of the form

$$W(x,t) = \frac{1}{d_1}\Big[\eta(x,t) + M(x,t)\Big],$$

where M is assumed to be small compared to η and W. Substituting the expression for W into (5.8) and neglecting higher-order terms, one has

$$\begin{cases} \eta_t = -\eta_x - M_x - \dfrac{d_2}{d_1}\eta_{xxx} - \dfrac{d_4}{d_1}(\eta^2)_x + \dfrac{d_5}{d_1}(\eta^3)_x \\[3mm] \eta_t = -\eta_x - M_t - d_3\eta_{xxt} - \dfrac{d_4}{2d_1}(\eta^2)_x + \dfrac{d_5}{d_1}(\eta^3)_x \end{cases}. \tag{5.9}$$

Comparing the two equations of (5.9), one has

$$M_x + \frac{d_2}{d_1}\eta_{xxx} + \frac{d_4}{d_1}(\eta^2)_x - \frac{d_5}{d_1}(\eta^3)_x = M_t + d_3\eta_{xxt} + \frac{d_4}{2d_1}(\eta^2)_x - \frac{d_5}{d_1}(\eta^3)_x.$$

As mentioned in section 5.1.2, one can consider that $M_x \approx -M_t$. Therefore, from the previous equation, one obtains

$$M_x = -\frac{1}{4}\frac{d_4}{d_1}(\eta^2)_x - \frac{1}{2}\frac{d_2}{d_1}\eta_{xxx} + \frac{1}{2}d_3\eta_{xxt}. \tag{5.10}$$

Substituting the expression for M_x into one of the equations of system (5.9) yields

$$\eta_t + \eta_x + \frac{3d_4}{4d_1}(\eta^2)_x - \frac{d_5}{d_1}(\eta^3)_x + \frac{d_2}{2d_1}\eta_{xxx} + \frac{d_3}{2}\eta_{xxt} = 0. \tag{5.11}$$

We have checked that the extended KdV equation (5.11) is in agreement with previously derived eKdV equations such as in Dias & Vanden-Broeck (2004) [20].

Let $V = 1 + c_1$ be the wave speed, with $|c_1|$ small compared to 1. In the moving frame of reference $X = x + x_0 - (1 + c_1)t$, $T = t$, (x_0 is an arbitrary constant), equation (5.11) becomes

$$-c_1 \eta_X + \eta_T + \frac{3d_4}{4d_1}(\eta^2)_X - \frac{d_5}{d_1}(\eta^3)_X + \frac{d_2}{2d_1}\eta_{XXX} + \frac{d_3}{2}\left[-(1+c_1)\eta_{XXX} + \eta_{XXT}\right] = 0.$$

One looks for stationary solutions. Therefore one studies the following equation

$$-c_1 \eta_X + \frac{3d_4}{4d_1}(\eta^2)_X - \frac{d_5}{d_1}(\eta^3)_X + \frac{d_2}{2d_1}\eta_{XXX} + \frac{d_3}{2}\left[-(1+c_1)\eta_{XXX}\right] = 0.$$

Integrating this equation with respect to X. Since the fluids are assumed to be at rest as $x \to \infty$, the integral constant takes value 0. Therefore

$$-c_1 \eta + \frac{3d_4}{4d_1}\eta^2 - \frac{d_5}{d_1}\eta^3 + \frac{1}{2}\left(\frac{d_2}{d_1} - d_3 - c_1 d_3\right)\eta_{XX} = 0. \tag{5.12}$$

Letting

$$\alpha_1 = \frac{3}{2}\frac{H^2 - r}{H(r + H)}, \quad \beta_1 = 3\frac{r(1 + H)^2}{H(r + H)^2}, \quad \lambda_1 = \frac{1}{6}\frac{H(rH + 1)}{r + H} - \frac{1}{4}\frac{HS}{r + H}c_1,$$

equation (5.12) becomes

$$-c_1 \eta + \frac{1}{2}\alpha_1\eta^2 - \frac{1}{3}\beta_1\eta^3 + \lambda_1\eta_{XX} = 0.$$

The previous equation has the solitary wave solutions

$$\eta(X) = \left(\frac{\alpha_1}{\beta_1}\right)\frac{1 - \epsilon^2}{1 + \epsilon\cosh(\sqrt{\frac{c_1}{\lambda_1}}X)}, \quad \text{with} \quad \epsilon = \frac{\sqrt{\alpha_1^2 - 6\beta_1 c_1}}{|\alpha_1|}. \tag{5.13}$$

One still has the conditions on S for well-posedness:

$$-(1 + rH) \leq S \leq -\frac{2}{3}(1 + rH).$$

One needs two following conditions for the existence of solution (5.13). The first once is

$$\lambda_1 c_1 > 0 \quad \text{or equivalently} \quad \left(\frac{1}{6}\frac{H(rH + 1)}{r + H} - \frac{1}{4}\frac{HS}{r + H}c_1\right)c_1 > 0.$$

The left hand side of this inequality has two solutions:

$$c_{10} = 0 \quad \text{and} \quad c_{11} = \frac{2}{3}\frac{1 + rH}{S}.$$

Since $S < 0$ one has $c_{11} < c_{10}$. The coefficient of c_1^2 in the inequality is positive. Consequently one must have

$$c_1 > c_{10} = 0 \quad \text{or} \ c_1 < c_{11} = \frac{2}{3}\frac{1 + rH}{S}$$

This second branch is not acceptable since

$$c_{11} = \frac{2}{3}\frac{1 + rH}{S} < \frac{2}{3}\frac{1 + rH}{-\frac{2}{3}(1 + rH)} = -1.$$

It is contradictory to the assumption that $|c_1|$ is very small compared to 1.
The second condition concerns the expression inside the root square in expression of ϵ. One needs

$$\alpha_1^2 - 6\beta c_1 \geq 0.$$

It will be satisfied if one takes

$$c_1 \leq \frac{(H^2 - r)^2}{8rH(1 + H)^2}.$$

Thus, the solitary waves are characterized by wave velocities larger than 1 ($c_1 > 0$). The maximum wave velocity $V_{\max}$ is

$$V_{\max} = 1 + \frac{(H^2 - r)^2}{8rH(1 + H)^2}.$$

In the fixed frame of reference, the profile of the solitary waves (5.13) is given by

$$\eta(x, t) = \left(\frac{\alpha_1}{\beta_1}\right) \frac{1 - \epsilon^2}{1 + \epsilon \cosh\left(\sqrt{\frac{V-1}{\lambda_1}}(x + x_0 - Vt)\right)}. \tag{5.14}$$

When $H^2 > r$ the solitary waves are of elevation. When $H^2 < r$ they are of depression. The parameter ϵ can take values ranging from 0 (infinitely wide solution) to 1 (solution of infinitesimal amplitude).

Since the fluids are assumed to be at rest as $x \to \infty$, one has $M(\pm\infty, t) = 0$. One can compute M explicitly by integrating equation (5.10) with respect to x and neglecting the integral constant

$$M = -\frac{d_4}{4d_1}\eta^2 - \frac{d_2}{2d_1}\eta_{xx} + \frac{d_3}{2}\eta_{xt}.$$

(a)   (b)
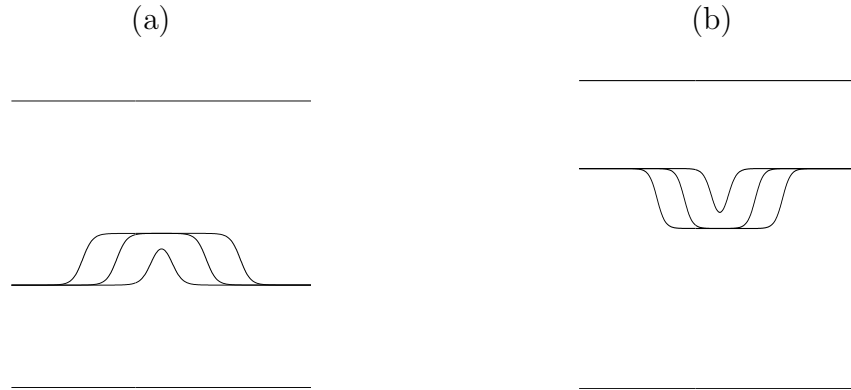

Figure 5.10: 'Table-top' solitary waves which are approximate solutions of the extended Boussinesq system (5.8). The horizontal velocities are taken on the top and the bottom so that $S = -(1 + rH)$. (a) $H = 1.8$, $r = 0.8$. The wave speeds V are, going from the smallest to the widest solitary wave, $V_{\max} - V \sim 10^{-3}, 10^{-9}, 10^{-15}$; (b) $H = 0.4$, $r = 0.9$. The wave speeds V are, going from the smallest to the widest solitary wave, $V_{\max} - V \sim 10^{-3}, 10^{-9}, 10^{-14}$.

Typical approximate solitary waves solutions are shown in Figure 5.10. Notice that the condition $|H^2 - r|$ small is not really satisfied for the selected values of H and r. The reason is that otherwise the waves would have been too small to be clearly visible.

In contrast to the solitary waves obtained by the Boussinesq system, where smaller amplitudes are wider, solitary wave solutions to the extended Boussinesq system with smaller amplitudes are narrower. The amplitude of wave increases when the velocity increases. As the upper limit of velocity V is approached, the wave begin to broaden until the maximum value of V noted $V_{\max}$ given above.

Similar to what was explained at the end of section 5.1.2, different positions of the initial solitary wave along the horizontal axis can be obtained by varying the values of x_0. The initial condition for the left-running wave is a pair $\eta(x, 0)$ and $-W(x, 0)$, where $\eta(x, 0)$ and $W(x, 0)$ form an initial condition for the right-running waves.

5.2.3 Numerical simulations for the extended Boussinesq system

In contrary to the Boussinesq system with quadratic nonlinear terms, where one can choose directly the amplitude of the initial solitary wave, the amplitude of the initial solitary wave of the extended Boussinesq system depends on the choice of c_1 and S. One will observe in the following numerical experiments that the solitary wave solutions to the extended Boussinesq system tend to be flat at an amplitude very small compared to the depth of both two layers.

Once the approximate solitary wave (5.14) has been obtained, it is again possible to make it cleaner by the iterative filtering that has been described in section 5.1.4. Qualitative results for non-filtered solitary waves will be given in this section. Some accurate results for run-ups and phase shifts with filtered waves will be described in the next section.

Figure 5.11 shows the propagation to the left of an almost perfect solitary waves of depression. All of the numerical experiments that we have done show that the solitary waves of small amplitude (not 'table top' waves) solution to the extended Boussinnesq system behave as waves obtained in section 5.1.

Figure 5.12 shows the head-on collision between two almost perfect 'table-top' solitary waves of elevation of equal amplitude moving in opposite directions. As in the case with only quadratic nonlinearities, the solution rises slightly to an amplitude larger than the sum of the amplitudes of the two incident solitary waves. After the collision, two similar waves emerge and return to the form of two separated 'table-top' solitary waves. As a result of this collision, the center of two resulting solitary waves are slightly retarded from the trajectories of the incoming centers.

Figure 5.13 shows the collision of two almost perfect solitary waves of depression of equal amplitude moving in opposite directions. The numerical simulations exhibit the same features that have been observed in the elevation case.

(a) $t = 0$

(b) $t = 400$

(c) $t = 1300$

(d) $t = 2000$

(e) $t = 2800$

(f) evolution in time
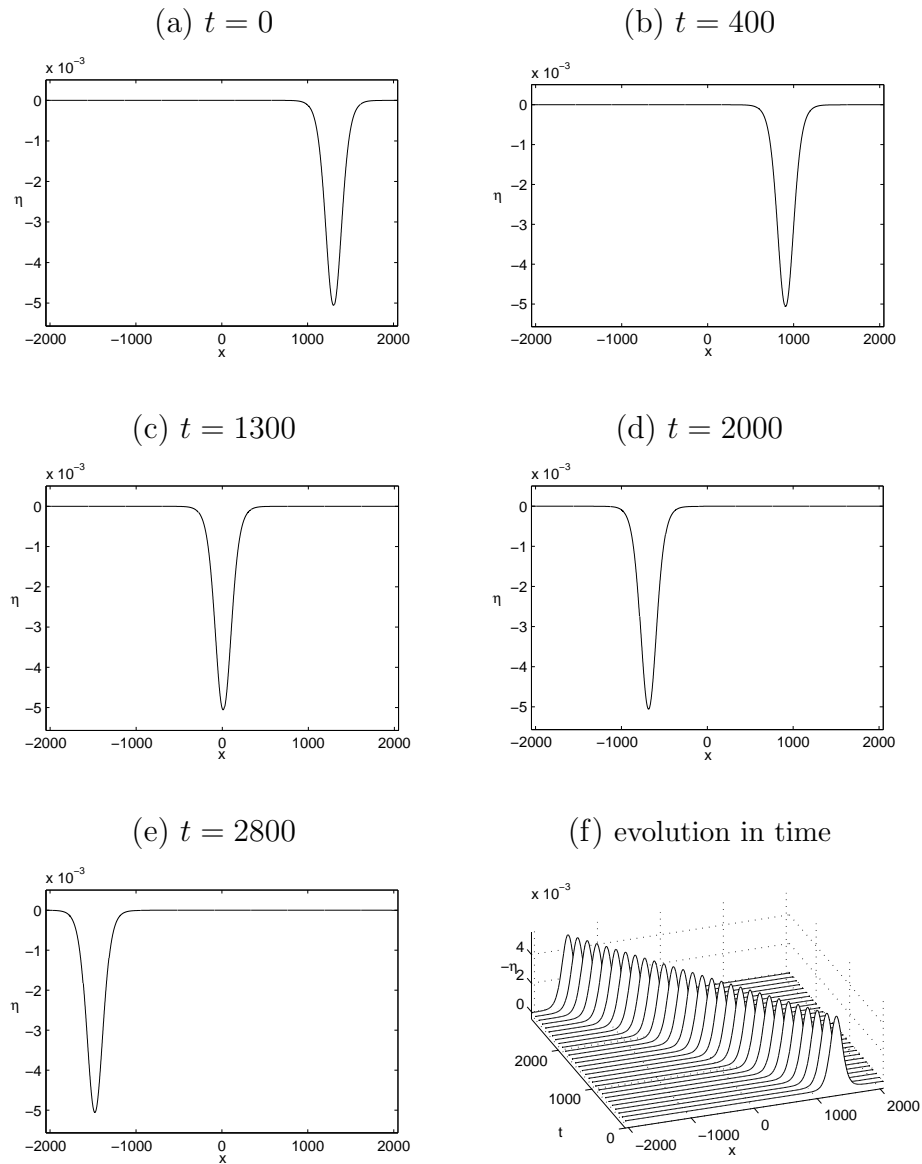
Figure 5.11: An approximate solitary wave of depression propagating to the left. This is a solution to the extended Boussinesq system (5.8) with parameters $H = 0.9$, $r = 0.85$, $L = 4096$, $N = 1024$, $S = -1 - rH$, $\Delta t = 6/N$, $x_0 = -2$, $V = 1 + 5 \times 10^{-5}$, $V_{\max} - V \sim 10^{-5}$. In plot (f), note that $-\eta(x,t)$ has been plotted for the sake of clarity.
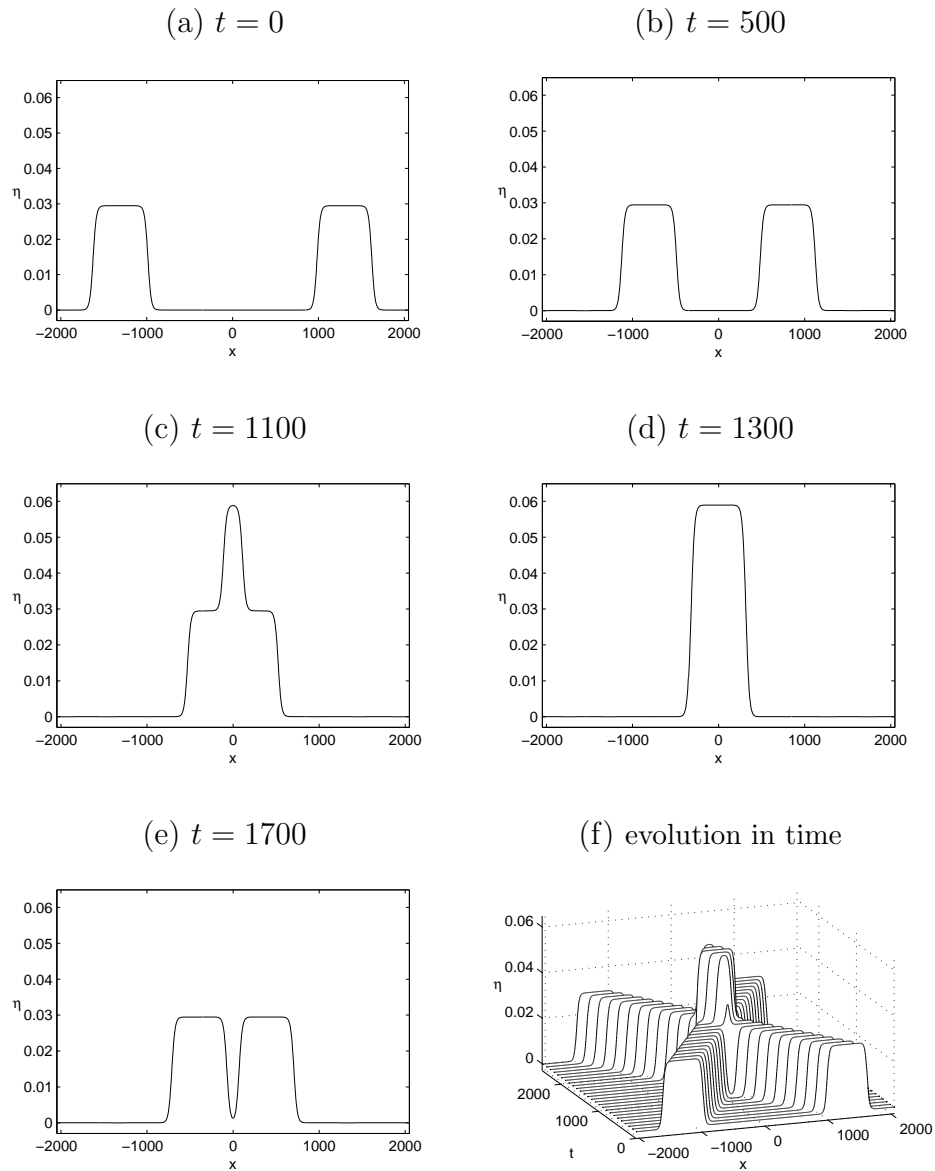
Figure 5.12: Head-on collision of two approximate 'table-top' elevation solitary waves of equal size. This is a solution to the extended Boussinesq system(5.8), with parameters $H = 0.95$, $r = 0.8$, $L = 4096$, $N = 1024$, $S = -1 - rH$, $\Delta t = 2/N$, $x_0^\ell = 2$, $x_0^r = -2$, $V = 1 + 4.544383023634 \times 10^{-4}$, $V_{\max} - V \sim 10^{-17}$.
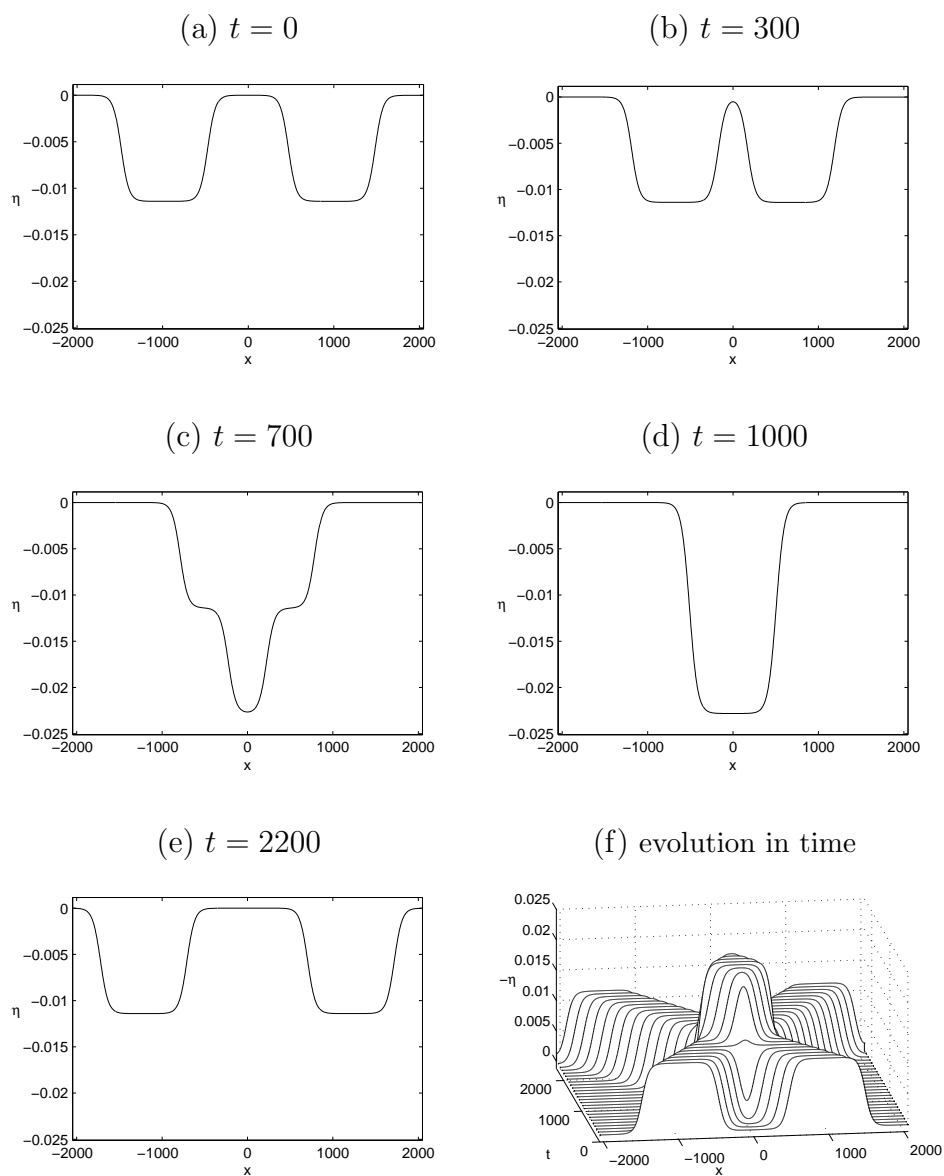
Figure 5.13: Head-on collision of two approximate 'table-top' solitary waves of depression of equal size. This is a solution to the extended Boussinesq system (5.8), with parameters $H = 0.9$, $r = 0.85$, $L = 4096$, $N = 1024$, $S = -1 - rH$, $\Delta t = 2/N$, $x_0^\ell = 1.5$, $x_0^r = -1.5$, $V = 1 + 7.24204732 \times 10^{-5}$, $V_{\max} - V \sim 10^{-14}$. In plot (f), note that $-\eta(x,t)$ has been plotted for the sake of clarity.

(a) $t = 0$

(b) $t = 280$

(c) $t = 520$

(d) $t = 600$

(e) $t = 800$

(f) evolution in time
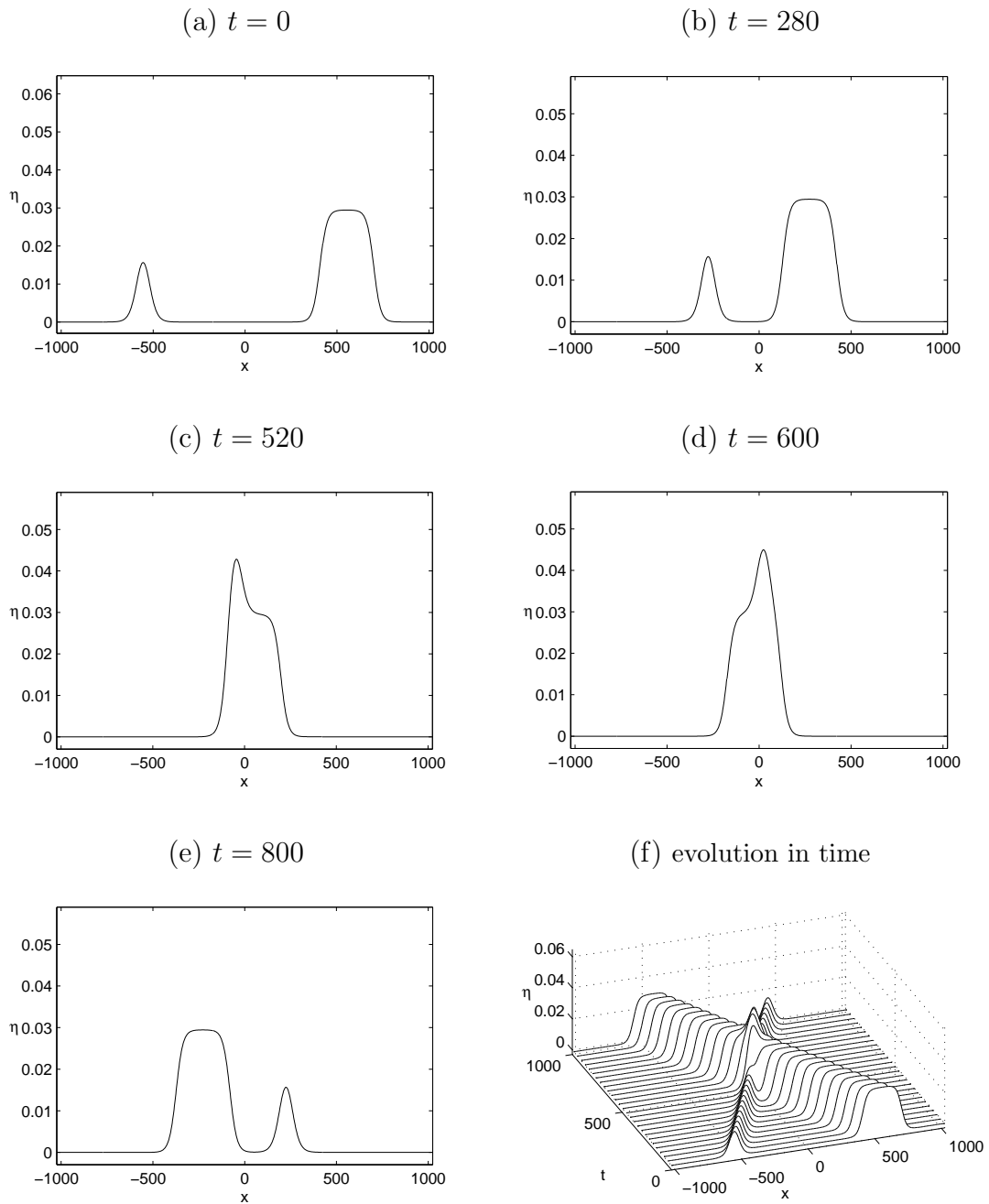
Figure 5.14: Head-on collision of a solitary wave of elevation and a 'table-top' solitary wave of elevation. This is a solution to the extended Boussinesq system (5.8), with parameters $H = 0.95$, $r = 0.8$, $L = 2048$, $N = 1024$, $S = -1 - rH$, $\Delta t = 7/N$, $x_0^\ell = 1.7$, $x_0^r = -1.7$, $V^\ell = 1 + 3.54436 \times 10^{-4}$, $V^r = 1 + 4.54438 \times 10^{-4}$, $V_{\max} - V^\ell \sim 10^{-4}$, $V_{\max} - V^r \sim 10^{-10}$.

Figure 5.14 shows the collision of an almost perfect 'table-top' solitary wave of elevation with a solitary wave of elevation moving in the opposite direction. The numerical simulations exhibit a number of the same features that have been observed in the symmetric case of two 'table top' solitary waves.

Note that in the quadratic as well as in the cubic cases, it is not possible to consider the collision between a solitary wave of depression and a solitary wave of elevation. Indeed the sign of $H^2 - r$ determines whether the wave is of elevation or of depression.

5.2.4   The run-ups and phase shifts

In this section, one concentrates on quantitative studies of run-ups and phase shifts resulting from the collision between two solitary waves solutions to the extended Boussinesq system.

In order to make the high accuracy numerical experiments concerning the collision between two solitary waves, the iterative filtering described in section 5.1.4 will be applied to obtain the initial solitary waves. But in this case much more iterations are needed.

Figure 5.15 shows the effect of cleaning. Starting with a 'table top' solitary wave of amplitude
$$\eta_{\max} = 0.06347607,$$
after 400 iterations of cleaning, one obtains a solitary wave of amplitude

$$\eta_{\max} = 0.06812113.$$

Thus, after several iterations of filtering, the amplitude of the solitary wave reaches an asymptotic level. The resulting waves will propagate in a perfectly stable manner. That is why one will use them to study the run-ups and phase shifts which need high accuracy.

Figure 5.16 shows the collision between two clean 'table-top' solitary waves obtained in the the work showed in Figure 5.15. Two incident solitary waves have the same amplitude
$$\eta_{\max} = 0.06812113$$

(a)

(b)   (c)

(d)   (e)
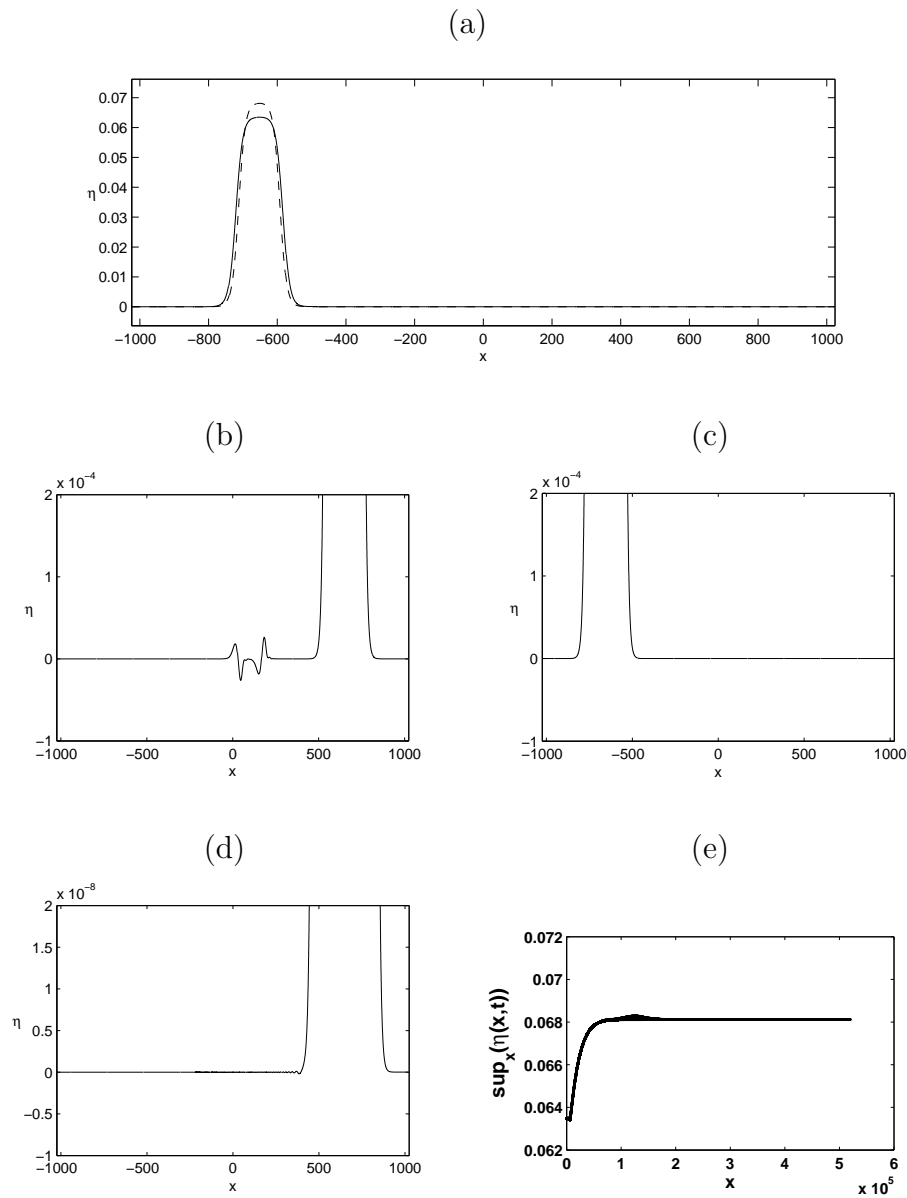
Figure 5.15: Flat solitary wave produced by iterative cleaning. This is a solution to the extended Boussinesq system (5.8) with parameters $H = 1.1$, $r = 0.95$, $L = 2048$, $N = 2^{13}$, $S = -1 - rH$, $\Delta = 8/N$, $x_0 = 2$, $ss = 128$, $V = 1.00183359$, $V_{\max} - V \sim 10^{-8}$. (a) Difference in the profile before (solid line) and after (dashed line) cleaning. (b) Profile of the approximate solitary wave (5.14) after one propagation across the domain. (c) Profile (b) after cleaning and translation to the left of the domain. (d) Profile after several cleanings. Notice the change of scale in the vertical axis. (e) Evolution of the maximum amplitude $\eta_{\max}$ as cleaning is repeated over and over. The amplitude reaches an asymptotic level.

(a)

(b)   (c)

(d)   (e)
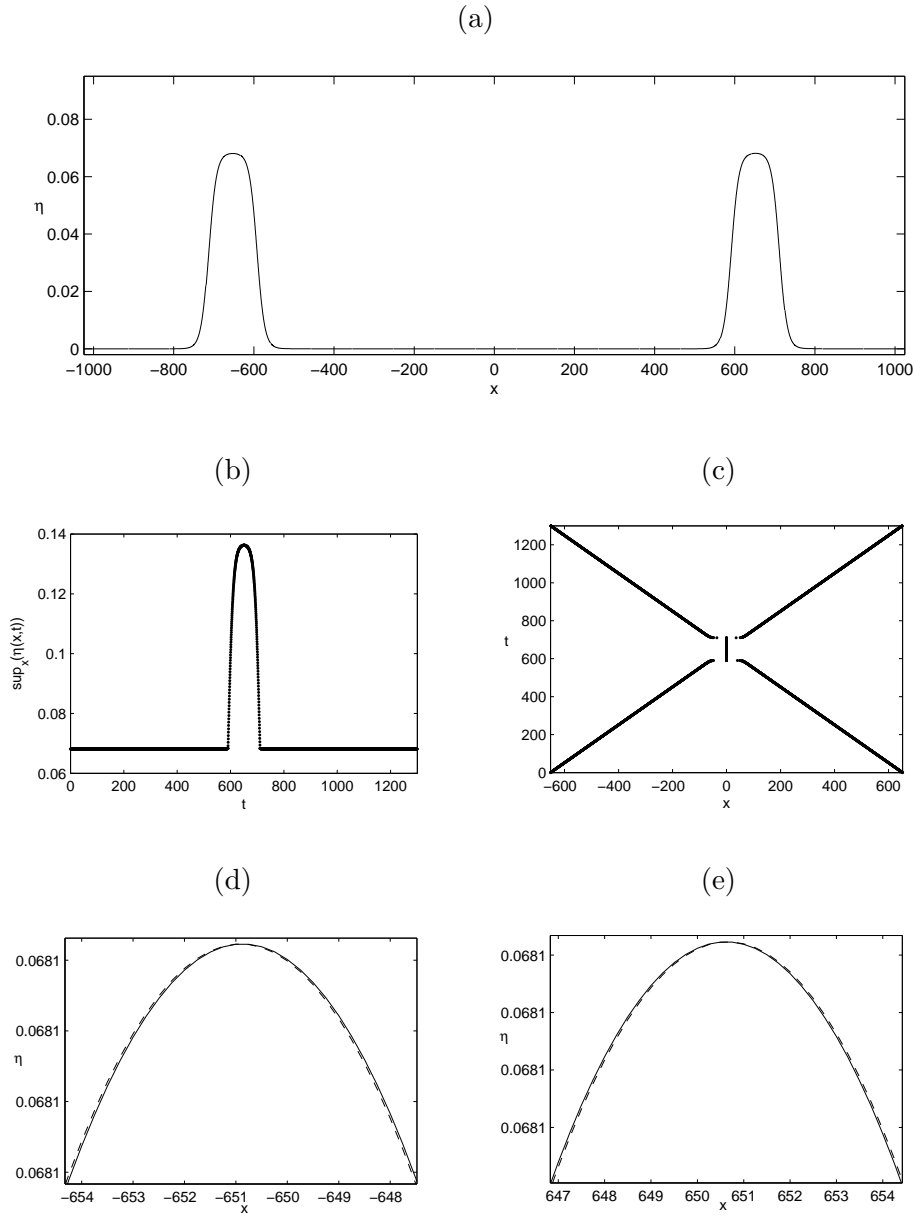
Figure 5.16: A head-on collision between two clean 'table-top' solitary waves of equal height. This is a solution to the system of extended Boussinesq equations (5.8) with parameters $H = 1.1$, $r = 0.95$, $L = 2048$, $N = 2^{13}$, $S = -1 - rH$, $\Delta t = 8/N$, $\eta_{\max}^{\ell} = \eta_{\max}^{r} = 0.06812113$. (a) Initial profiles. (b) Time evolution of the amplitude $\eta_{\max}$. (c) Crest trajectory. (d) Phase shift of the left-running wave, dashed curve represents a left-running wave which propagates without collision. (e) Phase shift of the right-running wave, dashed curve represents a right-running wave which propagates without collision.

The run-up during collision is extremely small. The amplitude of the solution reaches

$$\eta_{\max} = 0.13624323,$$

at collision, which is slightly larger than

$$2 \times 0.06812113 = 0.13624226.$$

After the collision, both resulting solitary waves shift backward an extremely small distance.

Figure 5.17 shows the collision between the clean 'table-top' solitary wave obtained in the work shown in Figure 5.15 and a clean solitary wave.

This shorter clean solitary wave has been obtained by using iterative cleaning from a solitary wave of amplitude

$$\eta_{\max} = 0.03647847.$$

After 230 iterations of cleaning, it reached

$$\eta_{\max} = 0.03719492.$$

The run-up during collision is again extremely small, even if it is larger than in the previous case. Indeed, the amplitude of solution reaches

$$\eta_{\max} = 0.10556057,$$

at collision, which is slightly larger than the sum of the amplitudes of the two incident solitary waves

$$0.06812113 + 0.03719492 = 0.10531605.$$

As in the previous case, the phase shifts after this collision are very small. The crest trajectory shows an interesting path.

Figure 5.18 shows the collision between two 'table-top' clean solitary waves of depression of the same amplitude:

$$-\eta_{\min} = 0.05693521.$$

(a)

(b)   (c)

(d)   (e)

Figure 5.17: A collision between a clean solitary wave and a clean 'table-top' solitary wave. This is a solution to the extended Boussinesq system (5.8) with parameters $H = 1.1$, $r = 0.95$, $L = 2048$, $N = 2^{13}$, $S = -1 - rH$, $\Delta t = 8/N$, $\eta^\ell_{\max} = 0.06812113$, $\eta^r = 0.03719492$. (a) Initial profiles. (b) Time evolution of the amplitude $\eta_{\max}$. (c) Crest trajectory. (d) Phase shift of the left-running wave, dashed curve represents a left-running wave which propagates without collision. (e) Phase shift of the right-running wave, dashed curve represents a right-running wave which propagates without collision.

Figure 5.18: A collision between two 'table-top' clean solitary waves of depression of the same amplitude. This is a solution to the system of extended Boussinesq equations (5.8) with parameters $H = 0.88$, $r = 0.98$, $N = 4096$, $L = 4096$, $S = -1 - rH$, $\Delta t = 8/N$, $-\eta_{\min}^{\ell} = -\eta_{\min}^{r} = 0.05693521$. (a) Initial profiles. (b) Time evolution of the amplitude $\eta_{\min}$. (c) Crest trajectory. (d) Phase shift of left-running wave, dashed line represent a left-running wave which propagates without collision. (e) Phase shift of right-running wave, dashed line represent a right-running wave which propagates without collision.

This solitary wave was obtained from a wave of amplitude $-\eta_{\min} = 0.055149$ after 275 iterations of cleaning.

During the collision, the amplitude reaches

$$-\eta_{\min} = 0.11387060,$$

which is larger than

$$2 \times 0.05693521 = 0.11387042.$$

As in the two previous numerical experiments, after the collision the centers of two solitary waves are retarded from the trajectories of the incoming centers.

Figure 5.19 shows a head-on collision between the 'table-top' clean solitary waves described in the previous numerical experiment and a shorter clean solitary waves. The shorter wave has amplitude

$$-\eta_{\min} = 0.01261376.$$

It was obtained from a solitary wave of amplitude $-\eta_{\min} = 0.01257633$ after 275 iterations of cleaning.

During the collision, the amplitude of the solution reaches

$$-\eta_{\min} = 0.06956701.$$

This is slightly larger than the sum of the amplitudes of the two incident solitary waves:

$$0.05693521 + 0.01261376 = 0.06954897.$$

Similar to the three previous cases, the resulting solitary waves of the collision are retarded from their trajectories.

The overall conclusion is that run-ups and phase shifts are smaller for 'table-top' solitary waves than for 'classical' solitary waves.

Figure 5.20 shows the overtaking collision between two solitary waves of depression of amplitudes

$$-\eta_{\min} = 0.0569 \quad \text{and} \quad -\eta_{\min} = 0.0126.$$

The iterative cleaning that we used to obtain them has been mentioned in the two previous experiments.

(a)

(b)

(c)

(d)

(e)
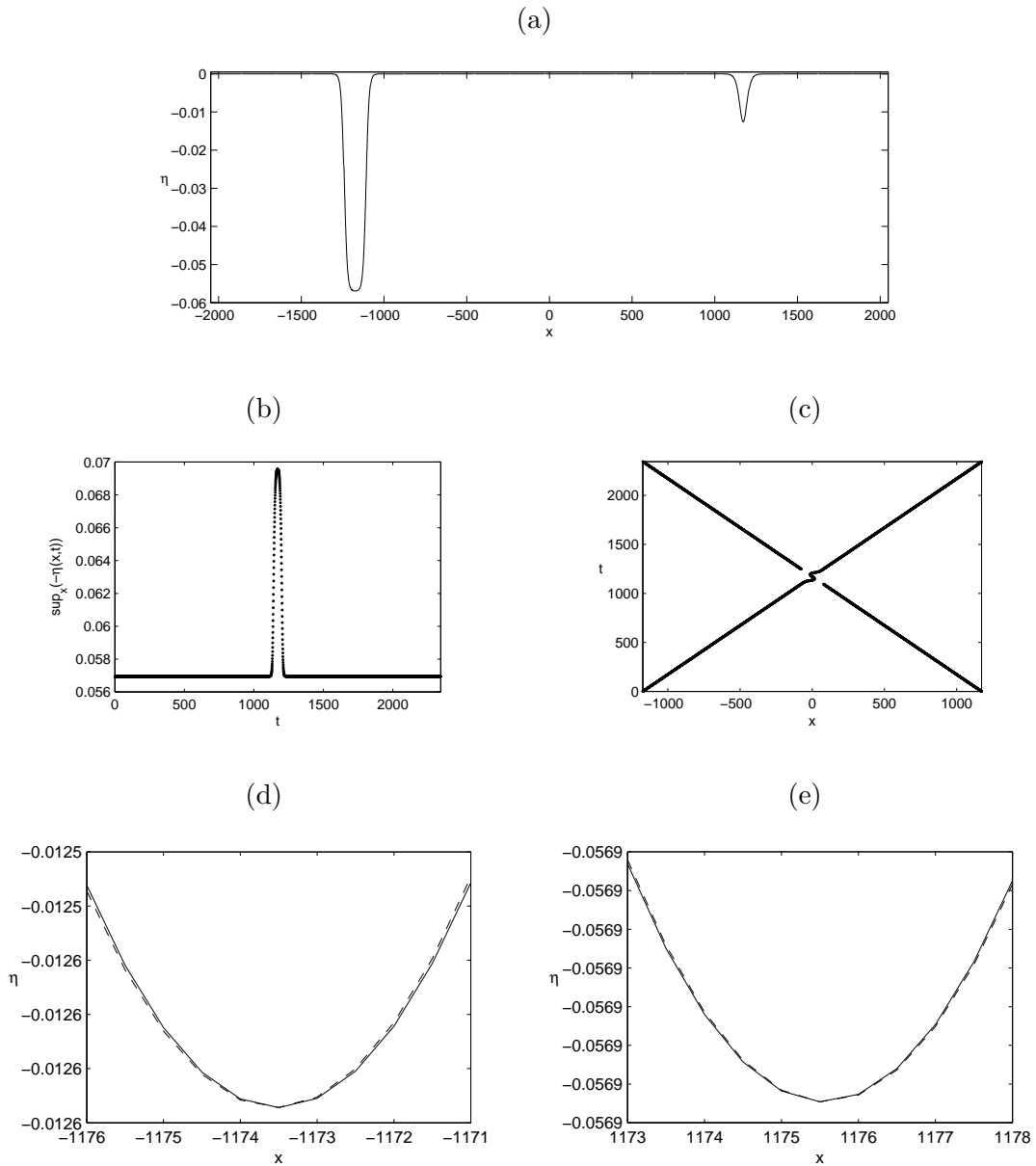
Figure 5.19: A head-on collision between a clean solitary wave of depression and a 'table-top' clean solitary wave of depression. This is a solution to the extended Boussinesq system (5.8) with parameters $H = 0.88$, $r = 0.98$, $L = 4098$, $N = 2^{13}$, $S = -1 - rH$, $\Delta t = 8/N$, $-\eta_{\min}^\ell = 0.05693521$, $-\eta_{\min}^r = 0.01261376$. (a) Initial profiles. (b) Time evolution of the amplitude $-\eta_{\min}$. (c) Crest trajectory. (d) Phase shift of the left-running wave, dashed line represents a left-running wave which propagates without collision. (e) Phase shift of the right-running wave, dashed line represents a right-running wave which propagates without collision.

(a)

(b)

(c)
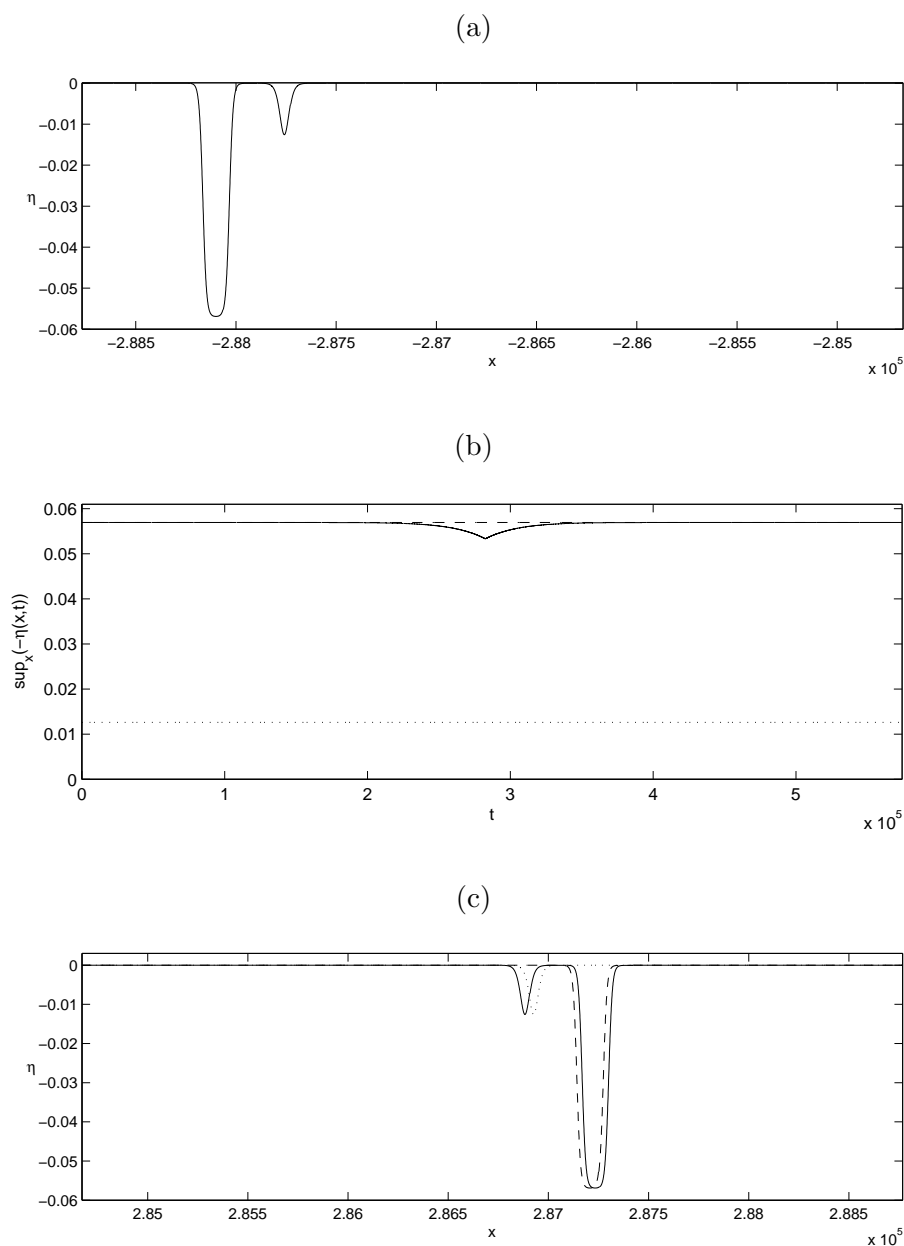
Figure 5.20: Overtaking collision between two solitary waves of depression of different amplitudes. This is a solution to the extended Boussinesq system (5.8) with parameters $H = 0.88$, $r = 0.98$, $L = 4096 \times 141$, $N = 2^{13} \times 141$, $S = -1 - rH$, $\Delta t = 8/N$, $-\eta^\ell_{\min} = 0.0569$, $-\eta^r_{\min} = 0.0126$.(a) Initial profiles. (b) Time evolution of the amplitude $-\eta_{\min}$. (c) Phase shift; dashed and dotted curves represent respectively the propagation of the small and the large waves without overtaking collision.

Similar to what has been shown in Figure (5.9), during this overtaking collision the amplitude of the solution $\eta(x, t)$ never exceeds that of the higher solitary wave, nor does it dip below the amplitude of the shorter.

As a result of the overtaking collision, the higher solitary wave is advanced while the shorter one is retarded from its trajectories. The distance that the shorter wave shifts is larger.

Conclusion and perspectives

In this thesis, two models for interfacial waves have been obtained by using two different methods.

The first model was established by using a perturbation method. It is a model of three equations with three variables: interfacial displacement, horizontal velocities at the interface. This model can be extended to the case where the nonlinear and dispersive parameters α and β are of the same order (not necessary equal), but it requires a lot of tedious calculations.

The second model is a Boussinesq system of three equations with three variables: interfacial displacement, horizontal velocities at the bottom and at the top. This model then has been written with horizontal velocities at arbitrary fluid levels. If one chooses the fluid levels at the interface, this model for $\alpha = \beta$ recovers the first model.

For numerical purpose, we wrote the model with arbitrary horizontal velocities in the form of a system of two equations with two variables: interfacial displacement and combination of horizontal velocities. In the critical case, where the square of the thickness ratio is close to the density ratio, the nonlinear terms become small compared to the dispersive terms. The extended Boussinesq system with cubic nonlinear terms was found to model this situation. This system permits flat solitary wave solutions.

The numerical simulations based on the two previous Boussinesq systems are carried out. We studied the propagation of a solitary wave as well as a flat solitary wave from right to left or left to right of the domain. In the next level of complexity, we studied the head-on collision and the overtaking collision of the solitary waves. We observed the run-ups during the head-on collision and the phase shifts after the collision of both kinds. In order to study quantitatively these phenomena, we used the clean solitary waves resulting from iterative filtering.

We took the horizontal velocities at the bottom and on the roof for most of our experiments. By choosing horizontal velocities at other fluid levels, we can vary the dispersion relation of the Boussinesq systems and study the dispersion effect on the waves. This is one of our perspectives.

From the numerical point of view, we would like to study the stability of our numerical scheme. This work will permit to choose optimal time steps.

In future research, we plan to study the interfacial waves of two-layer fluid in the case where the bottom is not flat.

Appendix A

Intermediate steps in the derivation of the equations by using a perturbation method

It is worth noting that equations (3.77), (3.81) and (3.82) are correct up to order $O(\alpha^2)$. Therefore one can add or eliminate terms of order $O(\alpha^3)$ without disturbing the level of approximation.

The intermediate steps to obtain (3.80)

Combining the 3th and 4th terms of (3.77) gives

$$
\begin{aligned}
& \frac{\alpha}{1 + \frac{r}{H}} \left[(u_0 \eta_{0t} + \frac{r}{H} u_0' \eta_{0t})_x - \alpha (u_0 u_1 - r u_0' u_1')_{xx} \right] \\
= & \frac{\alpha}{1 + \frac{r}{H}} \left[(u_0 \eta_{0t} - \alpha u_{0x} u_1 - \alpha u_0 u_{1x})_x + \left(\frac{r}{H} u_0' \eta_{0t} + \alpha r u_{0x}' u_1' + \alpha r u_0' u_{1x}' \right)_x \right] \\
= & \frac{\alpha}{1 + \frac{r}{H}} \left[(-u_0 u_{0x} - \alpha u_{0x} u_1 - \alpha u_0 u_{1x}) + (r u_0' u_{0x}' + \alpha r u_{0x}' u_1' + \alpha r u_0' u_{1x}') \right]_x \\
= & \frac{\alpha}{1 + \frac{r}{H}} \left[(-u_0 u_{0x} - \alpha u_{0x} u_1 - \alpha u_0 u_{1x} - \alpha^2 u_1 u_{1x}) + \hspace{2cm} \text{(A-1)} \right. \\
& \left. (r u_0' u_{0x}' + \alpha r u_{0x}' u_1' + \alpha r u_0' u_{1x}' + r \alpha^2 u_1' u_{1x}') \right]_x \\
= & \frac{\alpha}{1 + \frac{r}{H}} [-(u_0 + \alpha u_1)(u_{0x} + \alpha u_{1x}) + r(u_0' + \alpha u_1')(u_{0x}' + \alpha u_{1x}')]_x \\
= & -\frac{\alpha}{1 + \frac{r}{H}} (u u_x - r u' u_x')_x.
\end{aligned}
$$

123

The 5th term of (3.77) can be written in the form

$$-\frac{\alpha^2(1-r)}{1+\frac{r}{H}}(\eta_{0t}\eta_{0xt})_x = -\frac{\alpha^2}{1+\frac{r}{H}}(\eta_{0t}\eta_{0xt} - r\eta_{0t}\eta_{0xt})_x$$

$$= -\frac{\alpha^2}{1+\frac{r}{H}}(u_{0x}u_{0xx} - rH^2u'_{0x}u'_{0xx})_x \qquad (A\text{-}2)$$

$$= -\frac{\alpha^2}{1+\frac{r}{H}}(u_xu_{xx} - rH^2u'_xu'_{xx})_x.$$

The 6th term of (3.77) can be written in the form

$$-\frac{\alpha^2(1-r)}{1+\frac{r}{H}}(\eta_0\eta_{0tt})_{xx} = -\frac{\alpha^2}{1+\frac{r}{H}}(\eta_0\eta_{0tt} - r\eta_0\eta_{0tt})_{xx}$$

$$= -\frac{\alpha^2}{1+\frac{r}{H}}(-\eta_0u_{0xt} - rH\eta_0u'_{0xt})_{xx} \qquad (A\text{-}3)$$

$$= \frac{\alpha^2}{1+\frac{r}{H}}(\eta u_{xt} + rH\eta u'_{xt})_{xx}.$$

Combining the 7th, 8th and 9th terms of (3.77) will be done in two steps. First, one combines the 7th and 8th terms as follows:

$$\frac{\alpha}{1+\frac{r}{H}}(u_0\eta_{0x} + \frac{r}{H}u'_0\eta_{0x} + \alpha u_0\eta_{1x} + \alpha\frac{r}{H}u'_0\eta_{1x})_t + \alpha\frac{\frac{r}{H^2}-1}{1+\frac{r}{H}}(\eta_0\eta_{0t} + \alpha\eta_1\eta_{0t})_t$$

$$= \frac{\alpha}{1+\frac{r}{H}}\Big[(u_0\eta_{0x} + \alpha u_0\eta_{1x} - \eta_0\eta_{0t} - \alpha\eta_1\eta_{0t})$$

$$+(\frac{r}{H}u'_0\eta_{0x} + \alpha\frac{r}{H}u'_0\eta_{1x}) + \frac{r}{H^2}(\eta_0\eta_{0t} + \alpha\eta_1\eta_{0t})\Big]_t$$

$$= \frac{\alpha}{1+\frac{r}{H}}\Big[(u_0\eta_{0x} + \alpha u_0\eta_{1x} + u_{0x}\eta_0 + \alpha u_{0x}\eta_1)$$

$$+\frac{r}{H}(u'_0\eta_{0x} + \alpha u'_0\eta_{1x} + u'_{0x}\eta_0 + \alpha u'_{0x}\eta_1)\Big]_t$$

$$= \frac{\alpha}{1+\frac{r}{H}}\Big[(u_0\eta_0 + \alpha u_0\eta_1) + \frac{r}{H}(u'_0\eta_0 + \alpha u'_0\eta_1)\Big]_{xt}.$$

Then we combine this result with the 9th term

$$\frac{\alpha}{1+\frac{r}{H}}\Big[(u_0\eta_0 + \alpha u_0\eta_1) + \frac{r}{H}(u'_0\eta_0 + \alpha u'_0\eta_1)\Big]_{xt} + \frac{\alpha^2}{1+\frac{r}{H}}(u_1\eta_0 + \frac{r}{H}u'_1\eta_0)_{xt}$$

$$
= \frac{\alpha}{1 + \frac{r}{H}} \left[(u_0 \eta_0 + \alpha u_0 \eta_1 + \alpha u_1 \eta_0) + \frac{r}{H} (u_0' \eta_0 + \alpha u_0' \eta_1 + \alpha u_1' \eta_0)_{xt} \right]_{xt} \quad \text{(A-4)}
$$

$$
= \frac{\alpha}{1 + \frac{r}{H}} (u\eta + \frac{r}{H} u' \eta)_{xt}.
$$

In order to combine the 10th, 11th, 12th, 13th and 14th terms of (3.77), one shows first that

$$
\begin{aligned}
\frac{\frac{\alpha}{3}}{1 + \frac{r}{H}} u_{xxxt} &= \frac{\frac{\alpha}{3}}{1 + \frac{r}{H}} (u_0 + \alpha u_1)_{xxxt} \\
&= \frac{\frac{\alpha}{3}}{1 + \frac{r}{H}} u_{0xxxt} + \frac{\frac{\alpha^2}{3}}{1 + \frac{r}{H}} u_{1xxxt} \\
&= -\frac{\frac{\alpha}{3}}{1 + \frac{r}{H}} \eta_{0xxtt} + \frac{\frac{\alpha^2}{3}}{1 + \frac{r}{H}} (-w_{1z})_{xxt} \quad \text{(A-5)} \\
&= -\frac{\frac{\alpha}{3}}{1 + \frac{r}{H}} \eta_{0xxtt} + \frac{\frac{\alpha^2}{3}}{1 + \frac{r}{H}} (\frac{1}{3} \eta_{0xxt} + \eta_0 \eta_{0t} - \eta_{1t} - u_0 \eta_{0x})_{xxt} \\
&= -\frac{\frac{\alpha}{3}}{1 + \frac{r}{H}} \eta_{0xxtt} + \frac{\frac{\alpha^2}{9}}{1 + \frac{r}{H}} \eta_{0xxxxtt} + \frac{\frac{\alpha^2}{3}}{1 + \frac{r}{H}} (\eta_0 \eta_{0t})_{xxt} \\
&\quad - \frac{\frac{\alpha^2}{3}}{1 + \frac{r}{H}} \eta_{1xxtt} - \frac{\frac{\alpha^2}{3}}{1 + \frac{r}{H}} (u_0 \eta_{0x})_{xxt}.
\end{aligned}
$$

Then

$$
\begin{aligned}
-\frac{\frac{\alpha r H^2}{3}}{1 + \frac{r}{H}} u'_{xxxt} &= -\frac{\frac{\alpha r H^2}{3}}{1 + \frac{r}{H}} (u_0' + \alpha u_1')_{xxxt} \\
&= -\frac{\frac{\alpha r H^2}{3}}{1 + \frac{r}{H}} u'_{0xxxt} - \frac{\frac{\alpha^2 r H^2}{3}}{1 + \frac{r}{H}} u'_{1xxxt} \\
&= -\frac{\frac{\alpha r H}{3}}{1 + \frac{r}{H}} \eta_{0xxtt} - \frac{\frac{\alpha^2 r H^2}{3}}{1 + \frac{r}{H}} (-w'_{1z})_{xxt} \quad \text{(A-6)} \\
&= -\frac{\frac{\alpha r H}{3}}{1 + \frac{r}{H}} \eta_{0xxtt} + \frac{\frac{\alpha^2 r H^2}{3}}{1 + \frac{r}{H}} (\frac{H}{3} \eta_{0xxt} - \frac{1}{H^2} \eta_0 \eta_{0t} - \frac{1}{H} \eta_{1t} - \frac{1}{H} u_0' \eta_{0x})_{xxt} \\
&= -\frac{\frac{\alpha r H}{3}}{1 + \frac{r}{H}} \eta_{0xxtt} + \frac{\frac{\alpha^2 r H^3}{9}}{1 + \frac{r}{H}} \eta_{0xxxxtt} - \frac{\frac{\alpha^2 r}{3}}{1 + \frac{r}{H}} (\eta_0 \eta_{0t})_{xxt} \\
&\quad - \frac{\frac{\alpha^2 r H}{3}}{1 + \frac{r}{H}} \eta_{1xxtt} - \frac{\frac{\alpha^2 r H}{3}}{1 + \frac{r}{H}} (u_0' \eta_{0x})_{xxt}.
\end{aligned}
$$

Finally, adding term by term equations (A-5) and (A-6) yields

$$\frac{\frac{\alpha}{3}}{1+\frac{r}{H}}u_{xxxt} - \frac{\frac{\alpha r H^2}{3}}{1+\frac{r}{H}}u'_{xxxt} = -\alpha\frac{\frac{1+rH}{3}}{1+\frac{r}{H}}\eta_{0xxtt} - \alpha^2\frac{\frac{1+rH}{3}}{1+\frac{r}{H}}\eta_{1xxtt}$$

$$+ \frac{\frac{\alpha^2}{9}}{1+\frac{r}{H}}\eta_{0xxxxtt} + \frac{\frac{\alpha^2 r H^3}{9}}{1+\frac{r}{H}}\eta_{0xxxxtt}$$

$$+ \frac{\frac{\alpha^2(1-r)}{3}}{1+\frac{r}{H}}(\eta_0\eta_{0t})_{xxt} - \frac{\frac{\alpha^2}{3}}{1+\frac{r}{H}}(u_0\eta_{0x} + rHu'_0\eta_{0x})_{xxt}$$

$$= \left(\textit{The sum of the }10^{th},\ 11^{th},\ 12^{th},\ 13^{th},\textit{ and }14^{th}\textit{ terms}\right.$$

$$\left.\textit{of }(3.77)\right) + \frac{\alpha^2\frac{2}{15}}{1+\frac{r}{H}}(\eta_{0xxxxtt} + rH^3\eta_{0xxxxtt})$$

$$= \left(\textit{The sum of the }10^{th},\ 11^{th},\ 12^{th},\ 13^{th},\textit{ and }14^{th}\textit{ terms}\right.$$

$$\left.\textit{of }(3.77)\right) - \frac{\alpha^2\frac{2}{15}}{1+\frac{r}{H}}(u_{0xxxxxt} - rH^4u'_{0xxxxxt}).$$

One deduces from the previous equation that

$$\textit{The sum of the }10^{th},\ 11^{th},\ 12^{th},\ 13^{th},\textit{ and }14^{th}\textit{ terms of }(3.77)$$

$$= \frac{\frac{\alpha}{3}}{1+\frac{r}{H}}u_{xxxt} - \frac{\frac{\alpha r H^2}{3}}{1+\frac{r}{H}}u'_{xxxt} + \frac{\alpha^2\frac{2}{15}}{1+\frac{r}{H}}(u_{0xxxxxt} - rH^4u'_{0xxxxxt}) \qquad \text{(A-7)}$$

Combining (A-1),(A-2),(A-3),(A-4) and (A-7) with the first and the second terms of (3.77) one obtains the following equation to model interfacial waves:

$$\eta_{tt} - \frac{1-r}{1+\frac{r}{H}}\eta_{xx} - \frac{\alpha}{1+\frac{r}{H}}(uu_x - ru'u'_x)_x$$

$$-\frac{\alpha^2}{1+\frac{r}{H}}(u_xu_{xx} - rH^2u'_xu'_{xx})_x + \frac{\alpha^2}{1+\frac{r}{H}}(\eta u_{xt} + rH\eta u'_{xt})_{xx}$$

$$+\frac{\alpha}{1+\frac{r}{H}}(u\eta + \frac{r}{H}u'\eta)_{xt} + \frac{\frac{\alpha}{3}}{1+\frac{r}{H}}u_{xxxt} - \frac{\frac{\alpha r H^2}{3}}{1+\frac{r}{H}}u'_{xxxt}$$

$$+\frac{\alpha^2\frac{2}{15}}{1+\frac{r}{H}}(u - rH^4u')_{xxxxxt} = 0$$

The intermediate steps to obtain (3.81):

Equation (3.78) can be written in the form

$$
\begin{aligned}
u_x &= -\eta_t + \alpha\frac{1}{3}\Big(\eta_{0xxt} + \alpha\eta_{1xxt}\Big) + \alpha\Big(\eta_0\eta_{0t} + \alpha\eta_1\eta_{0t} - \alpha\eta_0 u_{1x}\Big) \\
&\quad -\alpha\Big(u_0\eta_{0x} + \alpha u_0\eta_{1x} + \alpha u_1\eta_{0x}\Big) \\
&\quad +\alpha^2\frac{1}{45}\eta_{0xxxxt} - \alpha^2\frac{1}{3}(\eta_0\eta_{0t} - u_0\eta_{0x})_{xx}
\end{aligned}
\tag{A-8}
$$

The 2th term of (A-8):

$$
\alpha\frac{1}{3}\Big(\eta_{0xxt} + \alpha\eta_{1xxt}\Big) = \alpha\frac{1}{3}\eta_{xxt}
\tag{A-9}
$$

The 3th term of (A-8):

$$
\begin{aligned}
\alpha\Big(\eta_0\eta_{0t} + \alpha\eta_1\eta_{0t} - \alpha\eta_0 u_{1x}\Big) &= \alpha\Big((\eta_0 + \alpha\eta_1)\eta_{0t} - \alpha\eta u_{1x}\Big) \\
&= \alpha(\eta\eta_{0t} - \alpha\eta u_{1x}) \\
&= -\alpha(\eta u_{0x} + \alpha\eta u_{1x}) \\
&= -\alpha\eta u_x
\end{aligned}
\tag{A-10}
$$

The 4th term of (A-8):

$$
\begin{aligned}
-\alpha\Big(u_0\eta_{0x} + \alpha u_0\eta_{1x} + \alpha u_1\eta_{0x}\Big) &= -\alpha\Big(u_0(\eta_{0x} + \alpha\eta_{1x}) + \alpha u_1\eta_x\Big) \\
&= -\alpha(u_0\eta_x + \alpha u_1\eta_x) \\
&= -\alpha(u_0 + \alpha u_1)\eta_x \\
&= -\alpha u\eta_x
\end{aligned}
\tag{A-11}
$$

The 5th term of (A-8):

$$
\begin{aligned}
&\alpha^2\frac{1}{45}\eta_{0xxxxt} - \alpha^2\frac{1}{3}(\eta_0\eta_{0t} - u_0\eta_{0x})_{xx} \\
&= \alpha^2\frac{1}{45}\eta_{xxxxt} - \alpha^2\frac{1}{3}(\eta\eta_t - u\eta_x)_{xx}
\end{aligned}
\tag{A-12}
$$

Substituting (A-9)-(A-12) in (A-8) yields

$$
\begin{aligned}
u_x &= -\eta_t + \alpha\frac{1}{3}\eta_{xxt} - \alpha(u\eta)_x \\
&\quad +\alpha^2\frac{1}{45}\eta_{xxxxt} - \alpha^2\frac{1}{3}(\eta\eta_t - u\eta_x)_{xx}
\end{aligned}
\tag{A-13}
$$

The intermediate steps to obtain (3.82):

Equation (3.79) can be written in the form

$$
\begin{aligned}
u'_x \;=\;& \frac{1}{H}\eta_t - \alpha\frac{H}{3}\Big(\eta_{0xxt} + \alpha\eta_{1xxt}\Big) && \text{(A-14)}\\
&+\alpha\frac{1}{H}\Big(\frac{1}{H}\eta_0\eta_{0t} + \frac{1}{H}\alpha\eta_1\eta_{0t} + \alpha\eta_0 u'_{1x}\Big)\\
&+\alpha\frac{1}{H}(u'_0\eta_{0x} + \alpha u'_0\eta_{1x} + \alpha u'_1\eta_{0x})\\
&-\alpha^2\frac{H^3}{45}\eta_{0xxxxt} - \alpha^2\frac{1}{3}(\eta_0\eta_{0t} + Hu'_0\eta_{0x})_{xx}
\end{aligned}
$$

The 2th term of (A-14):

$$
-\alpha\frac{H}{3}\Big(\eta_{0xxt} + \alpha\eta_{1xxt}\Big) = -\alpha\frac{H}{3}\eta_{xxt} \tag{A-15}
$$

The 3th term of (A-14):

$$
\begin{aligned}
&\alpha\frac{1}{H}\Big(\frac{1}{H}\eta_0\eta_{0t} + \frac{1}{H}\alpha\eta_1\eta_{0t} + \alpha\eta_0 u'_{1x}\Big)\\
&= \alpha\frac{1}{H}\Big(\frac{1}{H}(\eta_0 + \alpha\eta_1)\eta_{0t} + \alpha\eta u'_{1x}\Big)\\
&\qquad = \alpha\frac{1}{H}\Big(\frac{1}{H}\eta\eta_{0t} + \alpha\eta u'_{1x}\Big) \tag{A-16}\\
&\qquad\qquad = \alpha\frac{1}{H}\Big(\eta u'_{0x} + \alpha\eta u'_{1x}\Big)\\
&\qquad\qquad\qquad = \alpha\frac{1}{H}\eta u'_x
\end{aligned}
$$

The 4th term of (A-14):

$$
\begin{aligned}
&\alpha\frac{1}{H}\Big(u'_0\eta_{0x} + \alpha u'_0\eta_{1x} + \alpha u'_1\eta_{0x}\Big)\\
&= \alpha\frac{1}{H}\Big(u'_0(\eta_{0x} + \alpha\eta_{1x}) + \alpha u'_1\eta_x\Big) \tag{A-17}\\
&\qquad = \alpha\frac{1}{H}\Big(u'_0\eta_x + \alpha u'_1\eta_x\Big)\\
&\qquad\qquad = \alpha\frac{1}{H}(u'_0 + \alpha u'_1)\eta_x\\
&\qquad\qquad\qquad = \alpha\frac{1}{H}u'\eta_x
\end{aligned}
$$

The 5th term of (A-14):

$$-\alpha^2\frac{H^3}{45}\eta_{0xxxxt} - \alpha^2\frac{1}{3}(\eta_0\eta_{0t} + Hu'_0\eta_{0x})_{xx} \qquad\qquad \text{(A-18)}$$
$$= -\alpha^2\frac{H^3}{45}\eta_{xxxxt} - \alpha^2\frac{1}{3}(\eta\eta_t + Hu'\eta_x)_{xx}$$

Substituting (A-15)-(A-18) into (A-14) yields

$$\begin{aligned} u'_x &= \frac{1}{H}\eta_t - \alpha\frac{H}{3}\eta_{xxt} + \alpha\frac{1}{H}(\eta u')_x \\ &\quad -\alpha^2\frac{H^3}{45}\eta_{xxxxt} - \alpha^2\frac{1}{3}(\eta\eta_t + Hu'\eta_x)_{xx} \end{aligned} \qquad\qquad \text{(A-19)}$$

Appendix B

Intermediate steps used to derive the results in chapter 4

a. Intermediate steps to obtain the dispersion relations (4.40) and (4.41)

Look for solutions η, u and u' proportional to $\exp(ikx - i\omega t)$. In Fourier space, system (4.39) can be written as

$$
\begin{pmatrix}
-i\omega & ik + \dfrac{\beta}{2}(\theta^2 - \dfrac{1}{3})(ik)^3 & 0 \\[2ex]
-i\omega & 0 & -Hik - \dfrac{\beta}{2}H(\theta'^2 - \dfrac{H^2}{3})(ik)^3 \\[2ex]
(1-r)(ik) & -i\omega + \dfrac{\beta}{2}(\theta^2 - 1)(ik)^2(-i\omega) & -r(-i\omega) - \dfrac{\beta}{2}r(\theta'^2 - H^2)(ik)^2(-i\omega)
\end{pmatrix}
\begin{pmatrix}
\hat{\eta} \\[2ex]
\hat{w} \\[2ex]
\hat{w}'
\end{pmatrix}
= 0
$$

or equivalently

$$
\begin{pmatrix}
-i\omega & ik\left(1 - \dfrac{\beta}{2}(\theta^2 - \dfrac{1}{3})k^2\right) & 0 \\[2ex]
-i\omega & 0 & -Hik\left(1 - \dfrac{\beta}{2}(\theta'^2 - \dfrac{H^2}{3})k^2\right) \\[2ex]
(1-r)(ik) & -i\omega\left(1 - \dfrac{\beta}{2}(\theta^2 - 1)k^2\right) & r(i\omega)\left(1 - \dfrac{\beta}{2}(\theta'^2 - H^2)k^2\right)
\end{pmatrix}
\begin{pmatrix}
\hat{\eta} \\[2ex]
\hat{w} \\[2ex]
\hat{w}'
\end{pmatrix}
= 0.
$$

System (4.39) has a non-trivial solution only if the previous matrix is not invertible,

i.e.

$$
\begin{vmatrix}
-i\omega & ik\left(1 - \frac{\beta}{2}(\theta^2 - \frac{1}{3})k^2\right) & 0 \\[2mm]
-i\omega & 0 & -Hik\left(1 - \frac{\beta}{2}(\theta'^2 - \frac{H^2}{3})k^2\right) \\[2mm]
(1-r)(ik) & -i\omega\left(1 - \frac{\beta}{2}(\theta^2 - 1)k^2\right) & r(i\omega)\left(1 - \frac{\beta}{2}(\theta'^2 - H^2)k^2\right)
\end{vmatrix} = 0.
$$

It follows that

$$
\frac{\omega^2}{k^2} =
$$

$$
\frac{H(1-r)\left(1 - \frac{\beta}{2}(\theta^2 - \frac{1}{3})k^2\right)\left(1 - \frac{\beta}{2}(\theta'^2 - \frac{1}{3}H^2)k^2\right)}{H\left(1 - \frac{\beta}{2}(\theta^2 - 1)k^2\right)\left(1 - \frac{\beta}{2}(\theta'^2 - \frac{1}{3}H^2)k^2\right) + r\left(1 - \frac{\beta}{2}(\theta^2 - \frac{1}{3})k^2\right)\left(1 - \frac{1}{2}\beta(\theta'^2 - H^2)k^2\right)}.
$$

In order to obtain the dispersion relation written in physical variables, we switching back to physical variables

$$
x = \frac{1}{\ell}x^*, \quad t = \frac{c_0}{\ell}t^*, \quad \eta = \frac{1}{A}\eta^*, \quad w = \frac{c_0}{gA}w^*, \quad w' = \frac{c_0}{gA}w'^*.
$$

System (4.39) is written as

$$
\begin{cases}
\eta_t + hw_x + \frac{1}{2}h^3\left(\theta^2 - \frac{1}{3}\right)w_{xxx} = 0 \\[3mm]
\eta_t - Hhw'_x - \frac{1}{2}Hh^3\left(\theta'^2 - \frac{1}{3}H^2\right)w'_{xxx} = 0 \\[3mm]
g(1-r)\eta_x + w_t + \frac{1}{2}h^2(\theta^2 - 1)w_{xxt} - rw'_t - \frac{1}{2}h^2 r(\theta'^2 - H^2)w'_{xxt} = 0
\end{cases}
\qquad . \quad \text{(B-1)}
$$

Similarly, one looks for solution η, u, u' proportional to $\exp(ikx - i\omega t)$. In Fourier space, the previous system becomes

$$
\begin{pmatrix}
-i\omega & ikh + \frac{h^3}{2}(\theta^2 - \frac{1}{3})(ik)^3 & 0 \\[2mm]
-i\omega & 0 & -Hhik - \frac{h^3 H}{2}(\theta'^2 - \frac{1}{3}H^2)(ik)^3 \\[2mm]
g(1-r)(ik) & -i\omega + \frac{h^2}{2}(\theta^2 - 1)(ik)^2(-i\omega) & -r(-i\omega) - \frac{h^2 r}{2}(\theta'^2 - H^2)(ik)^2(-i\omega)
\end{pmatrix}
\begin{pmatrix}
\hat{\eta} \\[2mm]
\hat{w} \\[2mm]
\hat{w}'
\end{pmatrix} = 0
$$

or equivalently

$$
\begin{pmatrix}
-i\omega & ikh\left(1 - \frac{h^2}{2}\left(\theta^2 - \frac{1}{3}\right)k^2\right) & 0 \\[2mm]
-i\omega & 0 & -Hhik\left(1 - \frac{h^2}{2}\left(\theta'^2 - \frac{H^2}{3}\right)k^2\right) \\[2mm]
g(1-r)(ik) & -i\omega\left(1 - \frac{h^2}{2}(\theta^2 - 1)k^2\right) & r(i\omega)\left(1 - \frac{h^2}{2}(\theta'^2 - H^2)k^2\right)
\end{pmatrix}
\begin{pmatrix}
\hat{\eta} \\[2mm] \hat{w} \\[2mm] \hat{w}'
\end{pmatrix} = 0.
$$

System (B-1) has a not-trivial solution only if the previous matrix is not invertible, i.e

$$
\begin{vmatrix}
-i\omega & ikh\left(1 - \frac{h^2}{2}\left(\theta^2 - \frac{1}{3}\right)k^2\right) & 0 \\[2mm]
-i\omega & 0 & -Hhik\left(1 - \frac{h^2}{2}\left(\theta'^2 - \frac{H^2}{3}\right)k^2\right) \\[2mm]
g(1-r)(ik) & -i\omega\left(1 - \frac{h^2}{2}(\theta^2 - 1)k^2\right) & r(i\omega)\left(1 - \frac{h^2}{2}(\theta'^2 - H^2)k^2\right)
\end{vmatrix} = 0.
$$

It follows that

$$
\frac{\omega^2}{k^2} =
$$

$$
\frac{ghH(1-r)\left(1 - \frac{h^2}{2}(\theta^2 - \frac{1}{3})k^2\right)\left(1 - \frac{h^2}{2}(\theta'^2 - \frac{H^2}{3})k^2\right)}{H\left(1 - \frac{h^2}{2}(\theta^2 - 1)k^2\right)\left(1 - \frac{h^2}{2}(\theta'^2 - \frac{H^2}{3})k^2\right) + r\left(1 - \frac{h^2}{2}(\theta^2 - \frac{1}{3})k^2\right)\left(1 - \frac{h^2}{2}(\theta'^2 - H^2)k^2\right)}.
$$

b. Intermediate steps to obtain equations (4.60) and (4.61).

Adding H times equation (4.35) to r times equation (4.36) yields

$$
(r + H)\eta_t + H(w_x - rw'_x) + \alpha[(Hw + rw')\eta]_x
$$
$$
+ \frac{H}{2}\beta\left[(\theta^2 - \frac{1}{3})w_{xxx} - r(\theta'^2 - \frac{1}{3}H^2)w'_{xxx}\right]
$$
$$
+ \frac{1}{2}\alpha\beta\left[H(\theta^2 - 1)(\eta w_{xx})_x + r(\theta'^2 - H^2)(\eta w'_{xx})_x\right]
$$
$$
+ \frac{5H}{24}\beta^2\left[\left(\theta^2 - \frac{1}{5}\right)^2 w_{xxxxx} - r\left(\theta'^2 - \frac{1}{5}H^2\right)^2 w'_{xxxxx}\right] = 0. \qquad \text{(B-2)}
$$

Replacing the variables w and w' in (B-2) by their expressions (4.57)–(4.59) in terms of W and let

$$F = \frac{1+H}{r+H}, \quad G = H \frac{(\theta'^2 - \frac{1}{3}H^2) - (\theta^2 - \frac{1}{3})}{r+H}.$$

We will consider all the terms of (B-2) one by one:

The second term of (B-2):

$$H(w_x - rw'_x) = HW_x \tag{B-3}$$

The term in α of (B-2):
One deduces rw' from both sides of equation (4.58) in order to make appear W

$$w - rw' = -(r+H)w' - \alpha FW\eta + \frac{1}{2}\beta GW_{xx}.$$

Dividing the previous equation to $(r+H)$, one has

$$w' = -\frac{1}{r+H}W - \alpha\frac{1}{r+H}FW\eta + \frac{1}{2}\beta\frac{1}{r+H}GW_{xx}. \tag{B-4}$$

Similarly, multiplying equation (4.59) to $(-r)$, and then adding w to both sides yields

$$w - rw' = w + \frac{r}{H}w + \alpha\frac{r}{H}FW\eta - \frac{1}{2}\beta\frac{r}{H}GW_{xx}.$$

Dividing both sides of the previous equation by $\frac{r+H}{H}$ yields

$$w = \frac{H}{r+H}W - \alpha\frac{r}{r+H}FW\eta + \frac{1}{2}\beta\frac{r}{r+H}GW_{xx}. \tag{B-5}$$

Combining (B-4) and (B-5) yields

$$Hw + rw' = \frac{H^2 - r}{r+H}W - \alpha\frac{r(1+H)}{r+H}FW\eta + \frac{1}{2}\beta\frac{r(1+H)}{r+H}GW_{xx}.$$

Therefore

$$\alpha\left[(Hw + rw')\eta\right]_x = \alpha\frac{H^2 - r}{r+H}(W\eta)_x - \alpha^2\frac{r(1+H)^2}{(r+H)^2}(W\eta^2)_x \tag{B-6}$$
$$+ \frac{1}{2}\alpha\beta\frac{rH(1+H)\left((\theta'^2 - \frac{1}{3}H^2) - (\theta^2 - \frac{1}{3})\right)}{(r+H)^2}(W_{xx}\eta)_x.$$

Term in β of (B-2):
Using (B-4) and (B-5) one has

$$\frac{H}{2}\beta\left[(\theta^2 - \frac{1}{3})w_{xxx} - r(\theta'^2 - \frac{1}{3}H^2)w'_{xxx}\right]$$

$$
\begin{aligned}
= \quad &\frac{1}{2}\beta H\frac{H(\theta^2 - \frac{1}{3}) + r(\theta'^2 - \frac{1}{3}H^2)}{r + H}W_{xxx} \\
&+\frac{1}{2}\alpha\beta r H(1 + H)\frac{(\theta'^2 - \frac{1}{3}H^2) - (\theta^2 - \frac{1}{3})}{(r + H)^2}(W\eta)_{xxx} \\
&-\frac{1}{4}\beta^2 r H^2\frac{\left((\theta'^2 - \frac{1}{3}H^2) - (\theta^2 - \frac{1}{3})\right)^2}{(r + H)^2}W_{xxxxx}.
\end{aligned}
\qquad \text{(B-7)}
$$

Term in $\alpha\beta$ and term in β^2 of (B-2):
Since only the terms up to order 2 in α and/or β will be retained in the final equation, one can apply (4.57) to terms in $\alpha\beta$ or β^2

$$\frac{1}{2}\alpha\beta\left[H(\theta^2 - 1)(\eta w_{xx})_x + r(\theta'^2 - H^2)(\eta w'_{xx})_x\right]$$
$$= \frac{1}{2}\alpha\beta\frac{H^2(\theta^2 - 1) - r(\theta'^2 - H^2)}{r + H}(W_{xx}\eta)_x, \qquad \text{(B-8)}$$

and

$$\frac{5}{24}H\beta^2\left[\left(\theta^2 - \frac{1}{5}\right)^2 w_{xxxxx} - r\left(\theta'^2 - \frac{1}{5}H^2\right)^2 w'_{xxxxx}\right]$$
$$= \frac{5}{24}H\beta^2\frac{H(\theta^2 - \frac{1}{5})^2 + r(\theta'^2 - \frac{1}{5}H^2)^2}{r + H}W_{xxxxx}. \qquad \text{(B-9)}$$

Substituting (B-3), (B-6), (B-7), (B-8) and (B-9) into equation (B-2) yields the first

equation of the extended Boussinesq system

$$(r+H)\eta_t + HW_x + \alpha\frac{H^2-r}{r+H}(W\eta)_x$$

$$+\frac{1}{2}\beta\frac{H\left(H(\theta^2-\frac{1}{3})+r(\theta'^2-\frac{1}{3}H^2)\right)}{r+H}W_{xxx} - \alpha^2\frac{r(1+H)^2}{(r+H)^2}(W\eta^2)_x$$

$$+\frac{1}{2}\alpha\beta rH(1+H)\frac{(\theta'^2-\frac{1}{3}H^2)-(\theta^2-\frac{1}{3})}{(r+H)^2}(W\eta)_{xxx}$$

$$+\frac{1}{2}\alpha\beta\frac{rH(1+H)}{(r+H)^2}\left((\theta'^2-\frac{1}{3}H^2)-(\theta^2-\frac{1}{3})\right)(W_{xx}\eta)_x \qquad\text{(B-10)}$$

$$+\frac{1}{2}\alpha\beta\frac{H^2(\theta^2-1)-r(\theta'^2-H^2)}{r+H}(W_{xx}\eta)_x$$

$$-\frac{1}{4}\beta^2\frac{rH^2\left((\theta'^2-\frac{1}{3}H^2)-(\theta^2-\frac{1}{3})\right)^2}{(r+H)^2}W_{xxxxx}$$

$$+\frac{5}{24}\beta^2 H\frac{H(\theta^2-\frac{1}{5})^2+r(\theta'^2-\frac{1}{5}H^2)^2}{r+H}W_{xxxxx} = 0.$$

We proceed the same way for equation (4.37).

Term in α of (4.37):
Using (B-4) and (B-5), one has

$$ww_x - rw'w'_x$$

$$= \left(\frac{H}{r+H}W - \alpha\frac{r}{r+H}FW\eta + \frac{1}{2}\beta\frac{r}{r+H}GW_{xx}\right)$$

$$\left(\frac{H}{r+H}W_x - \alpha\frac{r}{r+H}F(W\eta)_x + \frac{1}{2}\beta\frac{r}{r+H}GW_{xxx}\right)$$

$$-r\left(-\frac{1}{r+H}W - \alpha\frac{1}{r+H}FW\eta + \frac{1}{2}\beta\frac{1}{r+H}GW_{xx}\right)$$

$$\left(-\frac{1}{r+H}W_x - \alpha\frac{1}{r+H}F(W\eta)_x + \frac{1}{2}\beta\frac{1}{r+H}GW_{xxx}\right)$$

$$= \frac{H^2}{(r+H)^2}WW_x - \alpha\frac{rH}{(r+H)^2}F(W^2\eta)_x + \frac{1}{2}\beta\frac{rH}{(r+H)^2}G(WW_{xx})_x$$

$$-r\frac{1}{(r+H)^2}WW_x - \alpha r\frac{1}{(r+H)^2}F(W^2\eta)_x + \frac{1}{2}\beta r\frac{1}{(r+H)^2}G(WW_{xx})_x$$

$$= \frac{H^2-r}{(r+H)^2}WW_x - \alpha\frac{r(H+1)}{(r+H)^2}F(W^2\eta)_x + \frac{1}{2}\beta\frac{r(H+1)}{(r+H)^2}G(WW_{xx})_x$$

Multiplying this equation by α yields

$$\alpha(ww_x - rw'w'_x) = \alpha\frac{H^2-r}{(r+H)^2}WW_x - \alpha^2\frac{r(H+1)^2}{(r+H)^3}(W^2\eta)_x$$

$$+\frac{1}{2}\alpha\beta\frac{rH(H+1)\left((\theta'^2 - \frac{1}{3}H^2) - (\theta^2 - \frac{1}{3})\right)}{(r+H)^3}(WW_{xx})_x$$

$$\text{(B-11)}$$

Term in β of (4.37):
Inserting (4.58)-(4.59) into this term, one has

$$\frac{1}{2}\beta\left[(\theta^2-1)w - r(\theta'^2-H^2)w'\right]_{xxt} =$$

$$\frac{1}{2}\beta\frac{H(\theta^2-1) + r(\theta'^2-H^2)}{r+H}W_{xxt} - \frac{1}{2}\alpha\beta\frac{r(1+H)\left((\theta^2-1) - (\theta'^2-H^2)\right)}{(r+H)^2}(W\eta)_{xxt}$$

$$+\frac{1}{4}\beta^2\frac{rH\left((\theta^2-1) - (\theta'^2-H^2)\right)\left((\theta'^2-\frac{1}{3}H^2) - (\theta^2-\frac{1}{3})\right)}{(r+H)^2}W_{xxxxt} \qquad \text{(B-12)}$$

Since only the terms up to order 2 in α and/or β will be retained in the final result, one can apply (4.57) to the last four terms of (4.37)

$$\frac{1}{2}\beta^2\Big[(\theta^2-1)(5\theta^2-1)w - r(\theta'^2-H^2)(5\theta'^2-H^2)w'\Big]_{xxxxt}$$
$$= \frac{1}{2}\beta^2\frac{H(\theta^2-1)(5\theta^2-1)+r(\theta'^2-H^2)(5\theta'^2-H^2)}{r+H}W_{xxxxt}. \quad \text{(B-13)}$$

and

$$-\alpha\beta\Big[(\eta w_{xt})_x + rH(\eta w'_{xt})_x\Big] = -\alpha\beta\frac{H(1-r)}{r+H}(W_{xt}\eta)_x, \quad \text{(B-14)}$$

and

$$\frac{1}{2}\alpha\beta\Big[(\theta^2-1)ww_{xxx} - r(\theta'^2-H^2)w'w'_{xxx}\Big]$$
$$= \frac{1}{2}\alpha\beta\frac{H^2(\theta^2-1)-r(\theta'^2-H^2)}{(r+H)^2}WW_{xxx}, \quad \text{(B-15)}$$

and

$$\frac{1}{2}\alpha\beta\Big[(\theta^2+1)w_xw_{xx} - r(\theta'^2+H^2)w'_xw'_{xx}\Big]$$
$$= \frac{1}{2}\alpha\beta\frac{H^2(\theta^2+1)-r(\theta'^2+H^2)}{(r+H)^2}W_xW_{xx}. \quad \text{(B-16)}$$

Substituting (B-11)–(B-16) to equation (4.37) yields the second equation of the

extended Boussinesq system

$$(1-r)\eta_x + W_t + \alpha\frac{H^2-r}{(r+H)^2}WW_x$$

$$+\frac{1}{2}\beta\frac{H(\theta^2-1)+r(\theta'^2-H^2)}{r+H}W_{xxt} - \alpha^2\frac{r(1+H)^2}{(r+H)^3}(W^2\eta)_x$$

$$+\frac{1}{2}\alpha\beta\frac{rH(H+1)\left((\theta'^2-\frac{1}{3}H^2)-(\theta^2-\frac{1}{3})\right)}{(r+H)^3}(WW_{xx})_x$$

$$-\alpha\beta\frac{H(1-r)}{r+H}(W_{xt}\eta)_x + \frac{1}{2}\alpha\beta\frac{H^2(\theta^2-1)-r(\theta'^2-H^2)}{(r+H)^2}WW_{xxx}$$

$$+\frac{1}{2}\alpha\beta\frac{H^2(\theta^2+1)-r(\theta'^2+H^2)}{(r+H)^2}W_xW_{xx}$$

$$-\frac{1}{2}\alpha\beta\frac{r(1+H)\left((\theta^2-1)-(\theta'^2-H^2)\right)}{(r+H)^2}(W\eta)_{xxt}$$

$$+\frac{1}{4}\beta^2\frac{rH\left((\theta^2-1)-(\theta'^2-H^2)\right)\left((\theta'^2-\frac{1}{3}H^2)-(\theta^2-\frac{1}{3})\right)}{(r+H)^2}W_{xxxxt}$$

$$+\frac{1}{2}\beta^2\frac{H(\theta^2-1)(5\theta^2-1)+r(\theta'^2-H^2)(5\theta'^2-H^2)}{r+H}W_{xxxxt}=0$$

(B-17)

c. Intermediate steps to obtain system (4.62)

One examines term by term of equations (4.60) and (4.61).

Let begin with the first one

$$\eta^*_{t^*} = (h\alpha\eta)_{\frac{h}{c_0\alpha}t} = c_0\alpha^2\eta_t,$$

$$W^*_{x^*} = \left(\frac{gh\alpha}{c_0}W\right)_{\frac{h}{\beta}x} = \frac{g}{c_0}\alpha\beta W_x,$$

$$(H^2 - r)(W^*\eta^*)_{x^*} = \alpha\mathcal{C}\left(\frac{gh\alpha}{c_0}Wh\alpha\eta\right)_{\frac{h}{\beta}x} = \frac{gh\mathcal{C}}{c_0}\alpha^3\beta(W\eta)_x,$$

$$W^*_{x^*x^*x^*} = \left(\frac{gh\alpha}{c_0}W\right)_{\frac{h^3}{\beta^3}xxx} = \frac{g}{c_0h^2}\alpha\beta^3 W_{xxx},$$

$$(W^*\eta^*)_{x^*x^*x^*} = \left(\frac{gh\alpha}{c_0}Wh\alpha\eta\right)_{\frac{h^3}{\beta^3}xxx} = \frac{g}{c_0h}\alpha^2\beta^3(W\eta)_{xxx},$$

$$(W^*_{x^*x^*}\eta)_{x^*} = \left(\frac{gh\alpha}{c_0}W_{\frac{h^2}{\beta^2}xx}(h\alpha\eta)\right)_{\frac{h}{\beta}x} = \frac{g}{c_0h}\alpha^2\beta^3(W_{xx}\eta)_x,$$

$$W^*_{x^*x^*x^*x^*x^*} = \left(\frac{gh\alpha}{c_0}W\right)_{\frac{h^5}{\beta^5}xxxxx} = \frac{g}{c_0h^4}\alpha\beta^5 W_{xxxxx}.$$

One decides to retain only terms up to order 4 in α and/or β, therefore the three last terms will be neglected.

For equation (4.61), one has

$$\eta^*_{x^*} = (h\alpha\eta)_{\frac{h}{\beta}x} = \alpha\beta\eta_x,$$

$$W^*_{t^*} = \frac{gh\alpha}{c_0}W_{\frac{h}{c_0\alpha}t} = g\alpha^2 W_t,$$

$$(H^2 - r)W^*W^*_{x^*} = \alpha\mathcal{C}\left(\frac{gh\alpha}{c_0}\right)^2 WW_{\frac{h}{\beta}x} = g\mathcal{C}\alpha^3\beta WW_x,$$

$$W^*_{x^*x^*t^*} = \left(\frac{gh\alpha}{c_0}\right)W_{\frac{h^2}{\beta^2}xx\frac{h}{c_0\alpha}t} = \frac{g}{h^2}\alpha^2\beta^2 W_{xxt},$$

$$(W^{*2}\eta^*)_{x^*} = \left(\left(\frac{gh\alpha}{c_0}\right)^2 W^2 h\alpha\eta\right)_{\frac{h}{\beta}x} = gh\alpha^3\beta(W^2\eta)_x,$$

$$(W^*W^*_{x^*x^*})_{x^*} = \left(\left(\frac{gh\alpha}{c_0}\right)^2 WW_{\frac{h^2}{\beta^2}xx}\right)_{\frac{h}{\beta}x} = \frac{g}{h^2}\alpha^2\beta^3(WW_{xx})_x,$$

$$(\eta^*W^*_{x^*t^*})_{x^*} = \left(\alpha h\eta\frac{gh\alpha}{c_0}W_{\frac{h}{\beta}x\frac{h}{c_0\alpha}t}\right)_{\frac{h}{\beta}x} = \frac{g}{h}\alpha^3\beta^2(\eta W_{xt})_x,$$

$$WW_{xxx} = \left(\frac{gh\alpha}{c_0}\right)^2 WW_{\frac{h^3}{\beta^3}} = \frac{g}{h^2}\alpha^2\beta^3 WW_{xxx},$$

$$(W^*\eta^*)_{xxt} = \left(\frac{gh\alpha}{c_0}Wh\alpha\eta\right)_{\frac{h2}{\beta^2}xx\frac{h}{c_0\alpha}t} = \frac{g}{h}\alpha^3\beta^2(W\eta)_{xxt},$$

$$W^*_{x^*x^*x^*x^*t^*} = \left(\frac{gh\alpha}{c_0}\right)W_{\frac{h4}{\beta^4}xxxx\frac{h}{c_0\alpha}t} = \frac{g}{h^4}\alpha^2\beta^4W_{xxxxt}.$$

Only terms up to order 4 in α and β will be retained, therefore the five last terms will be neglected.

Appendix C

Numerical simulations

C.1 The program is used to obtain the trajectories of the particles

Perturbation of the particles in the interior of two-layer fluid (linear case)

```
clear all;  close all;
M=1; % M takes value 1 or 2, depends on what we want to take
     % w(1) or w(2).
```

Parameters :

```
p = 2*pi;
g =  10;

k=0.5;
h =  1;    %the depth of the lower layer
h1 =  0.1; %the depth of the upper layer
r =  0.85; %density ratio

%k = 1;
%h = 1;     %the depth of the lower layer
%h1 = 1;    %the depth of the upper layer
%r = 0.98; %density ratio
```

```
%k=0.6;
%h = 0.6;  %the depth of the lower layer
%h1 = 0.2; %the depth of the upper layer
%r = 0.9;  %density ratio

%k = 1.2;
%h =  0.6; %the depth of the lower layer
%h1 = 0.2; %the depth of the upper layer
%r = 0.9;  %density ratio

c = -(h+h1)/2;
d = (h+h1)/2;
x0 = (c+d)/2;
C = 0.008;
x = c:p/200:d;
```

Two solutions of the dispersion relation

```
w(1) = sqrt((1-r)*g*k*tanh(k*h)*tanh(k*h1)/(tanh(k*h1)+r*tanh(k*h)));
w(2) = -sqrt((1-r)*g*k*tanh(k*h)*tanh(k*h1)/(tanh(k*h1)+r*tanh(k*h)));
```

Initial matrices

```
xtraj1 = [];
ztraj1 = [];
xtraj2 = [];
ztraj2 = [];
xf_particle_u=[];
zf_particle_u=[];
xe_particle_l=[];
ze_particle_l=[];
```

Main program contains a loop in time that takes place on a periodic domain 0<wt<2*pi

```
nb = 1;    %number of periods we want to observe
dt = 100;  %number of points represent

%%The form of the roof and the bottom:
paroi_superieure=h1*(x-x)+h1;
fond=-h*(x-x)-h;
```

```
for j = 1:dt+1
    t = nb*p*(j-1)/(dt*w(M));

%%The form of the interface:
    eta = -k*C/w(M)*tanh(k*h)*sin(k*x-w(M)*t) ;

%%Trajectories of the particles of the lower layer

e=6;  %Number of particles that we want to represent for the lower layer
for m=1:e
z0L = (m-e)/(e-1)*h; %Position of each particle in the interval [-h 0]

    xtraj10 = x0 - k*C/w(M)*cosh(k*(h+z0L))/cosh(k*h)*cos(k*x0-w(M)*t);
    ztraj10 = z0L - k*C/w(M)*sinh(k*(h+z0L))/cosh(k*h)*sin(k*x0-w(M)*t);

    xe_particle_l = [xe_particle_l xtraj10];
    ze_particle_l = [ze_particle_l ztraj10];
end
    xtraj1 = [xtraj1 ; xe_particle_l];
    ztraj1 = [ztraj1 ; ze_particle_l];
    xe_particle_l = [];
    ze_particle_l = [];

%%Trajectories of the particles of the upper layer

f=4;   %Number of particles that we want to represent for upper layer
for n=1:f
z0u = h1*(n-1)/(f-1); %Position of each particle in the interval [0 h1]

    xtraj20 = x0 - k*C/w(M)*cosh(k*(h1-z0u))*tanh(k*h)/sinh(k*h1)...
        *sin(k*x0-w(M)*t);
    ztraj20 = z0u + k*C/w(M)*sinh(k*(h1-z0u))*tanh(k*h)/sinh(k*h1)...
        *cos(k*x0-w(M)*t) ;

    xf_particle_u=[xf_particle_u  xtraj20];
    zf_particle_u=[zf_particle_u ztraj20];
end
    xtraj2 = [xtraj2; xf_particle_u];
    ztraj2 = [ztraj2; zf_particle_u];
    xf_particle_u = [];
    zf_particle_u = [];
```

Plot the trajectories, the boundaries and the interface:

```
plot(x,fond,'k',x,eta,'--k',x,paroi_superieure,'k',xtraj2,ztraj2,...
    'k.',xtraj1,ztraj1,'k');
axis([ c d -h-(h+h1)/10 h1+(h+h1)/10]);
xlabel x; ylabel z
set(get(gca,'ylabel'),'Rotation',0.0)

F(j) = getframe;

end
```

C.2 This program is used to study qualitatively the head-on collision between 2 elevation solitary waves of equal size which is solution to system (5.2)

```
clear all, close all
domaine = 512;
time = 300;
H = 1.2;  %thickness ratio
r = 0.8;  %density ratio
c = domaine/2/pi;
N = 1024; %space mesh
```

Fourier mode

```
k = [0:N/2-1 0 -N/2+1:-1]';
ik = i*k;
tmax = time/c;
```

Space step and time step

```
x = (2*pi/N)*(-N/2:N/2-1)';
dt = 1/N;% (dt<=9/N);
nmax = round(tmax/dt);
```

Initial condition

```
eta0 = 0.1; %initial amplitude
x0 = 2;     %initial position
theta = 0;  %water level in the lower fluid
theta1 = 0; %water level in the upper fluid
S = (theta^2-1)+r/H*(theta1^2-H^2);


d1 = H/(r+H);
d2 = H^2/(2*(r+H)^2)*(S+2/3*(1+r*H));
d3 = 1/2*S*d1;
d4 = (H^2-r)/((r+H)^2);


V = 1+d4*eta0/(2*d1);
K = sqrt(d4*eta0/(4*(d2-d1*d3-1/2*d3*d4*eta0)));

eta1 = eta0*(sech(K*c*(x+x0))).^2;
M1 = -1/4*d4/d1*eta1.^2 - eta0*K^2*(d2/d1+d3*V)...
    *(2./((cosh(K*c*(x+x0))).^2) - 3./((cosh(K*c*(x+x0))).^4));
u1 = (r+H)/H*(eta1+M1);

eta2 = eta0*(sech(K*c*(x-x0))).^2;
M2 = -1/4*d4/d1*eta2.^2 - eta0*K^2*(d2/d1+d3*V)...
    *(2./((cosh(K*c*(x-x0))).^2) - 3./((cosh(K*c*(x-x0))).^4));
u2 = -(r+H)/H*(eta2+M2);

eta = eta1+eta2;
u = u1+u2;

etan = eta1; %Initial condition for the right running-wave
un = u1;     %which propagates without collision

etam = eta2; %Initial condition for the left running-wave
um = u2;     %which propagates without collision
```

Coefficients of the system of 2 equations

```
d12k = (1/c^2*d2*k.^2 - d1).*ik;
d13k = - 1./(d1*(1-1/c^2*d3*k.^2)).*ik;
d34k = - d4./(2*(1-1/c^2*d3*k.^2)).*ik;
d4k = - d4.*ik;
```

Fourier

```
                    v1 = fft(eta);
                    v2 = fft(u);

                    v1n = fft(etan);
                    v2n = fft(un);

                    v1m = fft(etam);
                    v2m = fft(um);


peaks = max(abs(eta));
index_i = find(eta==max(eta));
left = min(index_i);
right = max(index_i);
tdata = 0;
tdata_left = 0;
tdata_right = 0;
aa = 0;
udata1 = eta;

for n = 1:nmax
            t = n*dt;
%RK4

a1 = d12k.*v2 + d4k.*fft(real(ifft(v2)).*real(ifft(v1)));
a2 = d13k.*v1 + d34k.*fft(real(ifft(v2)).^2);

b1 = d12k.*(v2+a2*dt/2)...
    + d4k.*fft(real(ifft(v2+a2*dt/2)).*real(ifft(v1+a1*dt/2)));
b2 = d13k.*(v1+a1*dt/2) + d34k.*fft(real(ifft(v2+a2*dt/2)).^2);

c1 = d12k.*(v2+b2*dt/2)...
    + d4k.*fft(real(ifft(v2+b2*dt/2)).*real(ifft(v1+b1*dt/2)));
c2 = d13k.*(v1+b1*dt/2) + d34k.*fft(real(ifft(v2+b2*dt/2)).^2);

d1 = d12k.*(v2+c2*dt)...
    + d4k.*fft(real(ifft(v2+c2*dt)).*real(ifft(v1+c1*dt)));
d2 = d13k.*(v1+c1*dt) + d34k.*fft(real(ifft(v2+c2*dt)).^2);

v1 = v1 + (a1 + 2*b1 + 2*c1 + d1)*dt/6;
v2 = v2 + (a2 + 2*b2 + 2*c2 + d2)*dt/6;
```

```
a1n = d12k.*v2n ...
    + d4k.*fft(real(ifft(v2n)).*real(ifft(v1n)));
a2n = d13k.*v1n + d34k.*fft(real(ifft(v2n)).^2);


b1n = d12k.*(v2n+a2n*dt/2)...
    + d4k.*fft(real(ifft(v2n+a2n*dt/2)).*real(ifft(v1n+a1n*dt/2)));
b2n = d13k.*(v1n+a1n*dt/2) + d34k.*fft(real(ifft(v2n+a2n*dt/2)).^2);


c1n = d12k.*(v2n+b2n*dt/2)...
    + d4k.*fft(real(ifft(v2n+b2n*dt/2)).*real(ifft(v1n+b1n*dt/2)));
c2n = d13k.*(v1n+b1n*dt/2) + d34k.*fft(real(ifft(v2n+b2n*dt/2)).^2);


d1n = d12k.*(v2n+c2n*dt)...
    + d4k.*fft(real(ifft(v2n+c2n*dt)).*real(ifft(v1n+c1n*dt)));
d2n = d13k.*(v1n+c1n*dt) + d34k.*fft(real(ifft(v2n+c2n*dt)).^2);


v1n = v1n + (a1n + 2*b1n + 2*c1n + d1n)*dt/6;
v2n = v2n + (a2n + 2*b2n + 2*c2n + d2n)*dt/6;




a1m = d12k.*v2m + d4k.*fft(real(ifft(v2m)).*real(ifft(v1m)));
a2m = d13k.*v1m + d34k.*fft(real(ifft(v2m)).^2);


b1m = d12k.*(v2m+a2m*dt/2)...
     + d4k.*fft(real(ifft(v2m+a2m*dt/2)).*real(ifft(v1m+a1m*dt/2)));
b2m = d13k.*(v1m+a1m*dt/2) + d34k.*fft(real(ifft(v2m+a2m*dt/2)).^2);


c1m = d12k.*(v2m+b2m*dt/2)...
     + d4k.*fft(real(ifft(v2m+b2m*dt/2)).*real(ifft(v1m+b1m*dt/2)));
c2m = d13k.*(v1m+b1m*dt/2) + d34k.*fft(real(ifft(v2m+b2m*dt/2)).^2);


d1m = d12k.*(v2m+c2m*dt)...
     + d4k.*fft(real(ifft(v2m+c2m*dt)).*real(ifft(v1m+c1m*dt)));
d2m = d13k.*(v1m+c1m*dt) + d34k.*fft(real(ifft(v2m+c2m*dt)).^2);


v1m = v1m + (a1m + 2*b1m + 2*c1m + d1m)*dt/6;
v2m = v2m + (a2m + 2*b2m + 2*c2m + d2m)*dt/6;
```

```
    u1 = real(ifft(v1)); h = waitbar(n/nmax);
    u1n = real(ifft(v1n));
    u1m = real(ifft(v1m));
    tdata = [tdata; t];
    udata1 = [udata1 u1];
    plot(c*x,u1,'k')
    title('Head-on collision of 2 elevation solitary waves of equal size')
    xlabel x; ylabel \eta
    set(get(gca,'ylabel'),'Rotation',0.0)
    axis([-c*pi c*pi -0.02 0.22])


    peaks = [peaks max(abs(u1))];
    index = find(u1==max(u1));% index can have 4 components
    [mm nn] = size(index);    % nn=1 car index is column vector

     if mm==1
         if index<N/2 left = [left index];
                     tdata_left = [tdata_left t];
         else right = [right index];
             tdata_right = [tdata_right t];
         end
     elseif mm==2
             left = [left min(index)];
             tdata_left = [tdata_left t];
             right = [right max(index)];
             tdata_right = [tdata_right  t] ;
     else
     aa=aa+1 %number of time index has more than 2 components
     end
end
%waterfall(c*x(1:5:end),tdata(:),udata1(1:5:end,:)');
    x_left = c*x(left);
    x_right = c*x(right);
    tdata_left = c*tdata_left;
    tdata_right = c*tdata_right;
    tdata = c*tdata;

scrsz = get(0,'ScreenSize');
```

Plot the evolution in time of the peaks (run-up)

```
figure('Position',[1 scrsz(4)/2 scrsz(3)/2 scrsz(4)/2])
plot(tdata, peaks', '.k');
set(gca,'FontWeight','bold');
xlabel ('t', 'fontsize', 14);
ylabel ('sup_x(\eta(x,t))', 'fontsize', 14 );
newsize = get(gca,'FontSize')*1.2;
set(gca,'FontSize',newsize);
axis([0 time 0.09 0.215]);
```

Plot the trajectory

```
figure('Position',[scrsz(3)/2 scrsz(4)/2 scrsz(3)/2 scrsz(4)/2]);
plot(x_left,tdata_left,'.k');
hold on;
plot(x_right,tdata_right,'.k');
set(gca,'FontWeight','bold');
xlabel ('x', 'fontsize', 14);
ylabel ('t', 'fontsize', 14 );
set(get(gca, 'ylabel'), 'Rotation',0.0)
newsize = get(gca,'FontSize')*1.2;
set(gca,'FontSize',newsize);
axis([ min(x_left)  max(x_right) 0 time ]);
```

Plot the phase shifts

```
figure('Position',[1 1 scrsz(3)/2 scrsz(4)/2]);
plot(c*x, u1, 'k');
hold on;
plot(c*x, u1n, 'k--');
plot(c*x, u1m, 'k--');
set(gca,'FontWeight','bold');
xlabel ('x', 'fontsize', 14);
ylabel ('\eta', 'fontsize', 14 );
set(get(gca, 'ylabel'), 'Rotation',0.0);
newsize = get(gca,'FontSize')*1.2;
set(gca,'FontSize',newsize);
```

C.3 The program is used to filter a solitary wave which is solution to the extended Boussinesq system (5.8)

```
clear all, close all
domain = 1024*4;     %real domain
time = 2600;         %real time propagating
H = 0.88;            %thickness ratio
r = 0.98;            %density ratio
c = domain/2/pi;     %compress coefficient: from real domain to Fourier domain
N = 1024*8;          %space mesh
c1_max = (H^2-r)^2/(8*r*H*(1+H)^2);
%c1_max = 0.001733531698205
```

Fourier mode

```
                        k = [0:N/2-1 0 -N/2+1:-1]';
                        ik = i*k;
                        tmax = time/c;
```

Space step and time step

```
                        x = (2*pi/N)*(-N/2:N/2-1)';
                        dt = 8/N;
                        nmax = round(tmax/dt);
```

Initial condition

```
c11 = 0.00173353;
x0 = 1.8;       %initial position
theta = 0;
theta1 = 0;
S = (theta^2-1)+r/H*(theta1^2-H^2); %S=-1-r*H

d1 = H/(r+H);
d2 = H^2/(2*(r+H)^2)*(S+2/3*(1+r*H));
d3 = 1/2*S*d1;
d4 = (H^2-r)/((r+H)^2);
d5 = r*(1+H)^2/((r+H)^3);

alpha = 3/2*(H^2-r)/(H*(r+H));
beta = 3*r*(1+H)^2/(H*(r+H)^2);
lambda = 1/6*H*(r*H+1)/(r+H) - 1/4*H*S/(r+H)*c11;
```

```
epsilon = sqrt(alpha^2-6*beta*c11)/alpha;
coh = cosh(sqrt(c11/lambda).*(c*(x+x0)));

eta = alpha/beta*(1-epsilon^2)./(1-epsilon*coh);
amp = min(eta);

plot(c*x,eta,'k--');
title ('Initial condition of \eta');
xlabel x; ylabel \eta
set(get(gca,'ylabel'),'Rotation',0.0);
axis([-c*pi c*pi amp*11/10 -amp/10 ]);


etaxx = -alpha*epsilon*c11*(epsilon^2-1)*(epsilon*coh.^2-2*epsilon+coh)...
    /beta/lambda./((1-epsilon*coh).^3);
etaxt = alpha*epsilon*c11*(epsilon^2-1)*(1+c11)*...
    (epsilon*coh.^2-2*epsilon+coh)/beta/lambda./((1-epsilon*coh).^3);
M = -d4/(4*d1)*eta.^2 - d2/(2*d1)*etaxx + d3/2*etaxt;
u = (r+H)/H*(eta+M);
```

Coefficients of the system of 2 equations with cubic terms

```
d12k = (1/c^2*d2*k.^2 - d1).*ik;
d4k = - d4.*ik;
d5k =  d5.*ik;
d13k = - 1./(d1*(1-1/c^2*d3*k.^2)).*ik;
d34k = - d4./(2*(1-1/c^2*d3*k.^2)).*ik;
d35k = d5./(1-1/c^2*d3*k.^2).*ik;

N012 = find(eta==min(eta));
peaks = min(eta);
fois = 0;
tdata = 0;

jmax=255;
```

Begin filter %***********************************

```
for j=1:jmax
% Fourier
                        v1=fft(eta);
```

```
                    v2=fft(u);

for n=1:nmax
            t=n*dt;

%RK4;

a1 = d12k.*v2 + d4k.*fft(real(ifft(v2)).*real(ifft(v1)))...
    + d5k.*fft(real(ifft(v2)).*real(ifft(v1)).^2) ;
a2 = d13k.*v1 + d34k.*fft(real(ifft(v2)).^2)...
    +d35k.*fft(real(ifft(v2)).^2.*real(ifft(v1)));

b1 = d12k.*(v2+a2*dt/2)...
    + d4k.*fft(real(ifft(v2+a2*dt/2)).*real(ifft(v1+a1*dt/2)))...
    + d5k.*fft(real(ifft(v2+a2*dt/2)).*real(ifft(v1+a1*dt/2)).^2);
b2 = d13k.*(v1+a1*dt/2)...
    + d34k.*fft(real(ifft(v2+a2*dt/2)).^2)...
    + d35k.*fft(real(ifft(v2+a2*dt/2)).^2.*real(ifft(v1+a1*dt/2)));

c1 = d12k.*(v2+b2*dt/2)...
    + d4k.*fft(real(ifft(v2+b2*dt/2)).*real(ifft(v1+b1*dt/2)))...
    + d5k.*fft(real(ifft(v2+b2*dt/2)).*real(ifft(v1+b1*dt/2)).^2);
c2 = d13k.*(v1+b1*dt/2)...
    + d34k.*fft(real(ifft(v2+b2*dt/2)).^2)...
    + d35k.*fft(real(ifft(v2+b2*dt/2)).^2.*real(ifft(v1+b1*dt/2)));

d1 = d12k.*(v2+c2*dt)...
    + d4k.*fft(real(ifft(v2+c2*dt)).*real(ifft(v1+c1*dt)))...
    + d5k.*fft(real(ifft(v2+c2*dt)).*real(ifft(v1+c1*dt)).^2);
d2 = d13k.*(v1+c1*dt)...
    + d34k.*fft(real(ifft(v2+c2*dt)).^2)...
    + d35k.*fft(real(ifft(v2+c2*dt)).^2.*real(ifft(v1+c1*dt)));

v1 = v1+(a1+2*b1+2*c1+d1)*dt/6;
v2 = v2+(a2+2*b2+2*c2+d2)*dt/6;

        u1 = real(ifft(v1)); waitbar(n/nmax);
        u2 = real(ifft(v2));
        tdata = [tdata (j-1)*tmax+t];
        peaks = [peaks min(u1)];
        plot(c*x,u1,'k')
```

```
        title('Evolution in time of \eta at this filter step')
        xlabel x; ylabel \eta
        set(get(gca,'ylabel'),'Rotation',0.0)
        axis([-c*pi c*pi amp*11/10 -amp/10])
end
ss = find(u1==min(u1));
eta = zeros(N,1);
u = zeros(N,1);


eta(round(N/8):N-ss+N012,1) = u1(ss-N012+round(N/8):N,1);
u(round(N/8):N-ss+N012,1) = u2(ss-N012+round(N/8):N,1);


fois=fois+1;
end
```

End filter **

```
etaeta = eta;
uu = u;

scrsz = get(0,'ScreenSize');
```

Plot the values of \eta

```
figure('Position',[1 scrsz(4)/2 scrsz(3)/2 scrsz(4)/2])
plot(c*x,u1,'k')
title ('\eta at the end of filter step');
xlabel x; ylabel \eta
set(get(gca,'ylabel'),'Rotation',0.0)
axis([-c*pi c*pi  amp*11/10 -amp/10]);
```

Plot the values of peaks

```
figure('Position',[scrsz(3)/2  1 scrsz(3)/2 scrsz(4)/2])
plot(c*tdata, -peaks,'.k')
title('Evolution in time of the peaks of \eta ')
xlabel t; ylabel sup_x(-\eta(x,t))
```

C.4   The program is used to study the overtaking collision between two solitary waves of depression which is solution to the extended Boussinesq system (5.8)

```
clear all, close all
domain=1024*4;
time=4100*40*3.5;
H=0.88;
r=0.98;
c=domain/2/pi;
N=1024*8;
c1_max=(H^2-r)^2/(8*r*H*(1+H)^2);
%c1_max = 0.001733531698205
```

Fourier mode

```
k=[0:N/2-1 0 -N/2+1:-1]';
ik=i*k;
```

Space step and phase steps

```
x=(2*pi/N)*(-N/2:N/2-1)';
dt=8/N;
tmax=time/c;
```

Initial condition

```
theta = 0;
theta1 = 0;
S = (theta^2-1)+r/H*(theta1^2-H^2); %S=-1-r*H

load c_filter_negative_normal_etaeta_uu_275times.mat etaeta uu

u1 = zeros(N,1);
eta1 = zeros(N,1);
eta1(round(N/30):N-1,1) = etaeta(1:N-round(N/30),1);
u1(round(N/30):N-1,1) = uu(1:N-round(N/30),1);

etan = eta1;
un = u1;
```

```
load c_negative_modi1_etaeta_uu_255time.mat etaeta uu

u2 = zeros(N,1);
eta2 = zeros(N,1);
eta2(1:N-round(N/20),1) = etaeta(round(N/20)+1:N,1);
u2(1:N-round(N/20),1) = uu(round(N/20)+1:N,1);

etam = eta2;
um = u2;

eta = eta1+eta2;
u = u1+u2;
```

Coefficients of the system of 2 equations with cubic terms

```
d1 = H/(r+H);
d2 = H^2/(2*(r+H)^2)*(S+2/3*(1+r*H));
d3 = 1/2*S*d1;
d4 = (H^2-r)/((r+H)^2);
d5 = r*(1+H)^2/((r+H)^3);

d12k = (1/c^2*d2*k.^2 - d1).*ik;
d4k = - d4.*ik;
d5k =  d5.*ik;
d13k = - 1./(d1*(1-1/c^2*d3*k.^2)).*ik;
d34k = - d4./(2*(1-1/c^2*d3*k.^2)).*ik;
d35k = d5./(1-1/c^2*d3*k.^2).*ik;
```

Fourier

```
                        v1=fft(eta);
                        v2=fft(u);

                        v1n=fft(etan);
                        v2n=fft(un);

                        v1m=fft(etam);
                        v2m=fft(um);

nplt=floor((tmax/600)/dt);
nmax=round(tmax/dt);
```

```
udata1=eta;
udata2=u;
tdata=0;

h=waitbar(0,'just hold on...');

peaks=[];
peaksn=[];
peaksm=[];
x_peaks_real=[];
x_peaks=[];
t_peaks=[];
index_real=0;

periodic=0;

for n=1:nmax
             t=n*dt;

%Runge Kutta 4 scheme;

a1 = d12k.*v2 + d4k.*fft(real(ifft(v2)).*real(ifft(v1)))...
    + d5k.*fft(real(ifft(v2)).*real(ifft(v1)).^2) ;
a2 = d13k.*v1 + d34k.*fft(real(ifft(v2)).^2)...
    + d35k.*fft(real(ifft(v2)).^2.*real(ifft(v1)));

b1 = d12k.*(v2+a2*dt/2)...
    + d4k.*fft(real(ifft(v2+a2*dt/2)).*real(ifft(v1+a1*dt/2)))...
    + d5k.*fft(real(ifft(v2+a2*dt/2)).*real(ifft(v1+a1*dt/2)).^2);
b2 = d13k.*(v1+a1*dt/2)...
    + d34k.*fft(real(ifft(v2+a2*dt/2)).^2)...
    + d35k.*fft(real(ifft(v2+a2*dt/2)).^2.*real(ifft(v1+a1*dt/2)));

c1 = d12k.*(v2+b2*dt/2)...
    + d4k.*fft(real(ifft(v2+b2*dt/2)).*real(ifft(v1+b1*dt/2)))...
    + d5k.*fft(real(ifft(v2+b2*dt/2)).*real(ifft(v1+b1*dt/2)).^2);
c2 = d13k.*(v1+b1*dt/2)...
    + d34k.*fft(real(ifft(v2+b2*dt/2)).^2)...
    + d35k.*fft(real(ifft(v2+b2*dt/2)).^2.*real(ifft(v1+b1*dt/2)));

d1 = d12k.*(v2+c2*dt)...
```

```
       + d4k.*fft(real(ifft(v2+c2*dt)).*real(ifft(v1+c1*dt)))...
       + d5k.*fft(real(ifft(v2+c2*dt)).*real(ifft(v1+c1*dt)).^2);
d2 = d13k.*(v1+c1*dt)...
       + d34k.*fft(real(ifft(v2+c2*dt)).^2)...
       + d35k.*fft(real(ifft(v2+c2*dt)).^2.*real(ifft(v1+c1*dt)));


v1 = v1+(a1+2*b1+2*c1+d1)*dt/6;
v2 = v2+(a2+2*b2+2*c2+d2)*dt/6;




a1n = d12k.*v2n + d4k.*fft(real(ifft(v2n)).*real(ifft(v1n)))...
       + d5k.*fft(real(ifft(v2n)).*real(ifft(v1n)).^2) ;
a2n = d13k.*v1n + d34k.*fft(real(ifft(v2n)).^2)...
       + d35k.*fft(real(ifft(v2n)).^2.*real(ifft(v1n)));

b1n = d12k.*(v2n+a2n*dt/2)...
       + d4k.*fft(real(ifft(v2n+a2n*dt/2)).*real(ifft(v1n+a1n*dt/2)))...
       + d5k.*fft(real(ifft(v2n+a2n*dt/2)).*real(ifft(v1n+a1n*dt/2)).^2);
b2n = d13k.*(v1n+a1n*dt/2)...
       + d34k.*fft(real(ifft(v2n+a2n*dt/2)).^2)...
       + d35k.*fft(real(ifft(v2n+a2n*dt/2)).^2.*real(ifft(v1n+a1n*dt/2)));

c1n = d12k.*(v2n+b2n*dt/2)...
       + d4k.*fft(real(ifft(v2n+b2n*dt/2)).*real(ifft(v1n+b1n*dt/2)))...
       + d5k.*fft(real(ifft(v2n+b2n*dt/2)).*real(ifft(v1n+b1n*dt/2)).^2);
c2n = d13k.*(v1n+b1n*dt/2)...
       + d34k.*fft(real(ifft(v2n+b2n*dt/2)).^2)...
       + d35k.*fft(real(ifft(v2n+b2n*dt/2)).^2.*real(ifft(v1n+b1n*dt/2)));

d1n = d12k.*(v2n+c2n*dt)...
       + d4k.*fft(real(ifft(v2n+c2n*dt)).*real(ifft(v1n+c1n*dt)))...
       + d5k.*fft(real(ifft(v2n+c2n*dt)).*real(ifft(v1n+c1n*dt)).^2);
d2n = d13k.*(v1n+c1n*dt)...
       + d34k.*fft(real(ifft(v2n+c2n*dt)).^2)...
       + d35k.*fft(real(ifft(v2n+c2n*dt)).^2.*real(ifft(v1n+c1n*dt)));

v1n = v1n+(a1n+2*b1n+2*c1n+d1n)*dt/6;
v2n = v2n+(a2n+2*b2n+2*c2n+d2n)*dt/6;
```

```
a1m = d12k.*v2m + d4k.*fft(real(ifft(v2m)).*real(ifft(v1m)))...
      + d5k.*fft(real(ifft(v2m)).*real(ifft(v1m)).^2) ;
a2m = d13k.*v1m + d34k.*fft(real(ifft(v2m)).^2)...
      + d35k.*fft(real(ifft(v2m)).^2.*real(ifft(v1m)));


b1m = d12k.*(v2m+a2m*dt/2)...
      + d4k.*fft(real(ifft(v2m+a2m*dt/2)).*real(ifft(v1m+a1m*dt/2)))...
      + d5k.*fft(real(ifft(v2m+a2m*dt/2)).*real(ifft(v1m+a1m*dt/2)).^2);
b2m = d13k.*(v1m+a1m*dt/2)...
      + d34k.*fft(real(ifft(v2m+a2m*dt/2)).^2)...
      + d35k.*fft(real(ifft(v2m+a2m*dt/2)).^2.*real(ifft(v1m+a1m*dt/2)));

c1m = d12k.*(v2m+b2m*dt/2)...
      + d4k.*fft(real(ifft(v2m+b2m*dt/2)).*real(ifft(v1m+b1m*dt/2)))...
      + d5k.*fft(real(ifft(v2m+b2m*dt/2)).*real(ifft(v1m+b1m*dt/2)).^2);
c2m = d13k.*(v1m+b1m*dt/2)...
      + d34k.*fft(real(ifft(v2m+b2m*dt/2)).^2)...
      + d35k.*fft(real(ifft(v2m+b2m*dt/2)).^2.*real(ifft(v1m+b1m*dt/2)));

d1m = d12k.*(v2m+c2m*dt)...
      + d4k.*fft(real(ifft(v2m+c2m*dt)).*real(ifft(v1m+c1m*dt)))...
      + d5k.*fft(real(ifft(v2m+c2m*dt)).*real(ifft(v1m+c1m*dt)).^2);
d2m = d13k.*(v1m+c1m*dt)...
      + d34k.*fft(real(ifft(v2m+c2m*dt)).^2)...
      + d35k.*fft(real(ifft(v2m+c2m*dt)).^2.*real(ifft(v1m+c1m*dt)));

v1m = v1m+(a1m+2*b1m+2*c1m+d1m)*dt/6;
v2m = v2m+(a2m+2*b2m+2*c2m+d2m)*dt/6;

        u1 = real(ifft(v1)); h = waitbar(n/nmax);
        u1n = real(ifft(v1n));
        u1m = real(ifft(v1m));
        plot(c*x,u1,'k');

        peaks = [peaks min(u1)];
        peaksn = [peaksn min(u1n)];
        peaksm = [peaksm min(u1m)];
        t_peaks = [t_peaks t];
end
```

```
scrsz = get(0,'ScreenSize');
```

Plot the evolution in time of the peaks of the solition

```
figure('Position',[1 scrsz(4)/2 scrsz(3)/2 scrsz(4)/2])
plot(t_peaks, -peaks,'k')
hold on
plot(t_peaks, -peaksn,'k:')
plot(t_peaks, -peaksm,'k--')
xlabel t; ylabel sup_x(-\eta(x,t))
axis([0 max(t_peaks) 0 0.061 ])
```

Plot the phase shift

```
figure('Position',[scrsz(3)/2  1 scrsz(3)/2 scrsz(4)/2])
plot(c*(x+140*pi),u1,'k');
hold on
plot(c*(x+140*pi),u1n, 'k:');
plot(c*(x+140*pi),u1m,'k--');
set(get(gca,'ylabel'),'Rotation',0.0)
xlabel x; ylabel \eta
axis([c*139*pi c*141*pi -0.06 0.003])
```

Bibliography

[1] D.S. Agafontsev, F. Dias, E.A. Kuznetsov, Deep-water internal solitary waves near critical density ratio, *Physica D* **225** (2007) 153–168.

[2] R. Barros, S.L. Gavrilyuk, V.M. Teshukov, Dispersive nonlinear waves in two-layer flows with free surface. I. Model derivation and general properties, *Studies in Applied Mathematics*, **119** (2007) 191-211.

[3] T.B. Benjamin, T.J. Bridges, Reappraisal of the Kelvin–Helmholtz problem. I. Hamiltonian structure, *J. Fluid Mech.* **333** (1997) 301–325.

[4] J.L. Bona, M. Chen, A Boussinesq system for two-way propagation of nonlinear dispersive waves, *Physica D* **116** (1998) 417–430.

[5] J.L. Bona, M. Chen, J.-C. Saut, Boussinesq equations and other systems for small-amplitude long waves in nonlinear dispersive media. I: Derivation and linear theory, *J. Nonlinear Sci.* **12** (2002) 283–318.

[6] J.L. Bona, V.A. Dougalis, D.E. Mitsotakis, Numerical solution of KdV–KdV systems of Boussinesq equations. I. The numerical scheme and generalized solitary waves, *Mathematics and Computers in Simulation* **74** (2007) 214–228.

[7] J.L. Bona, W.G. Pritchard, L.R. Scott, An evaluation of a model equation for water waves, *Phil. Trans. R. Soc. Lond. A* **302** (1981) 457–510.

[8] J. V. Boussinesq, Théorie générale des mouvements qui sont propagés dans un canal rectangulaire horizontal *C. R. Acad. Sci. Paris* **73** (1871) 256–260.

[9] J. V. Boussinesq, Théorie des ondes et des remous qui se propagent le long d'un canal rectangulaire horizontal, en communiquant au liquide contenu dans ce canal des vitesses sensiblement pareilles de la surface au fond, *C. R. Acad. Sci. Paris* **17** (1872) 55–108.

[10] T.J. Bridges, N.M. Donaldson, Reappraisal of criticality for two-layer flows and its role in the generation of internal solitary waves, *Phys. Fluids* **19** (2007) 072111-072111-13.

[11] M. Chen, Exact solution of various Boussinesq system, *Appl. Math. Lett.* **11** (1998) 45–49.

[12] J. W. Choi, S. M. Sun, M. C. Shen, Internal capillary-gravity waves of a two-layer fluid with free surface over an obstruction–Forced extended KdV equation, *Phys. Fluids,* **8** (1996) 397–404.

[13] W. Choi, R. Camassa, Fully nonlinear internal waves in a two-fluid system, *J. Fluid Mech.* **396** (1999) 1–36.

[14] W. Craig, P. Guyenne, J. Hammack, D. Henderson, C. Sulem, Solitary water wave interactions, *Phys. Fluids* **18** (2006) 057106.

[15] W. Craig, P. Guyenne, H. Kalisch, A new model for large amplitude long internal waves, *C. R. Mecanique* **332** (2004) 525–530.

[16] W. Craig, P. Guyenne, H. Kalisch, Hamiltonian long wave expansions for free surfaces and interfaces, *Comm. Pure Appl. Math.* **58** (2005) 1587–1641.

[17] P. Daripa, Higher-order Boussinesq equations for two-way propagation of shallow water waves, *Eur. J. Mech. B/Fluids* **25** (2006) 1008–1021.

[18] F. Dias, T. Bridges, Geometric aspects of spatially periodic interfacial waves, *Stud. Appl. Math.* **93** (1994) 93–132.

[19] F. Dias, J.-M. Vanden-Broeck, On internal fronts, *J. Fluid Mech.* **479** (2003) 145–154.

[20] F. Dias, J.-M. Vanden-Broeck, Two-layer hydraulic falls over an obstacle, *Europ. J. Mech. B/Fluids* **23** (2004) 879–898.

[21] F. Dias, A. Il'ichev, Interfacial waves with free-surface boundary conditions: an approach via a model equation, *Physica D* **150** (2001) 278–300.

[22] V.A. Dougalis, D.E. Mitsotakis, Solitary waves of the Bona-Smith system, Advances in scattering theory and biomedical engineering, ed. by D. Fotiadis and C. Massalas, World Scientific, New Jersey, (2004), pp. 286-294.

[23] D. Dutykh, F. Dias, Dissipative Boussinesq equations. *C. R. Mecanique* **335** (2007) 559–583.

[24] W.A.B. Evans, M.J. Ford, An integral equation approach to internal (2-layer) solitary waves, *Phys. Fluids* **8** (1996) 2032–2047.

[25] D. Farmer, L. Armi, The Generation and Trapping of Internal Solitary Waves over Topography, *Science* **283** (1999) 188–190.

[26] C. Fochesato, F. Dias, R. Grimshaw, Generalized solitary waves and fronts in coupled Korteweg–de Vries systems, *Physica D* **210** (2005) 96–117.

[27] M. Funakoshi, M. Oikawa, Long internal waves of large amplitude in a two-layer fluid, *J. Phys. Soc. Japan* **55** (1986) 128–144.

[28] R. Grimshaw, D. Pelinovsky, E. Pelinovsky, A. Slunyaev, Generation of large-amplitude solitons in the extended Kortewegde Vries equation, *Chaos* **12** (2002) 1070–1076.

[29] R. Grimshaw, E. Pelinovsky, T. Talipova, The modified Korteweg-de Vries equation in the theory of large - amplitude internal waves, *Nonlinear Processes in Geophysics* **4** (1997) 237–250.

[30] K.R. Helfrich, W.K. Melville, Long nonlinear internal waves, *Annu. Rev. Fluid Mech.* **38** (2006) 395–425.

[31] R. S. Johnson, A Modern Introduction to the Mathematical Theory of Water Waves, *Cambridge University Press,* **Cambrige** (1997).

[32] E. M. de Jager, On the Origin of the Korteweg-de Vries Equations, *oai:arXiv.org:math/0602661 (2007-08-17)*

[33] T. Kataoka, The stability of finite-amplitude interfacial solitary waves, *Fluid Dynamics Research* **38** (2006) 831–867.

[34] O. Laget, F. Dias, Numerical computation of capillary-gravity interfacial solitary waves, *J. Fluid Mech.* **349** (1997) 221–251.

[35] H. Michallet, E. Barthélemy, Experimental study of interfacial solitary waves, *J. Fluid Mech.* **366** (1998) 159–177.

[36] T. P. Stanton, L. A. Ostrovsky, Observations of highly nonlinear internal solitons over the Continental Shelf, *Geophysical Research Letters* **25**, (1998) 2695-2698.